

University of Dundee

DOCTOR OF PHILOSOPHY

A functional study of the *Phytophthora infestans* Avr3a alleles and paralogs

Seman, Zulkifli Ahmad

Award date:
2013

[Link to publication](#)

General rights

Copyright and moral rights for the publications made accessible in the public portal are retained by the authors and/or other copyright owners and it is a condition of accessing publications that users recognise and abide by the legal requirements associated with these rights.

- Users may download and print one copy of any publication from the public portal for the purpose of private study or research.
- You may not further distribute the material or use it for any profit-making activity or commercial gain
- You may freely distribute the URL identifying the publication in the public portal

Take down policy

If you believe that this document breaches copyright please contact us providing details, and we will remove access to the work immediately and investigate your claim.

DOCTOR OF PHILOSOPHY

A functional study of the *Phytophthora infestans* Avr3a alleles and paralogs

Zulkifli Ahmad Seman

2013

University of Dundee

Conditions for Use and Duplication

Copyright of this work belongs to the author unless otherwise identified in the body of the thesis. It is permitted to use and duplicate this work only for personal and non-commercial research, study or criticism/review. You must obtain prior written consent from the author for any other use. Any quotation from this thesis must be acknowledged using the normal academic conventions. It is not permitted to supply the whole or part of this thesis to any other person or to post the same on any website or other online location without the prior written consent of the author. Contact the Discovery team (discovery@dundee.ac.uk) with any queries about the use or acknowledgement of this work.

**A functional study of the *Phytophthora infestans*
Avr3a alleles and paralogs**

Zulkifli Ahmad Seman

Doctor of Philosophy

College of Life Sciences
The University of Dundee
and
Cell and Molecular Sciences
The James Hutton Institute



May 2013

DECLARATION

The results presented here are of investigations conducted by myself. Work other than my own is clearly identified with references to relevant researchers and/or their publications. I hereby declare that the work presented here is my own and has not been submitted in any form for any degree at this or any other university.

Zulkifli A. Seman

We certify that Zulkifli Ahmad Seman has fulfilled the relevant ordinance and regulations of the University Court and is qualified to submit this thesis for the degree of Doctor of Philosophy.

Dr. Ingo Hein
Cell and Molecular Sciences
The James Hutton Institute

Prof. Paul R J Birch
College of Life Sciences
University of Dundee

TABLE OF CONTENTS

DECLARATION.....	i
TABLE OF CONTENTS.....	ii
LIST OF FIGURES.....	v
LIST OF TABLES.....	vii
ACKNOWLEDGMENTS.....	viii
PUBLICATION ARISING FROM THIS WORK.....	x
ABSTRACT.....	xi
ABBREVIATIONS.....	xiii
1 LITERATURE REVIEW	1
1.1 POTATO.....	1
1.2 LATE BLIGHT DISEASE	3
1.2.1 <i>Phytophthora infestans</i>	4
1.2.2 Life cycle of <i>P. infestans</i>	7
1.2.2.1 Asexual Life Cycle.....	7
1.2.2.2 Sexual Life Cycle	8
1.3 RESISTANCE MECHANISMS.....	9
1.3.1 Pathogen Associated Molecular patterns (PAMP) and PAMP-triggered immunity (PTI)	11
1.3.2 Effector triggered susceptibility (ETS).....	13
1.3.3 Effector triggered immunity (ETI)	17
1.4 THE OOMYCETE RXLR EFFECTORS	21
1.5 HOST-OOMYCETE CO-EVOLUTION	25
1.6 THE ROLE OF UBIQUITINATION AND E3 LIGASES IN PLANT PCD AND DEFENCE	27
1.7 <i>P. infestans</i> EFFECTOR Avr3a AND A STRATEGY TO IDENTIFY MORE DURABLE RESISTANCE	31
1.8 AIMS AND OBJECTIVES	34
2 MATERIAL AND METHODS	36
2.1 PLASMID CONSTRUCTION	36
2.1.1 Amplification of <i>Avr3a</i> alleles and paralogs <i>Pex147-2/Pex147-3</i>	36
2.1.2 DNA purification.....	37

2.1.3	Cloning of PCR fragments into the destination vector pGRAB using Gateway® technology.....	38
2.2	BACTERIAL TRANSFORMATION	38
2.2.1	Preparation of electro-competent cells.....	38
2.2.2	Transformation of bacterial cell using electroporation	39
2.3	SCREENING FOR POSITIVE CLONES.....	40
2.3.1	PCR Screening.....	40
2.3.2	Plasmid purification	40
2.3.3	Spectrophotometric determination of DNA concentration and sequencing.....	40
2.4	AGROBACTERIUM INFILTRATIONS	40
2.4.1	Plant material and growth conditions	40
2.4.2	Preparation of <i>A. tumefaciens</i> for Agro-infiltration.....	41
2.4.3	Agro-Infiltration.....	41
2.4.4	Cell death assay.....	42
2.5	COMPLEMENTATION STUDY	42
2.5.1	Sporangia Preparation of CS12 for leaf inoculation.....	42
2.5.2	Agro-infiltration and Inoculation	43
2.5.3	Trypan-blue staining	43
2.6	YEAST-2-HYBRID	44
2.6.1	Construction of prey plasmid.....	44
2.6.2	Preparing competent yeast cells MaV203	44
2.6.3	Yeast Transformation.....	45
2.6.4	Characterization of protein/protein interactions and yeast transformations.....	45
2.7	DETERMINATION OF PROTEIN STABILITY	46
2.7.1	Protein extraction	46
2.7.2	Protein extraction from yeast	47
2.7.3	Western Blot Analysis	47
2.7.4	Confocal imaging to determine <i>in planta</i> CMPG1 stabilization.....	48
3	RECOGNITION OF Avr3a ALLELES AND THE PARALOGS PEX147-2/PEX147-3 BY THE POTATO RESISTANCE PROTEIN R3a.....	50
3.1	INTRODUCTION	50
3.2	AIM	54
3.3	RESULTS	54

3.3.1	Establishment of a transient expression system	54
3.3.2	Modelling of Avr3a alleles.....	60
3.3.3	Modelling of <i>Pj</i> _PEX147-2.....	62
3.3.4	Recognition of Avr3a alleles and paralogs PEX147-2/PEX147-3 by the resistance protein <i>R3a</i>	63
3.3.5	Inhibition study of R3a-dependent recognition by Avr3a alleles	69
3.4	DISCUSSION	70
4	SUPPRESSION STUDY OF CMPG1-MEDIATED CELL DEATH RESPONSES BY Avr3a ALLELES AND THE PARALOGS PEX147-2 and PEX147-3	79
4.1	INTRODUCTION	79
4.2	AIM	80
4.3	RESULTS	81
4.3.1	Suppression study of INF1 and CF-4/Avr4 mediated cell death by Avr3a alleles and paralogs	81
4.3.2	<i>In planta</i> stabilisation of CMPG1 by Avr3a alleles and paralogs	87
4.3.3	Identification of common virulence targets for Avr3a alleles and paralogs using yeast-2-hybrid assays.....	91
4.4	DISCUSSION	96
5	<i>IN PLANTA</i> COMPLEMENTATION STUDY.....	103
5.1	INTRODUCTION	103
5.2	AIM	106
5.3	RESULTS	106
5.4	DISCUSSION	111
6	GENERAL DISCUSSION AND FUTURE WORK	116
6.1	GENERAL DISCUSSION	116
6.2	FUTURE WORK.....	126
7	REFERENCES	130

LIST OF FIGURES

Figure 1.1: Late blight disease symptoms on potato foliage.....	4
Figure 1.2: The five eukaryotic supergroups according to Keeling <i>et al.</i> (2005).....	6
Figure 1.3: Evolutionary distance between oomycetes and other phylogenetic groups based on comparison of rRNA sequences..	6
Figure 1.4: The asexual and sexual disease cycles of <i>P. infestans</i> (Judelson <i>et al.</i> , 1997). ..	9
Figure 1.5: The Zig-Zag model illustrating plant inducible defences against pathogen attack and their amplitude of response.....	11
Figure 1.6: Various mechanisms of oomycete effectors are utilised to suppress plant immunity.....	14
Figure 1.7: CMPG1 dependant cell death induced by <i>P. infestans</i> PAMP, INF1 and <i>C. fulvum</i> effector Avr4, illustrated in the Zig-Zag model.....	30
Figure 1.8: Model of CMPG1-dependent PCDs following pathogen elicitor recognition at the inner or outer surface of the plasma membrane.....	31
Figure 1.9: Alignment of the amino acid haplotypes observed at the Avr3a locus in the Northern Andean region.....	33
Figure 3.1: Graphical representation of the distribution of Avr3a alleles sampled from the Toluca Valley.....	52
Figure 3.2: C-terminal <i>P. infestans</i> Avr3a sequences from 82 isolates collected in the Toluca Valley.....	53
Figure 3.3: (a) Hypersensitive response development in <i>N. benthamiana</i> leaves following co-infiltration and transient expression of <i>R3a</i> with <i>Avr3a</i> alleles and empty vector control in different vector backgrounds.....	56
Figure 3.4: Quantification of autofluorescence associated with PCD.....	58
Figure 3.5: Amino acid alignments between the C-terminal region of <i>P. capsici</i> Avr3a11 [position 70-132], <i>P. infestans</i> Avr3a, Avr3a paralogs and Avr3a variants	61
Figure 3.6: Amino acid changes in <i>P. infestans</i> Avr3a are superimposed onto the structure of <i>P. capsici</i> Avr3a11.....	62
Figure 3.7: Amino acid changes in PEX147-2 compared to Pi_Avr3a which is superimposed on the structure of PcAvr3a11.....	63
Figure 3.8: Recognition of Avr3a alleles and paralogs by R3a.....	65

Figure 3.9: Autofluorescence associated with cell death responses in <i>N. benthamiana</i>	66
Figure 3.10: Expression of N-terminal CFP tagged Avr3a alleles and paralogs in <i>N. benthamiana</i>	67
Figure 3.11: N-terminal fusions of the Avr3a alleles with CFP were used to demonstrate stability of the constructs <i>in planta</i>	68
Figure 3.12: Avr3a alleles and paralogs do not inhibit cell death responses elicited by co-infiltration of Avr3a ^{KI} and R3a in <i>N. benthamiana</i>	70
Figure 4.1: Effects of the co-expression of Avr3a alleles and paralogs on CMPG1-dependent cell death responses triggered by transient expression of INF1 in <i>N. benthamiana</i>	82
Figure 4.2: Effects of Avr3a alleles and paralogs on CMPG1-dependent cell death responses triggered by transient expression of CF-4/Avr4 in <i>N. benthamiana</i>	85
Figure 4.3: The ability of Avr3a alleles and paralogs to stabilise CMPG1 <i>in planta</i>	90
Figure 4.4: Yeast-two-hybrid based protein-protein interaction study involving 13 potential Avr3a host virulence targets and PEX147-2 and PEX147-3.....	92
Figure 4.5: Yeast-two-hybrid based protein-protein interaction study involving 13 potential Avr3a host virulence targets and Avr3a ^{KI} and Avr3a ^{EM} derived alleles.....	94
Figure 4.6: N-terminal fusions of the Avr3a alleles and paralogs with the DNA-binding domain were used to demonstrate stability of the constructs in yeast.....	95
Figure 5.1: Avr3a-silenced line CS12 has lost its ability to infect the plants.....	105
Figure 5.2: Complementation study of Avr3a ^{EM} silenced <i>P. infestans</i> line, CS12.....	108
Figure 5.3: Complementation study of Avr3a ^{EM} silenced <i>P. infestans</i> line, CS12.....	109
Figure 6.1: Activity of Avr3a ^{KI} and Avr3a ^{EM} (both in bold) together with their allelic variants (blue for Avr3a ^{KI} and red for AVR3 ^{EM} -derived alleles) and paralogs, PEX147-2 and PEX147-3.....	122

LIST OF TABLES

Table 1.1: Identified host-translocated effectors of oomycetes pathogens.....	17
Table 2.1: List of primers used to amplify <i>Avr3a</i> alleles and the paralogs <i>Pex147-2</i> and <i>Pex147-3</i>	37
Table 2.2: PCR protocol using GoTaq DNA polymerase.	37
Table 2.3: Plates used for yeast-two-hybrid transformations selection and protein/protein interactions.	45
Table 2.4: List of primary and secondary antibodies used in Western blots.	48
Table 3.1: <i>P. infestans</i> <i>Avr3a</i> haplotypes of 82 isolates collected from the Toluca Valley.....	52
Table 3.2: Statistical analysis of autofluorescence emitted from <i>A. tumefaciens</i> co-infiltration sites of <i>Avr3a^{KI}</i> and <i>Avr3a^{EM}</i> with <i>R3a</i> in different vector backgrounds.	59
Table 3.3: Amino acid changes in PEX147-2 compared to Pc_ <i>Avr3a</i> 11, Pi_ <i>Avr3a</i> and Pi_ <i>Pex147-3</i>	63
Table 4.1: Statistical analysis (Mann-Whitney U-test method) of INF1 cell death suppression activity of <i>Avr3a</i> alleles and paralogs.	83
Table 4.2: Statistical analysis (Mann-Whitney U-test method) of CF-4/ <i>Avr4</i> cell death suppression activity of <i>Avr3a</i> alleles and paralogs.	86
Table 4.3: Statistical analysis (t-Test) of the recorded levels of YFP fluorescence following co-expression of C-terminal fusions of CMPG1 to YFP (<i>StCMPG1b::YFP</i>) with <i>Avr3a</i> alleles and paralogs in <i>N. benthamiana</i>	90
Table 4.4: Summary of observed interactions of the <i>Avr3a</i> alleles and paralogs in Y2H, Western and Confocal imaging analysis.	96
Table 5.1: Statistical analysis (Mann-Whitney U-test method) of <i>Avr3a^{EM}</i> silenced <i>P. infestans</i> line, CS12, complementation study by the <i>Avr3a</i> alleles and paralogs.	110

ACKNOWLEDGMENTS

This thesis would not have been possible without the guidance and the help of several individuals who in one or another form contributed and extended their valuable assistance in the preparation and completion of this study. First and foremost, I would like to express my sincere gratitude to my supervisor, Dr. Ingo Hein for the continuous support of my Ph.D. study and research, for his patience, motivation, enthusiasm, and immense knowledge whilst allowing me the room to work in my own way. His guidance helped me during my research and writing of this thesis. I could not have imagined having a better supervisor and mentor for my Ph.D. study. One simply could not wish for a better or friendlier supervisor.

A big 'thank you' also goes to my co-supervisors, Prof. Paul Birch and Dr. Glenn Bryan for their patience and steadfast encouragement to complete this study. Thanks guys for taking the time to read, provide comments and help editing this thesis. And of course, I would like to extend my thanks to my sponsor, Malaysian Agricultural Research and Development Institute (MARDI), for paying the tuition fees and most appreciatively for providing money to bring along my family during my study period in Scotland. I am extremely grateful for this huge contribution by MARDI and the James Hutton Institute towards my career progression.

There are so many people who I need to thank for their help over the past few years. Thank you to all who had the patience to teach me new skills, techniques and for taken the time from their own busy days to help me. Without you I would not have achieved any of this. To my colleagues, Florian, Brian (both of you were always available to

discuss my problems), Gaetan (my little brother, many thanks for your help and I really appreciate it), members in the lab that I had been working in (Nicky, Kelly, Karen, etc.), the plant pathology group (Petra, Elli, Miles, Stefan, Eva, Tanya, Susan, Hazel) and all my friends throughout the institute, thank you for being there along the way, through the ups and downs, for making me laugh and generally being there to motivate, encourage and inspire. To the glasshouse team, who sowed, pricked out, watered and took care of my plants, what a great job, thank you! To the media kitchen for providing media on request and for all that they do. A special 'thank you' to Philip Smith for proof reading my thesis prior to submission.

To my wife Noraini, my son Azri and my daughters Athirah and Quratul'ain, thanks for your endless positivity, encouragement and love. You will never know how important it is to have your endless support. You are always there for me and I cannot thank you enough. For my wife, thank you for reminding me that there is a light at the end of the tunnel and my life will be much more relaxed from this moment onwards. And finally, for my late father, you have always been my inspiration throughout my study...

'Never, never, never give up'

Sir Winston Leonard Spencer Churchill

PUBLICATION ARISING FROM THIS WORK

Steve A. Whisson, Anna O. Avrova, Petra C. Boevink, Miles R. Armstrong, **Zulkifli A. Seman**, Ingo Hein, Paul R. J. Birch (2011) Exploiting Knowledge of Pathogen Effectors to Enhance Late Blight Resistance in Potato. **Potato Research**, 54, 325–340.

Zulkifli A. Seman, Petra C. Boevink, Miles R. Armstrong, David E. L. Cooke, Eleanor M. Gilroy, Paul R. J. Birch and Ingo Hein (in preparation) The costs to late blight disease of virulence on potato R3a.

ABSTRACT

Late Blight disease, caused by *Phytophthora infestans*, is the most significant threat to potato production world-wide. Identifying and deploying more durable host resistance to *P. infestans* is a promising way forward to sustain the production of potato. To achieve this goal, it is important to seek key pathogen components that are essential for infection and which, upon detection by the host, trigger a resistance response. One such potential key pathogen molecule is the RXLR-containing effector *Avr3a*. *Avr3a* is highly up-regulated during infection and is also required for *P. infestans* pathogenicity. To date, all *P. infestans* isolates studied contain *Avr3a* alleles $E^{80}M^{103}$ and/or $K^{80}I^{103}$. However, a study of *Avr3a* diversity in the Toluca Valley, Mexico, has identified additional alleles such as $K^{80}I^{103}L^{139}$, $K^{80}I^{103}H^{133}$, $E^{80}M^{103}H^{133}$ and $E^{80}M^{103}G^{124}$. Functional studies of these alleles were conducted as part of this thesis, which also include the *Avr3a* paralogs *Pex147-2* and *Pex147-3*.

By examining the amino acid changes in relation to the established protein structure, it was determined that all alterations within the *Avr3a* variants occur at surface exposed amino acids. The change R124G that leads to $Avr3a^{EMG}$ is located in the α -helix loop 3 and the changes Q133H and M139L ($Avr3a^{KI^H}$, $Avr3a^{EM^H}$ and $Avr3a^{KI^L}$) locate to α helix 4. Whereas amino acid substitutions in PEX147-3 only affect surface exposed residues, amino acid changes that occur in PEX147-2 involves a 'buried' amino acid that is key to structure and stability. Indeed, with the exception of PEX147-2, all *Avr3a* variants and PEX147-3 are stable upon transient expression *in planta* and in yeast cells.

In terms of host recognition, the protein products of the *Avr3a* alleles derived from $Avr3a^{KI}$ are recognised by the cognate host resistance gene product R3a whereas those

derived from *Avr3a^{EM}* evade recognition. Similarly, PEX147-3 is recognised by R3a but PEX147-2 is not. In addition to host recognition, virulence functions of these alleles and paralogs have been elucidated. INF1 and AVR4/CF-4 induced cell death responses, which are dependent on the host defence protein CMPG1, are suppressed by *Avr3a^{KI}*, *Avr3a^{KIH}*, *Avr3a^{KIL}*, *Avr3a^{EM}* and *Avr3a^{EMG}* but not by *Avr3a^{EMH}*. All *Avr3a* variants interact with and stabilise the host E3 ubiquitin ligase CMPG1 to various degrees *in planta* and this interaction was found to be weakest for *Avr3a^{EMH}*. Interestingly, PEX147-3, which did not interact with or stabilise CMPG1, could only suppress INF1 cell death but not CF-4/AVR4 elicited responses.

A *P. infestans* isolate, CS12, which was stably silenced for *Avr3a^{EM}* expression and subsequently shown to be compromised in virulence on the normally susceptible host *Nicotiana benthamiana*, was used for *in planta* complementation studies. As shown previously, upon transient expression *in planta* prior to infection with C12, *Avr3a^{KI}* and *Avr3a^{EM}* successfully restore pathogenicity. Similar levels of virulence re-establishment were only observed for *Avr3^{KI}* derived alleles *Avr3a^{KIH}* and *Avr3a^{KIL}* but not for alleles derived from *Avr3a^{EM}*. This study concludes that *Avr3a^{EM}* is currently the only form of the essential effector that is fully functional and evades recognition by the known resistance gene product R3a. This functionality is the likely reason that 70% of all studied isolates in the Toluca Valley are homozygous for *Avr3a^{EM}*. This form of the effector is therefore a suitable target for identifying more durable resistances.

ABBREVIATIONS

µg	Micrograms
µl	Microliters
Avr	Avirulence
Bp	Base pairs
CBEL	Cellulose binding elicitor lectin
CFP	Cyan fluorescence protein
CRN	Crinkler
DBD	DNA binding domain
DMSO	Dimethylsulphoxide
dpi	Days post-inoculation
E1	Ubiquitin-activating enzyme
E2	Ubiquitin-conjugating enzyme
E3	Ubiquitin ligase
ECPD	The European Cultivated Potato Database
EF-Tu	Elongation factor
elf18	Translation elongation factor Tu
EPIC, EPI	Extracellular protease inhibitor
ETI	Effector-triggered immunity
ETS	Effector-triggered susceptibility
flg22	Flagellin
FLS2, EFR	Plant receptor kinases
GP42	<i>Phytophthora infestans</i> transglutaminase
H	Haplotype
HECT	Homologous to the E6-AP Carboxyl Terminus
HR	Hypersensitive response
INF1	Elicitin infestans 1
Kb	Kilobase
kDa	Kilodaltons
LB	Luria-Bertani medium
LRR	Leucine rich repeats
ml	Millilitres
NBS	Nucleotide-binding site
OD	Optical density
PAMPs	Pathogen associated molecular patterns
PCD	Programmed cell death
PCR	Polymerase chain reaction
PEXEL	Plasmodium export elements
PI3P	Phosphatidylinositol-3-phosphate
PRR	Pattern recognition receptors
PTI	PAMP-triggered immunity
PUB	Plant U-box
<i>R</i> gene	Resistance gene
Rcr3, C14, Pip1	Cysteine proteases
RIN	RPM1-interacting protein
RING	Really Interesting New Gene
RLKs	Receptor-like kinases
RNA	Ribonucleic acid
ROS	Reactive oxygen species
Rpm	Revolutions per minute

SNPs	Single nucleotide polymorphisms
T3SS	Type-three secretion system
UPS	Ubiquitin proteasome system
UV	Ultra violet
YFP	Yellow fluorescent protein
GW	Gateway
TMV	Tobacco mosaic virus
<i>P</i>	Statistical probability value
Pi	<i>Phytophthora infestans</i>
Pc	<i>Phytophthora capsici</i>
<i>Ori</i>	Bacterial replication origin
ICD	INF1 cell death
Y2H	Yeast-2-hybrid
KIPI	Avr3a ^{KI} protein interactor
EMPI	Avr3a ^{EM} protein interactor

CHAPTER 1

1 LITERATURE REVIEW

1.1 POTATO

The cultivated potato, *Solanum tuberosum*, is a member of the *Solanaceae* or nightshade family that comprises, amongst other economically important plants, tomato (*Solanum lycopersicum*), pepper (*Capsicum*), aubergine (*Solanum melongena*) and tobacco (*Nicotiana tabacum*) (Hunziker, 2001). Potatoes have been grown for more than 8000 years in the Andean region of southern America but were introduced to Europe as late as 1570 by the Spanish and independently brought to the UK between 1588 and 1593 (Hawkes, 1990). Adaptation to long days alongside other breeding efforts led to the success of potato, which eventually became an important carbohydrate source and staple food throughout the world. Today, potato is the third most important food crop in the world after rice and wheat and the second most valuable crop in the UK after wheat (FAOSTAT). The European Cultivated Potato Database (ECPD) recorded 4,100 cultivated varieties in 2005 and the potato growing area is estimated to be as high as 20 million hectares worldwide, producing over 300 million tonnes of the crop (Haverkort *et al.*, 2009).

The direct progenitors of cultivated potatoes are Andean and Chilean primitive indigenous cultivated potatoes, also referred to as landraces, that in turn originate from wild relatives within the *S. brevicaulle* complex of the *Solanum* section *Petota* that comprises tuber bearing species only (Spooner *et al.*, 2005). More than 190 wild potato species of the *Solanum* section *Petota* have been identified in diverse habitats

within 16 countries of northern and southern America, albeit the majority have been observed in Argentina, Bolivia, Mexico and Peru (Hijmans & Spooner, 2001). The landraces and the wild relatives are grown in very diverse habitats ranging from high altitude Andean grasslands to dry Mexican forests, strand vegetation on Chilean beaches and cool rainforest in the Andes (reviewed in Hijmans *et al.*, 2002). The diversity of habitats exposes these plants to various abiotic and biotic stresses and it is therefore not surprising that wild potatoes and landraces play an important role in modern breeding programmes.

Potato has one of the richest genetic resources of any cultivated plant, making wild species a useful resource to breed new cultivars that are resistant to a wide range of pests and diseases, tolerant to frost and drought, and with other useful traits (Spooner & Hijmans, 2001). However, it is not easy to make use of these resources as potato has a complicated polyploid genome and many important qualitative and quantitative agronomic traits are poorly understood (Spooner & Hijmans, 2001). About 70% of the wild potato species are diploid at $2n=2x=24$, with the remaining species comprising polyploids, such as tetraploids ($2n=4x=48$) or hexaploids ($2n=6x=72$) (Spooner & Salas, 2006). Indeed, the majority of cultivated potatoes are tetraploid and are heterozygous outbreeders, which makes the analysis of their genetic traits more difficult (Bryan & Hein, 2008).

The whole sequence of the potato genome has been estimated to be about 844 Mb and approximately 39,000 genes have been annotated across the 12 chromosomes (Potato Genome Sequencing Consortium, 2011). Potato is susceptible to a wide range of pests and pathogens. Consequently, many research groups have put the

identification of genes conferring disease resistance as their major focus (Vleeshouwers *et al.*, 2011). The potato genome sequence has provided a platform to identify proteins that contain a nucleotide-binding site (NBS) and leucine-rich-repeat (LRR) domains. Most of the disease resistance genes cloned to date encode proteins containing these domains (Ballvora *et al.*, 2002; Huang *et al.*, 2005; Lokossou *et al.*, 2009). The potato genome contains at least 438 NBS-LRR-encoding genes and some of them are highly related homologues to potato late blight resistance genes *R1*, *RB* (*Rpi-blb1*), *R2*, *R3a*, *Rpi-blb2* and *Rpi-vnt1.1* (Jupe *et al.*, 2012). Interestingly, comparison between these *R* genes with well-established functional *R* genes indicates that 39.4% of these NBS-LRR genes are pseudogenes, including some of those within the *R1*, *R3a* and *Rpi-vnt1.1* clusters (The Potato Genome Sequencing Consortium, 2011). This high rate of gene pseudogenization ties-in with the rapid evolution of effector genes that has been observed in *Phytophthora infestans*, the potato late blight pathogen (Haas *et al.*, 2009).

1.2 LATE BLIGHT DISEASE

Late blight disease, caused by the oomycete *P. infestans*, is the most significant threat to potato production worldwide (Fry, 2008). Annually, late blight disease causes approximately £55 million losses to the UK potato industry and the costs associated with crop losses and chemical control amount to €5.2 billion globally per year (Garthwaite *et al.*, 2008; Birch & Whisson, 2001; Haverkort *et al.*, 2009). The most dramatic event caused by *P. infestans* was the Irish potato famine in 1845–1846 where up to one million people died of starvation and a similar number of people emigrated to the rest of Europe and the USA (Fry, 2008). The disease spreads optimally under cool and moist weather conditions and lesions occur on both leaves and stems. Within

3–7 days post infection (dpi), the symptoms appear first as brownish specks followed by development of water-soaked lesions on the leaf surface or stems. Finally, in the asexual life cycle, the infected areas are covered with white sporangiophores of *P. infestans* particularly on the underside of the leaf (Fry, 2008). Potato tubers are typically infected by spores that are washed through to the soil. The surface of infected tubers displays irregularly shaped, slightly depressed brown to purplish areas on the skin. The symptoms under the skin manifest themselves as a reddish brown, dry, granular rot which extends into the tuber (Kirk *et al.*, 2004).



Figure 1.1: Late blight disease symptoms on potato foliage

(Source; <http://www.apsnet.org/edcenter/intropp/lessons/fungi/oomycetes/Pages/LateBlight.aspx>)

1.2.1 *Phytophthora infestans*

P. infestans is derived from the oomycetes class Peronosporomycetidae. Some of the most destructive plant pathogens are from this class, including other *Phytophthora* species, downy mildews, *Pythium* species, *Albugo* and other white rusts (reviewed in Jiang & Tyler, 2012). Oomycetes are classified as Stramenopiles or Heterokonts together with the Alveolates to form the Chromalveolates, one of the five supergroups in the tree of eukaryotes (Keeling *et al.*, 2005). For a long time, oomycetes are grouped with true fungi and only in the last decade has it become clear that both of them have independently evolved; fungi belong to a separate group named the Unikonts (Figure

1.2). However, oomycetes and fungi share many common traits that are important for a phytopathogenic lifestyle (Meng *et al.*, 2009). The 'common' traits include spores for air dispersal, appressoria, haustoria, or other forms of specialized infection hyphae, effector proteins to be delivered into host cells, and expanded families of hydrolytic enzymes (review in Jiang & Tyler, 2012; Meng *et al.*, 2009). However, in terms of cell structures, oomycetes have a distinct chemical composition in their cell walls, mainly cellulose and β -glucans compared to chitin-based cell walls found in most fungal pathogens (Judelson, 1997). Oomycetes also produce wall-less, biflagellated swimming spores termed zoospores in the structure called sporangia (Judelson, 1997). In addition, comparisons of rRNA sequences reveal that oomycetes are more related to chrysophytes and golden-brown algae (Forster *et al.*, 1990; Peer & De Wachter, 1997) (Figure 1.3).

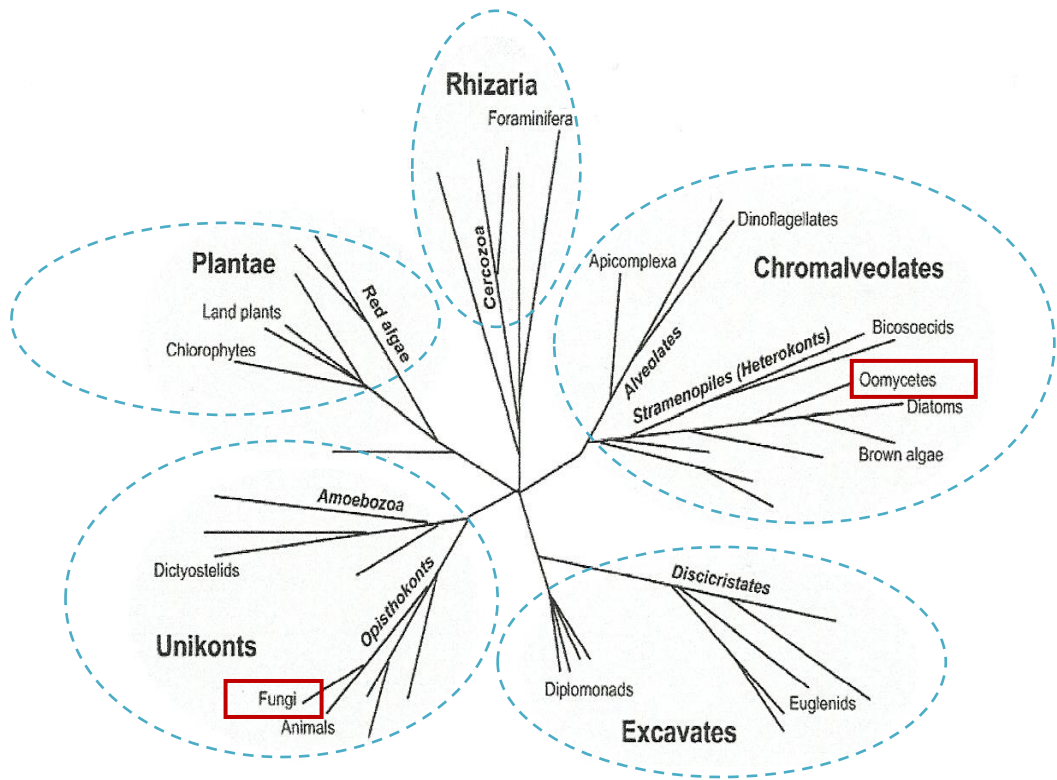


Figure 1.2: The five eukaryotic supergroups according to Keeling *et al.* (2005). Clearly shown (in red boxes) are the evolutionary distance between oomycetes and fungi. Taken from Govers & Gijzen (2006).

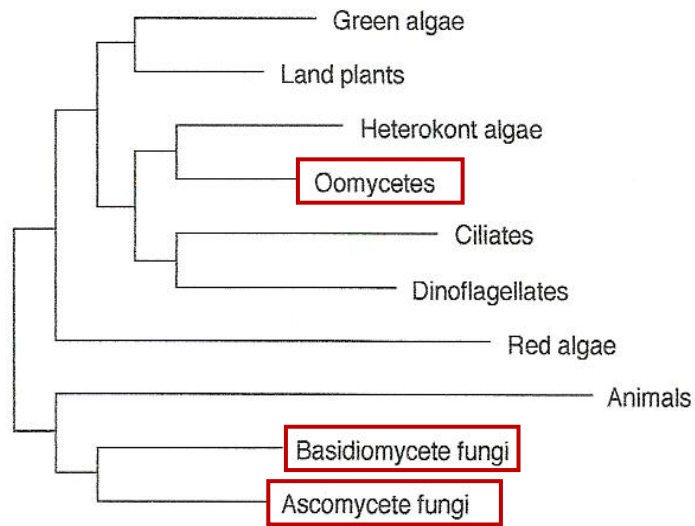


Figure 1.3: Evolutionary distance between oomycetes and other phylogenetic groups based on comparison of rRNA sequences. Adapted from Kamoun *et al.* (1999).

1.2.2 Life cycle of *P. infestans*

P. infestans, like many *Phytophthora* species, has a narrow host range and is considered a hemibiotrophic pathogen. It initiates infection biotrophically, with little direct damage of host tissue, and progresses to necrotrophic growth later once colonization has been established (Agrios & Beckerman, 2011; Fry, 2008). *P. infestans* takes approximately 2–3 dpi to complete the biotrophic stage (Fry, 2008). In its asexual form, the pathogen survives in the winter period either as mycelium on tubers in the soil, in potato waste piles or in stockrooms. In spring, infected shoots germinate from small portions of infected tubers and release the first airborne inoculum. The presence of free water greatly promotes spores to be dispersed to potato foliage where they can germinate and cause infection of the leaves.

1.2.2.1 Asexual Life Cycle

Asexual reproduction is manifested by sporangia, spores dispersed from sporangiophores (Figure 1.4). Sporangioophores are typically formed on the lower leaf surface and infected stems when relative humidity is < 90 %, in which sporulation can be initiated within an optimum temperature range of about 18–22 °C (Judelson *et al.*, 1997). In the presence of water and at cooler temperatures (around 10°C), sporangia germinate indirectly by undergoing cytoplasmic cleavage to form seven to eight swimming zoospores (Singh, 2010). After a mobile period, the zoospores will stop moving and a thick cell wall is then formed to create cysts. When the temperature is higher than 16°C, the cysts will start to germinate and penetrate the plant. Alternatively, sporangia can germinate directly and function as a single spore by producing a germ tube (Judelson *et al.*, 1997). An appressorium structure that forms on the tip of the germtube, either for germination cysts or sporangiospores, will

facilitate its ability to breach the plant cuticle and cell wall. To pass through the epidermis, hyphae grow mainly between the mesophyll of invading cells and form haustoria in the biotrophic stage (Haldar *et al.*, 2006). The necrotrophic phase of infection commences after approximately 3–4 dpi, in which the pathogen proceeds to kill the host plant tissue. In this stage, the hyphae emerge through the stomata carrying developed sporangia to start a new cycle of infection.

1.2.2.2 Sexual Life Cycle

Sexual reproduction of *P. infestans*, which is heterothallic (the male and female organs are on different individuals), requires the presence of two mating types termed A1 and A2, and potentially leads to extensive genetic recombination to create new populations (Figure 1.4). For sexual production to occur in nature, both A1 and A2 mating types have to infect the same plant or tuber. The two mating types differ in hormone production and response rather than in morphology of the different sexual forms. In response to hormones, the two mating types form male (antheridia) and female (oogonia) structures where meiosis occurs and asexual sporulation is inhibited (Judelson *et al.*, 1997). Individual haploid nuclei from both antheridia and oogonia will fuse to form gametangia in order to generate a diploid cell with a viable nucleus. In the progeny of hybrid gametangia (A1A2), only A1 or A2 types will develop from the germinated oospore (Judelson *et al.*, 1997). Oospores can survive several years in the soil (Flier *et al.*, 2001b) and under favourable conditions, can germinate to form sporangia to start the infection of tubers, stems and leaves. Additionally, infected tubers can facilitate oospore germination for the next season, as infected tubers are the most common source of inoculum at the beginning of the season.

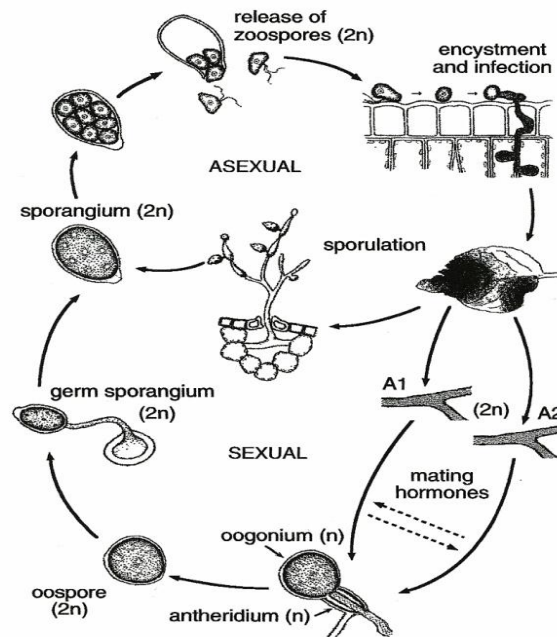


Figure 1.4: The asexual and sexual disease cycles of *P. infestans* (Judelson *et al.*, 1997).

1.3 RESISTANCE MECHANISMS

Plants must continually fight and prevent infection by the many pathogens they encounter. Unlike animals, which possess an adaptive immune system, plants rely on the innate immunity of each cell to recognise invading pathogens and also to respond to the systemic signals emanating from infection sites (Dangl & Jones, 2001; Ausubel, 2005). However, in addition to the inducible defences, plants also utilise preformed barriers and, for example, toxic compounds such as phytoanticipins to prevent infection (Lamothe *et al.*, 2009).

Successful pathogens must avoid, suppress, or tolerate plant defences to establish an interaction with the host for their benefit (Torto-Alalibo *et al.*, 2010). Thus, both prokaryotic and eukaryotic pathogens have evolved numerous strategies to gain nutrients from plants whilst suppressing defence mechanisms. Biotrophic and hemibiotrophic pathogens, including specialised fungi and oomycetes, require living

plants cells as their main source to retrieve nutrients (Hahn & Mendgen, 2001). These pathogens are dependent on their host to complete their life cycle. To gain access inside plant tissues, pathogens often use natural openings, such as stomata and wounds, to avoid specialised plant barriers such as leaf cuticles (Huckelhoven, 2007).

The next barrier for the pathogen to overcome is the apoplastic space, a very acidic area with a pH of about 3.2 which contains plant-secreted degrading defence enzymes and antimicrobial compounds (Huckelhoven, 2007). Plant cells are surrounded by a stable cell wall that cannot be easily penetrated by most microbes and therefore, some well adapted microbes are confined to the apoplastic space for proliferation (Gohre & Robatzek, 2008). To gain an intimate contact with plant cells, in order to suppress plant responses, some filamentous plant pathogens form specialised structures such as haustoria that are derived from penetrating hyphae (Catanzariti *et al.*, 2007) or, in case of bacteria, a specialised type-three secretion system (T3SS) that penetrates the host cell wall to inject effector molecules into the host cytoplasm (Jin *et al.*, 2003).

Efficient plant disease resistance is associated with inducible plant defences that consist of two overlapping components induced by microbial molecules (Thomma *et al.*, 2011; Jones & Dangl, 2006). These two evolutionarily linked forms of innate immunity have been illustrated by a Zig-Zag model (Figure 1.5) (Jones & Dangl, 2006; Hein *et al.*, 2009). In this model, the first layer of plant protection involves detection of pathogen associated molecular patterns (PAMPs) to induce PAMP-triggered immunity (PTI) in order to stop further pathogen invasion. However, well adapted pathogens promote virulence by delivering effector molecules that are able to interfere with PTI, resulting in effector-triggered susceptibility (ETS). To overcome ETS, plants have developed a second layer of protection that involves resistance (*R*) genes that

perceive, directly or indirectly, the pathogen effectors, which are then also referred to as avirulence (Avr) proteins and the consequent resistance response is known as effector-triggered immunity (ETI). However, adapted pathogens may be able to modify the recognised effectors to evade detection or to deliver additional effector molecules to suppress ETI, to re-establish ETS. In plant–pathogen co-evolution, the next step involves evolution of new *R* genes that recognize these effectors in order to regain ETI (Hein *et al.*, 2009).

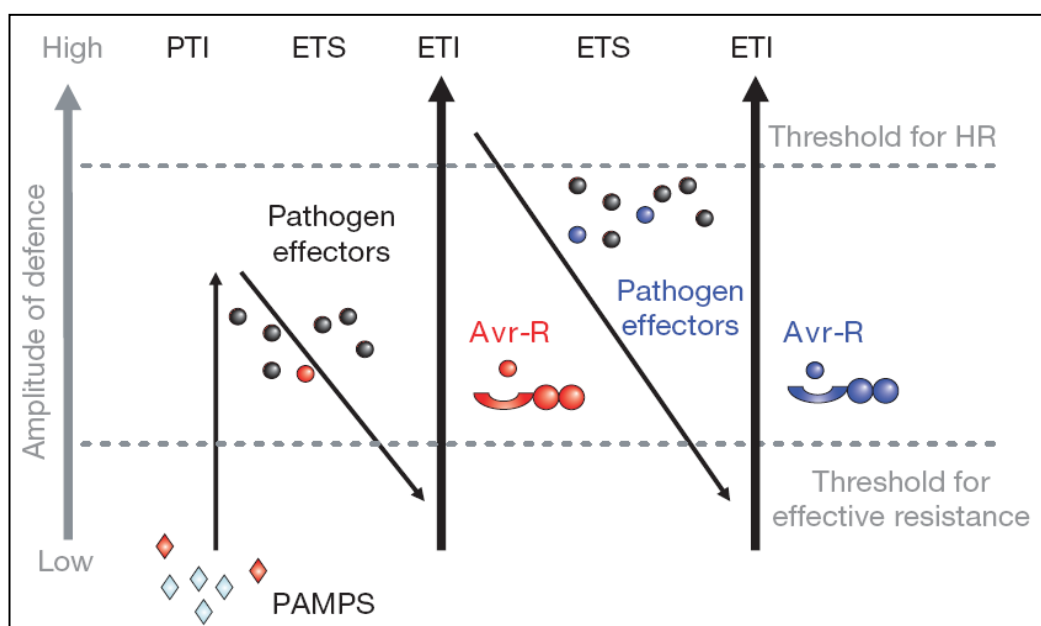


Figure 1.5: The Zig-Zag model illustrating plant inducible defences against pathogen attack and their amplitude of response. Pathogen associated molecular patterns (PAMPs) are recognised by host pattern recognising receptors (PRR) on the plasma membrane and subsequently activate PAMP triggered immunity (PTI). Effectors are secreted by the pathogen to suppress PTI resulting in effector-triggered susceptibility (ETS). In the second layer of inducible defences termed effector triggered immunity (ETI), plant resistance (*R*) gene products recognise translocated effectors and initiate an immune response that is also called the hypersensitive response (HR), a form of programmed cell death. To evade the host ETI response, pathogens deliver modified effectors which force the plant to evolve new *R* genes (taken from Jones & Dangl, 2006).

1.3.1 Pathogen Associated Molecular patterns (PAMP) and PAMP-triggered immunity (PTI)

Pathogen-associated molecular patterns (PAMPs) are commonly occurring microbial molecules, which trigger defences known as PAMP triggered immunity (PTI) in plants.

PTI is the first level of inducible plant defence which is activated upon perception of microbial PAMPs via cell surface receptor-like kinases (RLKs) (Nicaise *et al.*, 2009; Jones & Dangl, 2006). Pattern recognition receptors (PRR) or RLKs perceive molecular signatures characteristic of a whole class of microbes or PAMPs to trigger PTI (Schwessinger & Zipfel, 2008). Recently, *N. benthamiana* leucine-rich repeat receptor-like kinase (LRR-RLK) NbSERK3 has been shown to significantly contribute to resistance, triggered by the *P. infestans* PAMP elicitor protein INF1 (Chaparro-Garcia *et al.*, 2011). PAMPs are essential molecular components that are found to be highly conserved within a class of microbes where they carry out indispensable functions for fitness or survival and are not present in the hosts (Medzhitov & Janeway, 1997).

In the majority of cases, PTI is able to stop pathogen growth at an early infection stage by the induction of antimicrobial enzymes and peptides, antimicrobial chemicals [for example phytoalexins and reactive oxygen species (ROS)], deposition of callose and lignification to reinforce the cell wall at sites of infection and, in case of biotrophic and hemibiotrophic pathogens, programmed cell death (PCD) (Jones & Dangl, 2006). Flagellin (epitope flg22) and translation elongation factor Tu (epitope elf18) are the best-characterized bacterial PAMPs which are recognised by the plant receptor kinases Flagellin Sensing2 (FLS2) and EF-TU Receptor (EFR), respectively (Robatzek & Saijo, 2008). The protein flagellin is the building block of the flagellum and its recognition by most plants indicates this recognition event is evolutionarily ancient (Boller & Felix, 2009). The elongation factor Tu (EF-Tu) is one of the most abundant and conserved bacterial proteins and acts as an essential bacterial PAMP, detected by the receptor EFR in *Arabidopsis* and other members of the *Brassicaceae* family (Kunze *et al.*, 2004). Interestingly, expression of EFR in solanaceous plants, *Nicotiana benthamiana* and

tomato is also can give responsiveness to bacterial elongation factor Tu (EF-Tu), making them more resistant to a range of phytopathogenic bacteria (Lacombe, 2010). Many oomycete PAMPs and secreted elicitors are proteins, and resemble enzymes or protein toxins (Gijzen & Nurnberger, 2006). In addition to proteinaceous PAMPs and elicitors, surface-exposed oomycete glucans also trigger defences in host plants (Sharp *et al.*, 1984). Typical oomycete PAMPs include, for example, INF1, the transglutaminase GP42 (epitope pep13) and cellulose-binding elicitor lectin (CBEL) family members (Hein *et al.*, 2009).

1.3.2 Effector triggered susceptibility (ETS)

Most plant pathogens have developed sophisticated molecular strategies by evolving protein or chemical effectors to suppress or reprogramme PTI and ETI. Diverse effector molecules that are delivered into plant cells can suppress PTI and/or ETI, resulting in effector-triggered susceptibility (ETS) (Chen *et al.*, 2012; Halterman *et al.*, 2010; Torto-Alalibo *et al.*, 2009; Chisholm *et al.*, 2006; Jones & Dangl, 2006). Jiang & Tyler (2012) reviewed some of the various activities of oomycetes effectors in suppressing plant immunity (Figure 1.6).

Apoplasmic effectors secreted into the plant extracellular space play an important role in manipulating host counter-defence. Their mode of action can be diverse and include, for example, inhibition and protection against plant host hydrolytic enzymes such as proteases, glucanases and chitinases that accumulate in response to pathogen infection (Tian *et al.*, 2006; Kamoun, 2006). Examples of apoplasmic effector proteins are AVR2, AVR4, AVR9 and ECP2 from *Cladosporium fulvum* (Thomma *et al.*, 2005). Interestingly, *C. fulvum* does not form haustoria or haustoria-like structures that are

associated with effector translocation into the host cytoplasm (Rivas & Thomas, 2005). However, oomycetes such as *P. infestans* secrete both apoplastic and cytoplasmic effectors (Birch *et al.*, 2006; Kamoun, 2006). Examples of *P. infestans* apoplastic effectors are cysteine protease inhibitors, such as EPIC1 (member of Kazal-like protease inhibitor family) and EPIC2b (member of cystatin family) that can bind to cysteine proteases C14, PIP1 and RCR3 (Song *et al.*, 2009; Tian *et al.*, 2007).

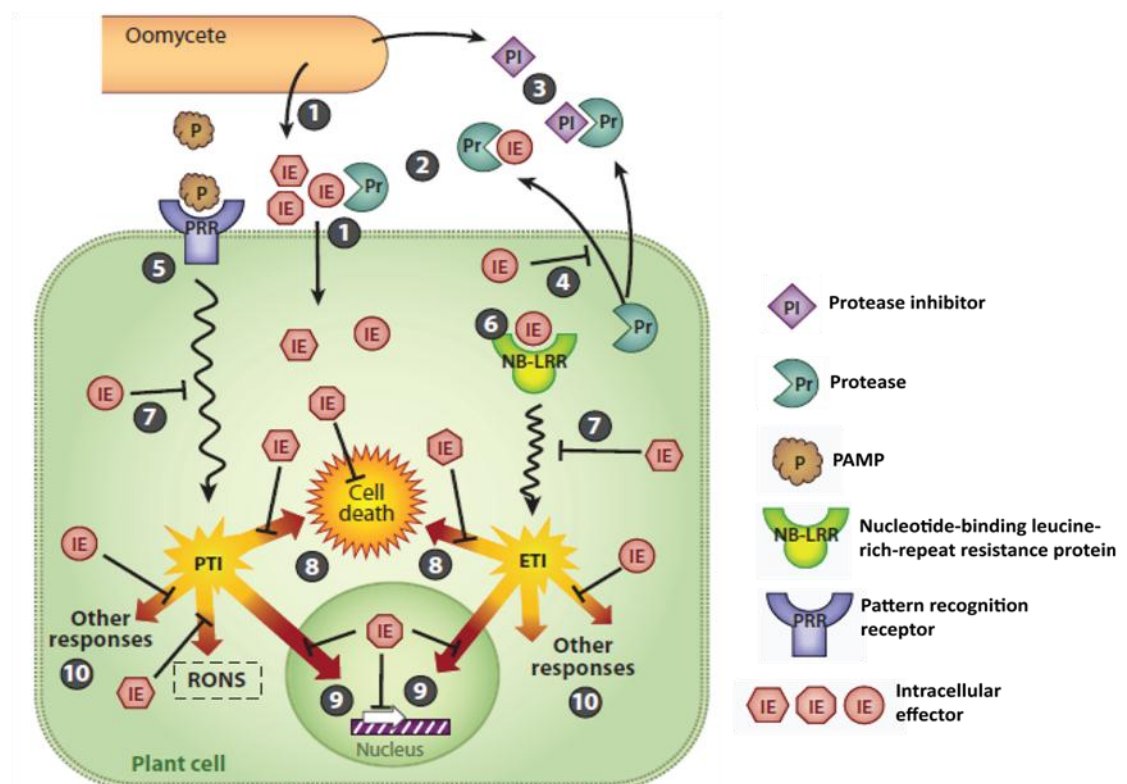


Figure 1.6: Various mechanisms of oomycete effectors are utilised to suppress plant immunity. Translocation of effectors (IEs) into the host cytoplasm (1) induces host proteases (Pr) to be secreted (2) into the apoplast to degrade them. To elude these proteases, the pathogen (3) may secrete protease inhibitors (PIs) or produce effectors to block secretion of host proteases (4). Recognition of PAMPs by PRRs (5) and intracellular effectors by NB-LRRs (6) induces PTI and ETI, respectively which is potentially inhibited by intracellular effectors (7). Induction of PTI and ETI may trigger programmed cell death (8) that can potentially be inhibited by effectors. Both PTI and ETI invoke transcriptional changes (9) which might be directly interfered with by nuclear-targeted effectors. Numerous other responses (10) are also involved in PTI or ETI signalling pathways such as production of reactive oxygen and nitrogen species (RONS) that may also to be interfered with by the effectors (modified from Jiang & Tyler, 2012).

In addition, Song *et al.* (2009) have shown that susceptibility of tomato plants to *P. infestans* was increased by mutation of the tomato *Rcr3* gene or silencing of C14. Thus,

the study has demonstrated the crucial role of cysteine protease inhibitors that are required for biotrophic fungi such as *C. fulvum* and *P. infestans* to infect the host (Song *et al.*, 2009). Furthermore, serine protease inhibitor EPI1 and EPI10 in *P. infestans* can bind to and inhibit a tomato protease P69B to abolish its activity in the apoplast (Tian *et al.*, 2004; 2005). Moreover, *Phytophthora* spp. are also known to secrete glucanase inhibitors that inhibit the host apoplastic enzyme endo- β -1,3 glucanase (Damasceno *et al.*, 2008; Rose *et al.*, 2002).

RXLR effectors include the products of avirulence genes and are initially translocated into the plant cytoplasm and target different subcellular compartments including nuclei, nucleolus, chloroplast, and Golgi (reviewed in Bozkurt *et al.*, 2011; Boevink *et al.*, 2011; Schornack *et al.*, 2010). This ties in with the identification of RXLR effectors by *R* genes that encode intracellular NBS-LRR proteins (Foster *et al.*, 2009; Goritschnig *et al.*, 2012; Huang *et al.*, 2005; Li *et al.*, 2011; Lokossou *et al.*, 2009). Pathogens use different means to deliver the effectors into the host cytoplasm and rely often on specialised structures. For example, Gram-negative bacteria use the type three secretion system (T3SS), a specialized secretion system, to deliver effector proteins inside host cells (Galan & Wolf-Watz, 2006; McCann & Guttman, 2008). In contrast, biotrophic fungi and oomycetes have evolved specialized structures termed haustoria (Meng *et al.*, 2009; Catanzariti *et al.*, 2007). The primary function of haustoria was initially thought to be nutrient uptake but, based on more recent findings, haustoria also take part in translocation of fungal and oomycete effectors (Whisson *et al.*, 2007; Catanzariti *et al.*, 2006). Thus, significant differentiation may occur between the haustorial cell wall, extrahaustorial space, and extrahaustorial membrane to facilitate

delivery of effectors from the pathogen and nutrients uptake from host plants (Meng *et al.*, 2009).

Subversion of PTI by microbial effectors is believed to be one of the key strategies of successful pathogens to grow and multiply in host plants (reviewed in Stassen & Van den Ackerveken, 2011; Hein *et al.*, 2009). The molecular mechanisms by which translocated effectors manipulate the plant defence or promote virulence are still largely unknown but on-going characterisation of individual effectors has shown that multiple processes are targeted, either as suppressors or as inducers of defence (Table 1.1) (Figure 1.6).

Most of the effector activity identified thus far is to suppress programmed cell death (PCD), which is associated with resistance towards biotrophic and hemibiotrophic pathogens (Stassen & Van den Ackerveken, 2011; Dangl & Jones, 2006) (Table 1.1). Conserved C-terminal W and Y motifs have been determined to be required for this activity (Dou *et al.*, 2008). As these motifs are present in many *Phytophthora* RXLR effectors, suppression of cell death activity has been suggested as a major function of oomycete effectors (Stassen & Van den Ackerveken, 2011). Indeed, potential effectors have been identified via cell death suppression assay by many research groups. Oh *et al.* (2009) for instance, revealed that the effector activity of PexRD8 and PexRD36₄₅₋₁ is sufficient to suppress cell death induced by INF1.

Another interesting function of RXLR effectors in suppressing ETI has been reported for the effector IPI-04, a sequence divergent member of the *P. infestans* IPI-O family (Halterman *et al.*, 2010; Chen *et al.*, 2012). IPI-04 is able to suppress ETI induced by the

effectors IPI-O1 and IPI-O2 in potato plants carrying the resistance gene *Rpi-blb1* (Halterman *et al.*, 2010).

Table 1.1: Identified host-translocated effectors of oomycetes pathogens. Their function, mechanism and host targets are shown where known. The table shows effectors identified thus far that contribute to virulence by interfering with plant immunity (Reviewed in Stassen & Van den Ackerveken, 2011).

Effector	Species	Class	ETI	Mechanisms	Host Target
AeCRN5	Ae	CRN		Cell death (via nucleus)	
ATR1	Ha	RXLR	AtRPP1	Contributes to virulence	
ATR5	Ha	?	AtRPP5		
ATR13	Ha	RXLR	AtRPP13	Suppresses callose deposition and ROS secretion	
AVR1	Pi	RXLR	R1		
AVR2	Pi	RXLR	R2		
Avr3a	Pi	RXLR	R3a	Stabilises host E3-ligase	CMPG1
AVR3b/10/11	Pi	RXLR	R3b/R10/R11		
AVR4	Pi	RXLR	R4		
AVRBlb2	Pi	RXLR	Rpi-Blb2	Interferes with protease secretion	
IPI-01	Pi	RXLR	Rpi-Blb1/Rpi-Sto1/Rpi-Pta1	Disruption PM-CW integrity	LecRK-1.9
IPI-02	Pi	RXLR	Rpi-Blb1/Rpi-Sto1/Rpi-Pta1		
IPI-04	Pi	RXLR		Suppresses IPI-01/IPI-02 ETI	
PexRD36₄₅₋₁	Pi	RXLR		Suppresses INF1 PTI	
PexRD8	Pi	RXLR		Suppresses INF1 PTI	
SNE1	Pi	RXLR?		Suppresses Avr3a ETI and NLP-induced cell death	
Various CRNs (e.g. CRN 1,2,8,16)	Pi	CRN		Cell death (via nucleus)	
AVR1a	Ps	RXLR	Rps1a		
AVR1b-1	Ps	RXLR	Rps1b	Suppresses BAX-induced cell death	
AVR1k	Ps	RXLR	Rps1k		
Avr3a	Ps	RXLR	Rps3a		
AVR3c	Ps	RXLR	Rps3k		
AVR4/6	Ps	RXLR	Rps4/Rps6		
PsCRN115	Ps	CRN		Suppresses PsCRN63/NLP-induced Cell death	
PsCRN63	Ps	CRN		Cell death (via nucleus)	

Class: CRN; Crinkler effector, **RXLR**; RXLR-motif effector, **RXLR?**; RXLR-like motif effector. **ETI:** corresponding *in planta* R gene. **Species (Sp.):** **Ae;** *Aphanomyces euteiches*, **Ha;** *Hyaloperonospora arabidopsidis*, **Pi;** *P. infestans*, **Ps;** *Phytophthora sojae*.

1.3.3 Effector triggered immunity (ETI)

The largest family of R genes identified to date encode nucleotide binding leucine-rich repeat (NB-LRR) proteins which act as immune receptors to mediate recognition of

pathogen-derived AVR effectors or their activity (Eitas & Dangl, 2010; Elmore *et al.*, 2011). Effectors, whilst being delivered by the pathogen to suppress PTI or promote virulence, also provide plants with an opportunity for detection via *R* gene products that mount a rapid and intense response termed effector triggered immunity (ETI). ETI typically culminates in a form of programmed cell death known as the hypersensitive response (Katagiri, 2004). Genes encoding pathogen effectors that induce *R* gene resistances are defined as avirulence (*Avr*) genes and interactions between effectors and their cognate *R* proteins are based on the gene-for-gene hypothesis (Gassmann & Bhattacharjee, 2012; Flor, 1971).

Interaction between avirulence effector molecules and their cognate *R* proteins can be either direct or indirect, the latter through modification of a host protein by the effector that is perceived by the *R* protein (Chisholm *et al.*, 2006; Jones & Dangl, 2006; van der Hoorn & Kamoun, 2008; Elmore *et al.*, 2011). Direct interaction between an *R* protein and its matching *Avr* protein has relatively rarely been observed (Dodds *et al.*, 2006; Ellis *et al.*, 2007a). However, a few examples of direct interaction between NB-LRR and effector have been confirmed in filamentous pathogens (Jia *et al.*, 2000; Dodds *et al.*, 2006; Krasileva *et al.*, 2010). *ATR1*, an effector from *Hyaloperonospora arabidopsidis*, is recognized by *Arabidopsis thaliana* *RPP1* via direct interaction with its LRR domain (Krasileva *et al.*, 2010). More recently, Chen *et al.* (2012) have shown evidence of direct interaction between *P. infestans* effector IPI-O (*AVRblb1*) and the coiled-coil domain of *RB* (*Rpi-blb1*).

The observation that effectors have specific targets in the host is an essential component of the Guard hypothesis, which explains an indirect perception mechanism

of R proteins by monitoring (guarding) the effector target (Van der Hoorn & Kamoun, 2008). Modification of effector targets by the effector are perceived by the R protein, which subsequently triggers a resistance response in the host (Van der Biezen & Jones, 1998; Dangl & Jones, 2001). Bacterial effectors are often recognized indirectly by the resistance protein via perception of modified host protein (Elmore *et al.*, 2011). A good example for the Guard model is the indirect perception of the *Pseudomonas syringae* effector AvrPTO by the tomato resistance proteins PTO and PRF (Zipfel & Rathjen, 2008). In addition, recognition of AvrB and AvrRPM1 by *Arabidopsis* NB-LRR protein RPM1 is also indirect by perception of modified host target protein RIN4 (Liu *et al.*, 2011). The Guard model also explains how multiple effectors secreted by the pathogen could be perceived by a single R protein, thus enabling a relatively small *R* gene repertoire to target the broad diversity of pathogen effectors (Dangl & Jones, 2001). However, in the absence of the cognate R protein, the alteration of effector targets (guardees) is indispensable for the virulence function (Rooney *et al.*, 2005; Hauck *et al.*, 2003).

Another example of indirect recognition involves the AvrBS3 effector protein from *Xanthomonas campestris*, which localises in the nucleus and binds to the promoter of the cognate *BS3* resistance gene product. This leads to *Bs3* transcript accumulation followed by HR induction (Römer *et al.*, 2007). Recently, based on this and additional findings, a modification of the Guard model was proposed by Van der Hoorn & Kamoun (2008), known as the Decoy model. This model takes into account the evolutionary aspects of the opposing selection forces on guarded virulence targets (Van der Hoorn & Kamoun, 2008). According to the model, the virulence target should maintain its guardee function if a guarding *R* gene is present to trigger ETI, whilst in the

absence of a corresponding *R* gene, the effector target should diversify to evade manipulation by the effector protein (Van der Hoorn & Kamoun, 2008).

Nonetheless, how these two models can be applied to the perception of filamentous pathogen AVR effectors by NB-LRR receptors is still unknown. Thus, it is important to uncover the host targets of filamentous pathogen effectors. Potato BSL1 has been identified recently to be a target of *P. infestans* AVR2. BSL1 mediates the indirect recognition of AVR2 by R2, supporting either the Guard or Decoy models (Saunders *et al.*, 2012).

As pathogens rely on effectors to infect host plants, *R* genes provide an excellent opportunity to protect plants by effector recognition mechanisms. Indeed, *R* genes from wild sources were exploited in early potato breeding programmes by focussing on the characterisation of the resistance spectrum and the introgression of 11 *R* genes from the wild Mexican hexaploid species *Solanum demissum* (Malcolmson & Black, 1966). Thus far, more than 20 functional late blight *R* genes have been cloned, which include *R1*, *R2*, *R3a*, and *R3b* from *Solanum demissum* (Ballvora *et al.*, 2002; Huang *et al.*, 2005; Lokossou *et al.*, 2009; Li *et al.*, 2011). Resistance genes have also successfully been isolated from other wild *Solanum* species such as *S. bulbocastanum* (Song *et al.*, 2003; van der Vossen *et al.*, 2003, 2005), *S. stoloniferum* and *S. papita*, (Vleeshouwers *et al.*, 2008), *S. venturii* and *S. mochiquense* (Pel *et al.*, 2009; Foster *et al.*, 2009). All of these cloned resistance genes belong to the coiled-coil (CC)-NB-LRR class.

Regardless of the generated cultivars containing these genes, rapidly changing populations of *P. infestans* have overcome the *R1-R11* genes (Malcolmson & Black,

1966). Indeed, *P. infestans* is a pathogen with high 'evolutionary potential' (McDonald & Linde, 2002) and changes in the *P. infestans* populations via migration and mutation are well documented (Fry & Goodwin, 1997). The *P. infestans* population that dominated Europe from 1845 to the mid-1970s contained only the A1 mating type but this was displaced when new lineages of both the A1 and A2 mating types were found in the 1970s (Drenth *et al.*, 1994). Such changes were probably driven by increases in aggressiveness, fitness and virulence against host resistance as well as resistance to fungicides (Cooke *et al.*, 2012). To enhance resistance durability against late blight resistance, stacking of multiple *R* genes has been shown to be a potential approach to strongly delay the onset of late blight symptoms (Kim *et al.*, 2012; Tan *et al.*, 2010). Sarpo Mira is one of the good examples of potato cultivars with significant levels of durable resistance to late blight disease and has recently been shown to contain at least five *R* genes (Rietman *et al.*, 2012).

Recent interest has focussed on transforming cloned *R* genes into existing potato varieties (Haverkort *et al.*, 2009). Thus, current *R* gene isolation and breeding efforts aim to combine at least two different broad spectrum *R* genes (Song *et al.*, 2003; van der Vossen *et al.*, 2005). Zhu *et al.* (2011) and Forch *et al.* (2010) have recently shown that transformation of multiple *R* genes into susceptible varieties can be used to add value to these varieties.

1.4 THE OOMYCETE RXLR EFFECTORS

Recently, a lot of attention has focused on oomycete RXLR effectors, one of the best-studied classes of virulence proteins (Kale & Tyler, 2011; Whisson *et al.*, 2011; Tyler, 2009; Hogenhout *et al.*, 2009). This class of effectors is the largest that has been

discovered from the available whole genome sequences of *Phytophthora* species (Grunwald, 2012) (Table 1.1). Oomycete RXLR containing effectors are typically modular proteins with an N-terminal domain associated with secretion and translocation into plant cells and a C-terminal domain linked to virulence function (Kamoun, 2006; Bos *et al.*, 2006). The RXLR motif was found to be conserved in divergent oomycete avirulence proteins (Rehmany *et al.*, 2005) and was used in bioinformatic screens to search for candidate effector genes from three *Phytophthora* genomes (Tyler *et al.*, 2006; Haas *et al.*, 2009; Oh *et al.*, 2009). C-terminal domains of RXLR containing effectors are distinct from each other whereas the N-terminal domains display more common features such as an acidic region (dEER) that often follows the RXLR motif (Jiang *et al.*, 2008; Whisson *et al.*, 2007).

The RXLR-EER motif has shown to be required for translocation of effector protein into the host (Duo *et al.*, 2008; Whisson *et al.*, 2007). However, the mechanisms of how this motif contributes to translocation of RXLR effectors remain unclear and under debate (Ellis & Dodds, 2011). A study of *P. sojae* effector AVR1b has shown a possible mechanism involving the RXLR domain binding to cell-surface phosphatidylinositol-3-phosphate (PI3P), potentially to stimulate endocytosis of the effector into the host (Plett *et al.*, 2011; Kale *et al.*, 2010). The RXLR-like motif, PEXEL/HL of the Malaria parasite *Plasmodium falciparum* has also been shown to be required to mediate PI3P binding for effector translocation into the host erythrocyte (Bhattacharjee *et al.*, 2012). However, Yaeno *et al.* (2011) have shown that the RXLR motifs of Avr3a and AVR1b do not interact with PIPs. Wawra *et al.* (2012a) has recently confirmed that Avr3a does not specifically bind to phospholipids to translocate into host cells. Interestingly, interactions with PIPs have shown to be mediated by surface patches of

positively charged amino acids located on equivalent locations in the C-terminal domain of each effector (Yaeno *et al.*, 2011). Recently, another potential cell surface protein with tyrosine-*O*-sulphate modification has been shown to be crucial for an effector of the oomycete fish pathogen *Saprolegnia parasitica*, SpHtp1, to translocate into host cells (Wawra *et al.*, 2012b).

RXLR effector genes display signatures of positive selection that may contribute to rapid evolution, presumably a consequence of their co-evolutionary arms race with plants (Win *et al.*, 2007; Oh *et al.*, 2009). The molecular mechanism underlying these evolutionary events to generate the effectors with new virulence functions and/or to evade the immune system is poorly understood. However, recently reported three-dimensional structures of RXLR effectors from *Phytophthora* have provided resource to investigate structure/function relationships in the C-terminal region between these effectors that provide information about their accelerated evolution.

To date, five structures of oomycete RXLR effector have been published: Avr3a4 and Avr3a11 from *Phytophthora capsici* (Yaeno *et al.*, 2011; Boutemy *et al.*, 2011), PexRD2 from *P. infestans* (Boutemy *et al.*, 2011) and ATR1 and ATR13 from *H. arabidopsidis* (Chou *et al.*, 2011; Leonelli *et al.*, 2011). Studies of PexRD2 and ATR1 structures have yielded the a striking finding that both share a conserved alpha-helical protein fold defined as W and Y motifs, regardless of the fact that *Phytophthora* and *H. arabidopsidis* effectors do not share any significant sequence similarity (Win *et al.*, 2012; Boutemy *et al.*, 2011). Based on structure-informed bioinformatic analyses of PexRD2 and ATR1, the three-helix bundle folds that are adopted by the repeating W-Y motifs have been suggested to form a structural unit which is observed in about 44%

of annotated *Phytophthora* RXLR effectors and 26% of *H. arabidopsidis* RXLR effectors (Win *et al.*, 2012; Boutemy *et al.* 2011). This structural unit of conserved W-Y motifs was named the WY-domain (Boutemy *et al.*, 2011). The WY-domain has been proposed as a flexible scaffold to provide both a degree of molecular stability and plasticity to support the rapid changes within effector proteins (Win *et al.*, 2012; Boutemy *et al.*, 2011). This is important for the effectors to maintain their virulence activities while evading recognition by the plant innate immune system during rapid co-evolution (Win *et al.*, 2012).

Many functionally important and polymorphic residues have been discovered by Boutemy *et al.* (2011) which map to the surface of RXLR proteins. This finding has led the authors to propose an evolution model of RXLR effectors at the structural level via adaptation of WY-domains of the protein which comprise: (i) insertion/deletions of amino acids in loop regions between helices; (ii) extensions of amino acid residues to the N and C termini; (iii) amino acid replacements that target surface residues, (iv) tandem domain duplications, and (v) oligomerization.

A genome-wide analysis of the sequenced *P. infestans* isolate T30-4 has identified 563 potential RXLR type effector genes (Haas *et al.*, 2009). Additionally, by considering that *P. infestans* contains potentially a further 196 crinkler effectors, the scope for functional redundancy is immense (Haas *et al.*, 2009; Birch *et al.*, 2008). Indeed, in comparison, bacterial pathogens contain typically between 25 and 35 T3SS effectors, and most of them are functionally redundant (Wilton & Desveaux, 2010). Furthermore, effector genes are located in dynamic regions of the *P. infestans* genome which is likely to facilitate rapid evolutionary changes and accounts for the considerable *P. infestans*

effector expansion compared to *P. sojae* and *Phytophthora ramorum* (Haas *et al.*, 2009). By comparison to other *Phytophthora* species, the RXLR genes in the *P. infestans* genome have expanded considerably and 70 out of 563 RXLR effector genes are rapidly diversifying (Haas *et al.*, 2009). Moreover, RXLR effector gene turnover has been associated with host co-evolution (Tyler *et al.*, 2006; Jiang *et al.*, 2008; Win *et al.*, 2007).

1.5 HOST-OOMYCETE CO-EVOLUTION

High levels of diversifying selection of the effectors are presumably the result of molecular co-evolution between a pathogen and its host plant. Most of the *P. infestans* effector genes that are induced *in planta* and show presence/absence polymorphism, copy number variation or high nonsynonymous substitution rates, are located within gene-sparse regions (GSRs) (Raffaele *et al.*, 2010). This is probably for flexibility of the potential effector genes to be evolutionarily changed in response to novel host resistance (Haas *et al.*, 2009). The *P. infestans* 13_A2 lineage, which is currently dominant in Europe, comprises some of the most aggressive *P. infestans* isolates and contains extensive genetic and expression polymorphisms particularly in effector genes (Cooke *et al.*, 2012). Copy number variations, gene gains and losses, amino-acid replacements and changes in expression patterns of disease effector genes within this isolate are likely to contribute to enhanced virulence and aggressiveness to drive the observed population displacement (Cooke *et al.*, 2012).

The introduction of nucleotide substitutions is one of the key strategies used by pathogens to evade recognition by resistance proteins. Proteins with amino acid changes might be able to escape recognition by the resistance protein. Single

nucleotide polymorphisms (SNPs) have been reported to provide virulent alleles of *Atr1* and *Atr13* from *H. arabidopsidis* (Allen *et al.*, 2004; Rehmany *et al.*, 2005) and also *Avr1b* and *Avr3c* from *P. sojae* (Shan *et al.*, 2004; Dong *et al.*, 2009).

An additional approach to retain virulence on a host plant that contains a resistance protein involves the pathogen 'jettisoning' the recognised effector. Loss of AVR4 function in *P. infestans* isolates that infect potato expressing R4 has been reported (Van Poppel *et al.*, 2008). Truncated versions of *Avr4* resulted from frame-shift mutations to generate probably non-functional and non recognised effector protein (Van Poppel *et al.*, 2008). Interestingly, mutation of *Avr4* does not interfere with pathogen fitness, which explains why virulent races evolve rapidly and at high frequency (Vleeshouwers *et al.*, 2011). Presumably, functional redundancy in the effector complement may compensate loss of an effector gene to maintain the pathogen fitness on susceptible plants (Birch *et al.*, 2008).

There are hundreds of NBS-LRR-encoding sequences within a typical plant genome (Lehmann, 2002; Jupe *et al.*, 2012). *R* genes located within plant genomes often exist as members of clustered gene families which have evolved through duplication and diversification (Lehmann, 2002). Compared to other genes in the plant genome, resistance genes have been found to evolve more rapidly and domains such as the leucine-rich repeat (LRR) are subjected to diversifying selection (Lehmann, 2002; Jupe *et al.*, 2012).

Arabidopsis thaliana has been reported to contain approximately 150 NB-LRR encoding genes, comprising up to 1% of the genome (Meyers *et al.*, 2003; 1999). The potato

genome potentially contains at least 438 NBS-LRR genes which represent 1.16% of the total number of annotated genes in the potato genome (Jupe *et al.*, 2012). This shows that plant species contain abundant, distantly related NBS-LRR *R* genes for the provision of recognition specificities. Most of the cloned resistance genes are members of multigene families, indicating that gene duplication and subsequent diversification are common processes in plant gene evolution (Martin *et al.*, 1993; Lawrence *et al.*, 1995). The potato *R3a* locus, for instance, is organised in three neighbouring homogeneous clusters that consist of 13 members with varying sizes that are thought to facilitate rapid evolution (Jupe *et al.*, 2012). Jupe *et al.* (2012) have shown that, unlike effector genes, potato resistance genes reside in indistinct genomic regions that are not significantly different compared to other regions of the potato genome.

1.6 THE ROLE OF UBIQUITINATION AND E3 LIGASES IN PLANT PCD AND DEFENCE

The ubiquitin proteasome system (UPS) is one of the most important cellular processes for protein modification and degradation in eukaryotic organisms. The overall process is to tag the target-protein with ubiquitin, which leads to a variety of fates. These tagging processes are mediated by an enzymatic cascade involving an ubiquitin-activating enzyme (E1), an ubiquitin-conjugating enzyme (E2), and an ubiquitin ligase (E3). 1-2 E1s, 50 E2s and E2-like genes, and more than 1000 E3s have been estimated to reside in plant genomes (reviewed by Vierstra, 2009). Thus, compared to E1 or E2 genes, E3 genes are highly abundant in plant genomes to allow plants to ubiquitinate a wide variety of substrates for many biological processes. Each E3 ubiquitin ligase is able to act in ubiquitination mechanism for only one or a few target proteins (Vierstra, 2009). This can be linked with specificity of the ubiquitination mechanism that mainly depends on the E3 ligase (Hershko *et al.*, 1983; Finley *et al.*, 2004). Based on the

subunit component and action modes, E3 ligases can be divided into two major types which can be a single protein or a protein complex (Vierstra, 2009). HECT, RING finger and U-box domain proteins have been classified as single protein E3 ligases (Moon *et al.*, 2004).

In *Arabidopsis*, the R proteins RPM1 and RPS2 are dependent on two RING finger E3 ligases, RPM1-interacting protein 2 (RIN2) and RIN3 to trigger an HR upon delivery of either the AvrRPM1 or AvrB type III effector proteins (Kawasaki *et al.*, 2005). In addition, *Arabidopsis* plant U-box (PUB) E3 ligase, PUB17, is required for RPM1 and RPS4 mediated ETI induced by the avirulence effectors, AvrB and AvrRPS4 respectively (Yang *et al.*, 2006). However, a homologous triplet of PUB22, PUB23 and PUB24 act as negative regulators of PTI in response to several distinct PAMPs (Trujillo *et al.*, 2008). In addition, PUB13 has recently been shown to be involved in regulation of cell death, defence and flowering time in *Arabidopsis* (Li *et al.*, 2012a).

The rice U-box E3 ligase, SPL11, has been successfully identified and characterized providing the first evidence for the role of ubiquitination in controlling resistance and PCD in monocot plants (Liu *et al.*, 2012; Zeng *et al.*, 2004). This was followed by identification of two RING finger E3 ligases which are BLAST AND BTH-INDUCED-1 (OsBBI1), that positively regulate resistance against *Magnaporthe oryzae* by modifying the rice cell wall (Li *et al.*, 2011) and XA21 BINDING PROTEIN 3 (XB3) that is required by rice bacterial blight resistance protein XA21 (Wang *et al.*, 2006). However, in tobacco, the E3 ligase CMPG1 has been shown previously to function as a positive regulator of plant defence and disease resistance and the U-box domain of this protein is essential for its activity (González-Lamothe *et al.*, 2006).

Oomycete plant pathogens belonging to the Peronosporales such as *Phytophthora* sp. have lost the ability to synthesize sterols and must acquire them from their host during pathogenesis (Tyler *et al.*, 2006). However, oomycete pathogens belonging to the Saprolegniales group are sterol prototrophs and the study by Gaulin *et al.*, (2010) has provided the first detailed analysis of a sterol biosynthesis pathway in an oomycete. INF1 is a sterol carrier that plays an important role in *Phytophthora* to uptake sterols from external sources (Tyler *et al.*, 2006; Hein *et al.*, 2009). However, some host plants perceive INF1 as a PAMP (Hein *et al.*, 2009) leading to induction of PTI (Bos *et al.*, 2006). PTI mediated by INF1 is dependent on CMPG1 (González-Lamothe *et al.*, 2006) and can be blocked by the action of Avr3a (Gilroy *et al.*, 2011a; Bos *et al.*, 2010) (Figure 1.7A).

The role of CMPG1 in plant defence signalling was extended by investigating the recognition of a range of pathogen-derived proteins in *Nicotiana* species (Gilroy *et al.*, 2011a). In addition to INF1, cell death triggered by another PAMP, CBEL, is also dependent on CMPG1 (Gilroy *et al.*, 2011a). CMPG1 has been reported to be required for HR induced by interaction of the *C. fulvum* effector, Avr9 with its cognate resistance protein from tomato, Cf-9 (González-Lamothe *et al.*, 2006). The study by Gilroy *et al.* (2011a) showed that interaction of another *C. fulvum* effector, Avr4 with its cognate resistance protein, Cf-4, also causes PCD that is dependent on CMPG1 (Figure 1.7B). Interestingly, all the PCD events that are dependent on CMPG1 are triggered at the host plasma membrane, suggesting that CMPG1 plays a critical role in signal transduction/regulatory processes following pathogen perception at the plasma membrane (Gilroy *et al.*, 2011a) (Figure 1. 8). However, the induced host immunity can be suppressed by *P. infestans* Avr3a effector (Gilroy *et al.*, 2011a; Bos *et al.*, 2010;

2006). $Avr3a^{KI}$ strongly interacts with and stabilizes CMPG1 *in planta* (Bos *et al.*, 2010). However, the same function is weakly performed by the virulent allele, $Avr3a^{EM}$, which evaded recognition by the cognate potato *R* gene product R3a (Armstrong *et al.*, 2005) and this function is lost with an $Avr3a^{KI/Y147del}$ mutant (Bos *et al.*, 2010).

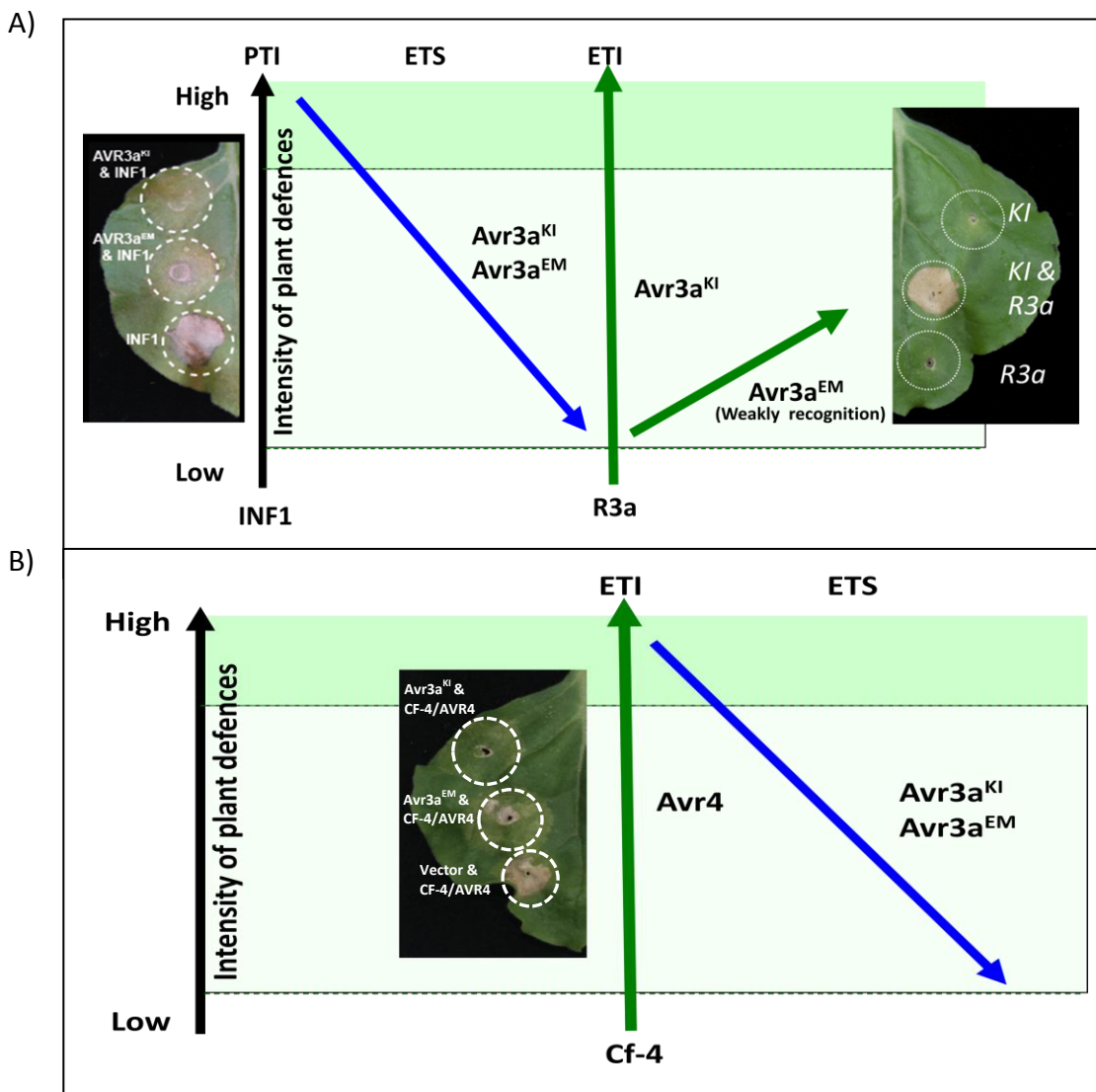


Figure 1.7: CMPG1 dependant cell death induced by *P. infestans* PAMP, INF1 and *C. fulvum* effector Avr4, illustrated in the Zig-Zag model (Jones & Dangl, 2006; Hein *et al.*, 2009). Perception of *P. infestans* PAMP, INF1 induces PTI which can be suppressed by effector $Avr3a^{KI}$ and $Avr3a^{EM}$. Presence of R3a elicits a strong HR following recognition of $Avr3a^{KI}$ but not of $Avr3a^{EM}$ (A). Induction of ETI by interaction between *C. fulvum* effector, Avr4, and tomato protein, CF-4, can also be suppressed by $Avr3a$ (B).

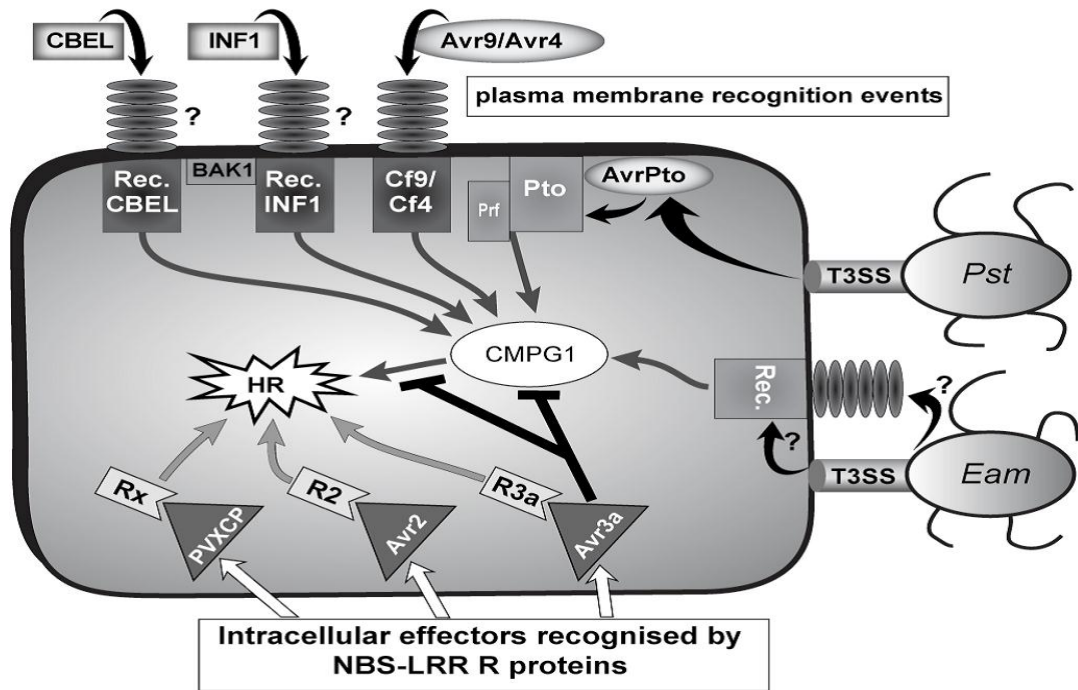


Figure 1.8: Model of CMPG1-dependent PCDs following pathogen elicitor recognition at the inner or outer surface of the plasma membrane. These responses can be suppressed by *P. infestans* effector Avr3a. Recognition of RXLR effectors by cognate NBS-LRRs or non-host responses toward *Erwinia amylovora* (*Eam*) are not suppressed by Avr3a. (Figure is taken from Gilroy *et al.*, 2011a).

1.7 *P. infestans* EFFECTOR Avr3a AND A STRATEGY TO IDENTIFY MORE DURABLE RESISTANCE

Generating new potato cultivars with good resistance to current late blight populations is difficult due to the genetic flexibility of *P. infestans* (Brasier, 1992). Moreover, co-evolution between *P. infestans* and *Solanum* species in Central and South America has contributed to remarkable sources of genetic diversity in *P. infestans* populations (Cardenas *et al.*, 2011). As indicated above, the genome size of *P. infestans* is about 240 megabases (Mb), the largest and most complex genome discovered so far in the chromalveolates (Haas *et al.*, 2009).

However, effectors have entered a new era of research that goes beyond unravelling their mode of action to promote virulence and utilises these pathogen genes as host

targets to identify more durable sources of resistance (Whisson *et al.*, 2011; Vleeshouwers *et al.*, 2011; 2008; Birch *et al.*, 2008). The ability of effectors (candidate Avr proteins) to trigger hypersensitive cell death on host genotypes with corresponding disease resistance *R* genes (Armstrong *et al.*, 2005; Song *et al.*, 2009) is one of the chief drivers of this work. However, functional redundancy of the effectors is important in current studies to seek the essential effectors for pathogen fitness and disease establishment (Birch *et al.*, 2008). The functional redundancy is most studied in bacterial effectors. The best examples are HopM1 and AvrE from *Pseudomonas syringae* pv. tomato, both of which are able to suppress callose deposition (DebRoy *et al.*, 2004). Functional redundancy was also described for AvrPto and AvrPtoB, both of which target the receptor-like kinase FLS2 (Gohre & Robatzek, 2008; Xiang *et al.*, 2008).

The RXLR domain has been used as a 'signature' to identify additional Avr gene candidates to enable the identification of key pathogen components or effectors that represent the pathogen's 'Achilles heels'. It is thought that the detection of essential molecules by the host could lead to more durable forms of resistance (Birch *et al.*, 2008). One such potential key effector that has been characterised to date is Avr3a which has been shown to be highly up-regulated during infection and is essential for pathogenicity (Bos *et al.*, 2010). A recent study has shown that *Avr3a* is induced during potato infection in *P. infestans* isolates T30-4, 06_3928A and NL07434 strains (Cooke *et al.*, 2012). In addition, *Avrblb1*, *Avrblb2* and Avr2/Avr2-like are also expressed in all *P. infestans* genotypes tested, and may thus be essential for pathogenicity (Cooke *et al.*, 2012; Gilroy *et al.*, 2011b).

When first identified, two alleles of *Avr3a* were described that encoded for two polymorphic proteins of 147 amino acids in length that differed in only two amino acids, *Avr3a*^{K80I103} and *Avr3a*^{E80M103}, in the mature protein (Armstrong *et al.*, 2005). All isolates studied today contain at least one of these two forms. *P. infestans* isolates that are avirulent on R3a containing potatoes express *Avr3a*^{KI}, which elicits a strong HR upon recognition, whereas virulent isolates carry only *Avr3a*^{EM} that evades recognition by the potato resistance gene product R3a (Armstrong *et al.*, 2005).

The polymorphisms in *Avr3a* have been used to determine the genetic diversity of *P. infestans* in the Northern Andean regions (Cardenas *et al.*, 2011). Six different alleles of *Avr3a* have been identified in this region and four of them were new allelic variants labelled as haplotypes H1 to H6 (Cardenas *et al.*, 2011) (Figure 1.9).



Figure 1.9: Alignment of the amino acid haplotypes observed at the *Avr3a* locus in the Northern Andean region. Shared amino acids are represented by dots and polymorphisms are represented as amino acid replacement. Different colours represent the different domains/regions of the gene: signal peptide (blue), RXLR-EER (red) and C-terminal (purple). (Adapted from Cardenas *et al.*, 2011).

In addition to the virulent form *Avr3a*^{EM} (H1) and the avirulent protein *Avr3a*^{KI} (H3), the study also identified two additional variants *Avr3a*^{KIL} and *Avr3a*^{KKGIL} based on the amino acid variants at the C-terminus (Cardenas *et al.*, 2011).

This study suggests that this gene is under diversifying selection. Interestingly, the amino acids KI or EM at positions 80 and 103 are maintained together in the population (Cardenas *et al.*, 2011; Armstrong *et al.*, 2005). In line with this, Armstrong *et al.*, (unpublished) identified *Avr3a* variants based on a genetic diversity study of *P. infestans* isolates collected from different areas in the Toluca Valley, Mexico, a centre for *P. infestans* and potato co-evolution (Flier *et al.*, 2003; Niklaus & Wilbert, 2005). Within the 82 isolates assessed, the majority are homozygous for *Avr3a*^{EM} whereas *Avr3a*^{KI} homozygous isolates are very rare. Interestingly, compared to the study by Cardenas *et al.* (2011), four additional alleles were found in this study: *Avr3a*^{KIH}, *Avr3a*^{KIL}, *Avr3a*^{EMH} and *Avr3a*^{EMG}. However, the frequency of these additional alleles was very low compared to the *Avr3a*^{EM} allele that dominates the population.

1.8 AIMS AND OBJECTIVES

The *Avr3a* effector has been shown to be essential for *P. infestans* pathogenicity (Bos *et al.*, 2010) and is thus a good target to combat late blight disease. *P. infestans* isolates have been identified which contain new alleles of *Avr3a*. The focus of this study is to elucidate their functionality and role in *P. infestans*'s infectivity. In addition, the *Avr3a* paralogs *Pex147-2* and *Pex147-3*, which are presumably derived from functional divergence of duplicated genes (Armstrong *et al.*, 2005), are also included in this study.

Plants have evolved mechanisms to recognize effector proteins, resulting in selective pressure on the effector to evade host recognition while maintaining its virulence activity. Thus, understanding the function of these alleles and paralogous proteins in *P. infestans* pathogenicity will assist us to reveal the underlying molecular mechanisms by

which effectors evolve to gain new virulence functions, adapt to their host targets, and/or evade the plant innate immune system.

The specific aims of this project were to:

- Test the recognition specificity of the *P. infestans* *Avr3a* alleles and paralogs with the potato *R* gene, *R3a*.
- Investigate whether *Avr3a* alleles and paralogs have a conserved virulence function by suppressing cell death dependant on the E3 ligase, CMPG1.
- To determine *in planta* stabilization of CMPG1 by *Avr3a* alleles and paralogs.
- Identify the common virulence targets that interact with *Avr3a* alleles and paralogs via Yeast-2-Hybrid assay.
- Determine the capability of *Avr3a* alleles and paralogs to complement *Avr3a* silenced *P. infestans* line CS12.
- To determine the relative contributions of *Avr3a* alleles to pathogen fitness, and thus the potential costs that may be associated with virulence on *R3a* plants.

CHAPTER 2

2 MATERIAL AND METHODS

2.1 PLASMID CONSTRUCTION

2.1.1 Amplification of *Avr3a* alleles and paralogs *Pex147-2/Pex147-3*

Naturally occurring *Avr3a* alleles were generated by overlap Polymerase Chain Reaction (PCR) using *Avr3a*^{KI} or *Avr3a*^{EM} without the signal peptide as a template. Since all alleles are mutated at the 3' end, the first PCR amplification was performed using the *Avr3a* forward primer and different mutagenic reverse primers (Table 2.1). The paralogous genes *Pex147-2* and *Pex147-3* were amplified using genomic DNA from the *P. infestans* isolate T30-4 and their specific forward and reverse primers (Armstrong *et al.*, 2005)(Table 2.1). Full AttB gateway recombination sites were added in a second PCR step using the primers AttB1 5'-GGGG ACA AGT TTG TAC AAA AAA GCA GGC TTC-3' and AttB2 5'-GGGG AC CAC TTT GTA CAA GAA AGC TGG GTT TTA-3' to facilitate cloning the genes into Gateway compatible vectors.

In general, all PCRs were conducted in a standard reaction volume of 50µl. Each reaction consisted of template DNA (10 - 200ng), 1X of Green GoTaq buffer (Promega, USA), 2mM of MgCl₂, 0.2mM dNTPs (Invitrogen, USA), 0.4µM forward primer, 0.4µM reverse primer, 0.25µl (5U/µl), GoTaq DNA polymerase, the volume being adjusted to 50µl with DNase-free water (SIGMA, USA). Reactions were mixed gently and briefly centrifuged to ensure even distribution of the components. The amplification protocol is shown in Table 2.2. The PCR products were separated by gel electrophoresis on a

1.5% agarose/1XTBE (89mM Tris-Base, 89mM Boric acid and 2mM EDTA pH8.0) gel containing 0.5µg/ml ethidium bromide.

Table 2.1: List of primers used to amplify *Avr3a* alleles and the paralogs *Pex147-2* and *Pex147-3*. Bases indicated in red are the partial sequence of the *AttB* sites and the bases indicated in blue are substitution of nucleotides to generate the previously identified alleles of the gene.

	5'-Primer (5'-3')	3'-Primer (5'-3')
<i>Avr3a</i> ^{K¹H}	5'- AA AAA GCA GGA TTC ATG GAC CAA ACC AAG GTC CTG-3'	5'- A GAA AGC TGG GTT TTA CTA ATA TCC AGT GAG CCC CAG GTG CAT CAT GTA GCT ATT GTA GAT GTG -3'
<i>Avr3a</i> ^{K¹L}	5'- AA AAA GCA GGA TTC ATG GAC CAA ACC AAG GTC CTG-3'	5'- A GAA AGC TGG GTT TTA CTA ATA TCC AGT GAG CCC CAG GTG CAT CAG -3'
<i>Avr3a</i> ^{EMH}	5'- AA AAA GCA GGA TTC ATG GAC CAA ACC AAG GTC CTG-3'	5'- A GAA AGC TGG GTT TTA CTA ATA TCC AGT GAG CCC CAG GTG CAT CAT GTA GCT ATT GTA GAT ATG -3'
<i>Avr3a</i> ^{EMG}	5'- AA AAA GCA GGA TTC ATG GAC CAA ACC AAG GTC CTG-3'	5'- A GAA AGC TGG GTT TTA CTA ATA TCC AGT GAG CCC CAG GTG CAT CAT GTA GCT ATT GTA GAT CTG ATT GTA CTT TGC GCC TTG CGT CTT GCC -3'
<i>Pex147-2</i>	5'- AA AAA GCA GGA TTC ATG GAC CAA ACC AAG GTT CTG ATG TAT GGG T -3'	5'- A GAA AGC TGG GTT TTA CTA ATA TGC AGT GAG CCC CAG GTG CAT CAG GT -3'
<i>Pex147-3</i>	5'- AA AAA GCA GGA TTC ATG GAC CAA ACC AAG GTT CTG ATG TAT GGG A -3'	5'- A GAA AGC TGG GTT TTA CTA ATA TGC AGT GAG CCC CAG GTG CAT CAG GT -3'

2.1.2 DNA purification

PCR products were purified from agarose gels using the QIAquick® Gel Extraction Kit (Qiagen, Valencia, CA) according to the manufacturer's specifications. The target DNA fragment was excised from the agarose gel using a clean and sharp scalpel. The final volume for elution of the gel-excised product was 30µl.

Table 2.2: PCR protocol using GoTaq DNA polymerase.

Initial Denaturation	95 °C	2 minutes
For Cycles 1-30		
Denaturation	95 °C	30 sec
Annealing	50-60 °C	30 sec
Extension	72 °C	1 minute
Final Extension	72 °C	5 minutes

2.1.3 Cloning of PCR fragments into the destination vector pGRAB using Gateway® technology

The Gateway® Technology is a cloning method that takes advantage of the site-specific recombination properties of the bacteriophage lambda to provide a rapid and highly efficient way to re-clone DNA sequences into multiple vector systems. In this study, all effectors have been amplified with suitable AttB sites flanking the effector using PCR-based mutagenesis. Prior to cloning into a destination vector, the PCR product was cloned into pDONR207 (Invitrogen, USA). The PCR product (150ng) was mixed with pDONR207 (150ng) and the volume adjusted with TE buffer (pH8.0) to 8µl. The individual components were mixed and 2µl of BP Clonase™II enzyme was added following by an overnight incubation at 25°C in a PCR machine. On the next day, 1 µl of Proteinase K was added and the reaction was incubated at 37°C for 10 minutes to stop the enzyme activity. Plasmids were introduced into *E. coli* by electroporation and sequences checked before proceeding. The binary vector pGRAB (Whisson *et al.*, 2007) was used in this study for *in planta* expression. Recombinant pDONR207 (150ng) was mixed together with pGRAB (150ng) and adjusted with TE buffer (pH8.0) to a final volume of 8µl. Two microliters of LR Clonase™II were added into the mixture prior to incubating overnight at 25°C in a PCR machine followed by adding 1 ul Proteinase K and incubated at 37°C, 10 minutes on the next day to stop the reaction.

2.2 BACTERIAL TRANSFORMATION

2.2.1 Preparation of electro-competent cells

A single bacterial colony from a fresh LB plate was inoculated into 10ml LB (0.01% (w/v) Bacto-peptone, 0.05% (w/v) Bacto yeast-extract, 0.05% (w/v) NaCl, 0.001% (w/v) Glucose, 0.015% (w/v) bacto agar adjusted to pH7.5 with 5M NaOH) containing the

appropriate antibiotics and incubated in a shaking incubator for 1–2 days at 28°C (*A. tumefaciens*) or 37°C overnight (*E. coli*) at 200rpm. A fraction of the culture (100µl) was added to 300ml fresh LB Glucose and shaken again until the OD₆₀₀ of the culture was between 0.3–0.6. The culture was chilled on ice for 30 minutes and the cells were harvested at 5000 rpm for 15 minutes at 4°C. The pellet was re-suspended in 250ml cold 10% glycerol and centrifuged for 15 min, 4°C at 5000 rpm to wash the cells. To make sure the cells are free from any salt, the washing step was repeated another six times. The pellet was re-suspended in a suitable volume of 10% glycerol depending on the size of the pellet. Approximately 100µl of cells were aliquoted into tubes. The tubes were frozen in liquid nitrogen prior to storage at -80°C.

2.2.2 Transformation of bacterial cell using electroporation

DNA constructs (one microliter at a concentration of 1-10µg/ml) and 25µl of DH10B electrocompetent cells were mixed together in a 0.5µl tube, transferred into a pre-chilled electroporation cuvette and then placed in the electroporator (*E. coli* Pulser, BioRad). The voltage of the electroporation device was set to 1800V and a 2ms pulse was applied. Immediately, after electroporation, 500µl of fresh SOC medium (2% bacto tryptone, 0.5% bacto yeast extract, 10mM NaCl, 2.5mM KCl, 20mM glucose, 10mM MgCl₂) was added into the cuvette and mixed gently by pipetting the bacteria up and down three times. To recover the transformed cells, two different conditions were used for *E. coli* and *A. tumefaciens* cells. For *E. coli*, the cells were incubated in a shaking incubator for 1 hour at 37°C and 2 hours at 27°C for *A. tumefaciens*. The transformed cells were plated on LB agar containing appropriate antibiotics and incubated at 37°C overnight for *E. coli* and 2–3 days at 27°C for *A. tumefaciens*.

2.3 SCREENING FOR POSITIVE CLONES

2.3.1 PCR Screening

A scaled down PCR reaction using ten microliters of PCR master mix (see above) was prepared to perform colony PCRs. Bacterial colonies presumed to be recombinant were picked up from plates by touching a sterile yellow tip onto the surface of a colony and stirred well into PCR reaction. The same colony was then used to inoculate LB media containing appropriate antibiotics and incubated at 37°C, overnight for *E. coli* or at 27°C, 2–3 days for *A. tumefaciens* using a shaking incubator.

2.3.2 Plasmid purification

Plasmid purification was carried out using the QIAprep Spin Miniprep Kit (Qiagen, Valencia, CA) according to the manufacturer's recommendation. DNA was eluted in 30µl of distilled water (Sigma-Aldrich Inc. USA) and stored at -20 °C until use.

2.3.3 Spectrophotometric determination of DNA concentration and sequencing

The concentration and purity of DNA was measured spectrophotometrically at 260–280 nm wavelengths using a NanoDrop (NanoDrop Technologies Inc., USA) instrument. The DNA was sent for sequence analysis at the JHI's sequencing facility.

2.4 AGROBACTERIUM INFILTRATIONS

2.4.1 Plant material and growth conditions

Nicotiana benthamiana plants were grown and maintained in JHI's glasshouse facilities with an ambient temperature of 22–25°C and 60–120µmol.m⁻².s⁻¹ light intensity. The three middle leaves of four to six week old *N. benthamiana* plants were used for Agro-infiltration and *P. infestans* infection assays and maintained in the

glasshouse/controlled environment throughout the experiments. In our experience, the cotyledon and the older leaves towards the plant base tend to be more susceptible to pathogens whereas the newly forming leaves at the top appear much more resistant to *P. infestans*. Thus, these leaves were not used in our studies.

2.4.2 Preparation of *A. tumefaciens* for Agro-infiltration

To initiate *A. tumefaciens* cultures, a single colony from an LB plate was inoculated into a sterile 15ml centrifuge tube containing 10ml of LB broth with the appropriate selection antibiotics. Cultures were grown at 27°C for 2–3 days in a shaking incubator. The cells were harvested by centrifugation at 4000 rpm for 10 minutes at 10°C. The pellet was re-suspended in 5ml of Agromix solution [(3',5'-dimethoxy-4'-hydroxyacetophenone (200µM), 2-(4-morpholino)ethanesulfonic acid pH5.6 (100mM), Magnesium Chloride (100mM)] and the suspended cells were kept in the dark at room temperature for at least 3 hours. The cell density was adjusted to 0.5 absorbance units OD₆₀₀. The cell density at OD₆₀₀ was obtained using a spectrophotometer (Cell density meter, WPA biowave) by mixing 100µl culture with 900µl of Agromix buffer.

2.4.3 Agro-Infiltration

When transiently producing a recombinant protein *in planta* via *A. tumefaciens* gene delivery, the goal of the infiltration process is to maximize contact between the *A. tumefaciens* cells and the plant cells within the leaf tissue. Suitable *N. benthamiana* leaves were infiltrated using a 1ml needleless syringe. The syringe was placed onto the abaxial (underneath) side of a leaf that was superficially wounded at the inoculation spot with a needle. By exerting a counter-pressure with a finger on the adaxial (top) side of the leaf, the solution was slowly injected into the leaf. Typically, for every

experiment, five plants with three leaves per plant were used for each biological replicate and at least three biological replicates were carried out for each experiment.

2.4.4 Cell death assay

Hypersensitive responses (HRs) on infiltrated sites were recorded and photographed between 4–8 days post-infiltration (dpi) depending on the elicitors used. An individual inoculation was counted as a positive response if more than 50% of the inoculated site developed a clear PCD lesion. The inoculation sites were also observed under ultraviolet (UV) light and fluorescence that was emitted at 505nm after excitation at 395nm was quantified using a SpectraMax M5 fluorometer (Molecular Devices). Observation and quantification of fluorescence was performed especially for the effector/resistance gene interaction studies that produced weak responses.

2.5 COMPLEMENTATION STUDY

2.5.1 Sporangia Preparation of CS12 for leaf inoculation

P. infestans Avr3a^{EM} silenced line CS12 has been used in this study as described by Bos *et al.* (2010). To isolate asexual sporangia of CS12, rye agar plates containing 10–12 days old *P. infestans* cultures were flooded with cold water and rubbed with a glass rod to harvest the sporangia. The sporangial suspension was transferred to a 50ml centrifuge tube and spun at 2500 g for 10 minutes. The pellet was re-suspended in 5ml cold sterile water and 10µl of the sample was used to count the number of sporangia under a microscope. The number of sporangia was set to between 100–150 sporangia per 10µl and used to inoculate plants.

2.5.2 Agro-infiltration and Inoculation

Preparation and infiltrations of *A. tumefaciens* samples in *N. benthamiana* leaves were carried out using the protocols described above in section 2.4. About 3–4 week old *N. benthamiana* plants were used in this study with 3 leaves per plant being infiltrated with *A. tumefaciens* samples. Two inoculation sites per half leaf contained the respective Avr3a allele and two inoculation sites for the other half contained the control pGRAB empty vector. The plants were left in the glasshouse for 3 days for protein expression before being transferred to the laboratory in sealed boxes for inoculation with *P. infestans* isolate CS12. The plants were arranged in propagators (6 plants per propagator and 3 plants per row) containing wet tissue to facilitate high humidity inside the propagators (nearly 100%) throughout the experiment. Every agro-infiltration site was inoculated with 10µl of the CS12 culture followed by sealing the propagators with plastic wrap to keep humidity close to 100% inside the propagators. Samples were kept in the dark for 24 hours and then stored at 20°C for 5–7 days for disease development. The occurrence of *P. infestans* lesions was recorded and representative leaves photographed. The statistical analysis was performed to identify statistically significant differences between the samples. Trypan-blue staining was performed on representative leaves to visualise disease symptoms further.

2.5.3 Trypan-blue staining

Trypan-blue staining was carried out by boiling leaf samples in 50ml Falcon tubes containing approximately 10ml trypan-blue solution (400ml contained 100mg Trypan-blue, 100ml water, 100ml Phenol, 100ml Lactic acid, 100ml Glycerol [add last after trypan blue has dissolved]) for 5 minutes in a water bath. After boiling, the leaf was washed 2 times with 20ml sterile distilled water, transferred to 10ml saturated chloral

hydrate solution (500g chloral hydrate dissolved in 200ml hot sterile distilled water) and then stored at room temperature overnight to remove non-specific staining. The chloral hydrate wash was repeated once and cleared leaves photographed.

2.6 YEAST-2-HYBRID

2.6.1 Construction of prey plasmid

Using Gateway cloning (Section 2.1.3) all genes were re-cloned into the yeast expression vector pDEST32 (Invitrogen, Paisley, UK). The constructs were transformed into yeast competent cells prior to use in the experiment.

2.6.2 Preparing competent yeast cells MaV203

A single colony of MaV203 (Invitrogen, Paisley, UK) was inoculated into 10ml of YPAD media (0.01% (w/v) Bacto-yeast extract, 0.02% (w/v) Bacto-peptone, 0.02% (w/v) Dextrose, 0.0001% (w/v) Adenine sulphate), supplemented with 2% (w/v) glucose and 0.003% Adenine hemisulfate. Yeast cells were grown overnight at 30°C, at 200 rpm in a shaking incubator. To obtain the bacterial cells at the log phase, the overnight culture was diluted to an OD₆₀₀ of 0.4 and incubated again for another 3 hours. The cells were harvested by centrifugation at 2500 rpm for 5 minutes and re-suspended in 20ml sterile water to wash the pellet. The cultures were spun again as before and the pellet was re-suspended in 1ml of 1X LiAc/0.5 XTE (10ml 10X LiAc [1M Lithium acetate], 5ml 10X TE [100mM Tris-HCl, 10mM EDTA, pH7.5], 85ml distilled water). For yeast transformations, competent MaV203 were used immediately.

2.6.3 Yeast Transformation

Yeast cells (10µl) were mixed with 100ng of each of the prey and bait constructs in the presence of 10µg of herring sperm DNA in 0.2ml PCR tubes. To each tube, 70 µl of 1 X LiAc/40% PEG-3350/1X TE was added and samples incubated at 30°C for 30 minutes. Finally, 8.8µl of DMSO was added to the tubes and a heat shock transformation was carried out by incubating the tubes at 42°C for 7 minutes. The tubes were then spun for 1 minute at 1000 × g and the pellet was re-suspended in 100µl of sterile distilled water. The cells were then plated onto double drop out plates (0.004% (w/v) Yeast nitrogen base without amino acids [Sigma-Aldrich, Dorset, UK], 0.000924% (w/v); Synthetic drop-out media without *Tryptophan* and *Leucine* [Sigma-Aldrich, Dorset, UK], 0.012% (w/v) agar, 40% Glucose) lacking amino acids *Leucine* and *Tryptophan*.

2.6.4 Characterization of protein/protein interactions and yeast transformations

Three reporter genes, *HIS3*, *URA3* and *lacZ*, function as selective markers for successful transformations. Induction of the *HIS3* and *URA3* reporter genes allows cell growth on plates lacking histidine (*HIS3*) or uracil (*URA3*), respectively whereas induction of the *lacZ* gene results in a blue colour when assayed with X-gal (5-bromo-4-chloro-3-indolyl-β-D-galactopyranoside). Thus, the transformants from 2.6.3 were plated out on the nutrient selection plate (Table 2.3).

Table 2.3: Plates used for yeast-two-hybrid transformations selection and protein/protein interactions.

synthetic complete (SC) drop-out media	Specific Induction
SC-Leu-Trp-Ura	<i>URA3</i> induction
SC-Leu-Trp-His	<i>HIS3</i> induction
SC-Leu-Trp	LacZ induction (The nitrocellulose membrane is placed on the surface of the agar to allow yeast cells to grow on the membrane)
SC-Leu-Trp	Control

Three single colonies of yeast transformants from 2.6.3 were picked up using sterile yellow pipette tips and swirled in 100µl sterile distilled water. Suspensions were spotted on synthetic complete (SC) drop-out media (Table 2.3) and incubated at 30°C for 24 hours prior to colony analysis. For β-galactosidase induction assays, the membrane was carefully peeled out from the agar and immediately immersed in liquid nitrogen for 30 seconds. The frozen membrane was immediately placed with the 'colony side up' on two layers of 3MM papers that had been saturated with X-gal solution (100µl X-gal in DMF [Sigma-Aldrich]), 60µl 2-mercaptoethanol, 10ml Z buffer [60mM Na₂HPO₄·7H₂O, 40mM NaH₂PO₄·H₂O, 10mM KCl, 1mM MgSO₄, pH7.0]). The membrane was covered and incubated at 37°C for 24 hours to monitor the appearance of blue colour as an indicator of β-galactosidase activity on the substrate X-gal.

2.7 DETERMINATION OF PROTEIN STABILITY

2.7.1 Protein extraction

Avr3a alleles and paralogs that had been cloned into the destination Gateway vector pGRAB were re-cloned into the donor vector pDONR211 using BP clonase® (Invitrogen) enzyme. To determine *in planta* protein stability, LR clonase® was used to recombine these constructs into the plant expression vector pB7WGC2 that yields C-terminal CFP-tagged proteins (Karimi *et al.*, 2002), whereas the genes were retained in pGRAB for *in planta* CMPG1 stabilisation (CMPG1 cloned in pB7YWG2) experiments. All bacterial transformation and agro-infiltration assays were performed as described earlier in sections 2.2 and 2.4. *N. benthamiana* leaves were infiltrated with the cultures set to an OD₆₀₀ of 0.5 to allow 1 cm² leaf discs to be cut out at 3 dpi for protein extraction. About 100mg of leaf discs were ground in liquid N₂, 200µl extraction buffer was added (200mM HEPES, 13 % sucrose, 1 mM EDTA, 1mM dithithreitol (DTT), proteinase

inhibitor cocktail tablet) and left to thaw on ice. A fraction of the lysate (20µl) was mixed with 20µl sodium dodecyl sulphate loading buffer. The samples were boiled for 5 min at 95°C and loaded onto a 4–12% Bis-Tris NuPAGE® Novex® Mini gel (Invitrogen, Paisley, UK).

2.7.2 Protein extraction from yeast

The double drop out liquid media (10ml) was inoculated with yeast transformants as described in section 2.6. Samples were incubated for 12 hours at 30°C in a shaking incubator at 200 rpm. From the culture, 2ml were transferred into a small tube and the yeast cells collected by centrifugation at 13,000 rpm for 10 minutes. Cell pellets were re-suspended in 200µl 0.1M NaOH and incubated at room temperature for 5 minutes. Cells were centrifuged again using the same conditions as before and the pellet was re-suspended in 50µl sample buffer (60mM Tris-HCl, pH6.8, 5% glycerol, 2% SDS, 4% β-mercaptoethanol, 0.0025% bromophenol blue). Cell suspensions were boiled for 5 minutes followed by centrifugation at 13,000 rpm for 5 minutes. The supernatant was carefully transferred into a fresh 1.5ml tube and 10µl loaded onto a 4–12% Bis-Tris NuPAGE® Novex® Mini gel (Invitrogen, Paisley, UK).

2.7.3 Western Blot Analysis

All protein samples were loaded onto a 12% Bis-Tris NuPAGE® Novex® Mini gel (Invitrogen, Paisley, UK) and run at 200V, 120mA and 25W for 1 hour in 1X NuPAGE MOPS buffer (Invitrogen, Paisley, UK). The gel was blotted onto a nitrocellulose membrane (Hybond-ECL, Amersham) for 2 hours at 25V using transfer buffer (1X NuPAGE Transfer buffer [Invitrogen, Paisley, UK], 10% (v/v) followed by soaking the blot into 15ml Ponceau solution (Sigma-Aldrich, Dorset, UK) to visualise the protein

samples. The blot was blocked with Blocking buffer (1X PBS, 5% milk powder, 0.01% Tween 20) either overnight or 1–2 hours at room temperature. The primary antibody was applied either for 2 hours at room temperature or overnight at 4°C whilst gently rotating (Table 2.4). The blot was washed three times for 10 minutes each with TBS-T (1X PBS, 0.01% Tween 20) and then incubated with the secondary antibody for 1 hour at room temperature whilst gently rotating (Table 2.4). The blot was washed again as before and proteins detected using enzymatic reactions. The ECL-Plus Western Blotting Detection Reagents (GE Healthcare, Hertfordshire, UK) were used for detection, according to the manufacturer’s instructions. The blot was exposed to an X-ray film and the luminescence was visualised by developing the film using an automatic X-ray Film Processor, Compact X4 (Xograph Imaging System, England). When necessary, the blot was stripped with stripping buffer (25mM Glycine, 1% SDS, pH 2.0 with HCl) for half an hour and probed again as described before.

Table 2.4: List of primary and secondary antibodies used in Western blots.

Assay	Tag protein	Primary antibody	Secondary antibody
<i>In-planta</i> protein stabilisation	Cyan Fluorescent Protein (CFP)	Monoclonal mouse <i>GFP</i> antibody (Sigma-Aldrich) Dilution; 1 : 1000	Goat antimouse immune-Globulin (Ig) horseradish peroxidase antibody (Sigma-Aldrich) Dilution; 1 : 5000
<i>In-yeast</i> protein stabilisation	DNA Binding Domain (DBD), GAL4.	Monoclonal mouse <i>GAL4</i> antibody (Sigma-Aldrich) Dilution; 1 : 1500	Goat antimouse immune-Globulin (Ig) horseradish peroxidase antibody (Sigma-Aldrich) Dilution; 1 : 5000
CMPG1 stabilisation <i>in-planta</i>	Yellow Fluorescent Protein (YFP) + Myc	Monoclonal rabbit <i>Myc</i> antibody (Sigma-Aldrich) Dilution; 1:5000	Goat antirabbit immune-Globulin (Ig) horseradish peroxidase antibody (Sigma-Aldrich) Dilution; 1 : 5000

2.7.4 Confocal imaging to determine *in planta* CMPG1 stabilization

Recombinant *A. tumefaciens* strain Agl1 containing the binary expression vector pB7YWG2 with the potato gene StCMPG1b-YFP (full-length StCMPG1b fused to yellow

fluorescent protein [YFP] at the C-terminus; Bos *et al.*, 2010) was mixed together with recombinant *A. tumefaciens* strain Agl1 containing *Avr3a* alleles and paralogs cloned into the vector pGRAB (GW) to final OD₆₀₀ of 0.01 before infiltrating into *N. benthamiana* leaves as described in section 2.4. The leaves were imaged after 2 days with the help of Dr Petra Boevink. Imaging was conducted on a Leica TCS-SP2 AOBS (Leica Microsystems) confocal microscope using HCX APO L 20X/0.5, 40X/0.8, and 63X/0.9 water dipping lenses. The excitation wavelength for YFP was 514 nm, and its emission was collected from 530–575 nm. The optimal pinhole diameter was maintained at all times. Photoshop CS software (Adobe System) was used for post-acquisition image processing. Mean intensities of regions of interest (ROIs) within single optical slice images of nuclei were measured for each of the combinations. ROIs were drawn within the nucleoplasm area, avoiding the dark nucleoli where they were visible. Images were all taken with identical settings on the Zeiss 710 CLSM (Carl Zeiss Microimaging GmbH, Germany). The averages of the mean intensities of ROIs of between 16 and 24 nuclei per combination were plotted.

CHAPTER 3

3 RECOGNITION OF *Avr3a* ALLELES AND THE PARALOGS PEX147-2/PEX147-3 BY THE POTATO RESISTANCE PROTEIN *R3a*

3.1 INTRODUCTION

Effectors are secreted by pathogens to perturb host defence responses and therefore to promote virulence and to aid in establishing disease. However, upon their detection by cognate plant disease resistance (*R*) gene products, effectors are known as avirulence (*Avr*) genes as their perception typically activates the innate host immune system. This response often invokes a hypersensitive response (HR), a form of programmed cell death that halts infection of biotrophic and hemibiotrophic pathogens (Dangl & Jones, 2001; Staskawicz *et al.*, 1995).

The potato resistance gene *R3a* is a member of the nucleotide-binding (NB) and leucine-rich repeat (LRR) motif containing family of resistance genes, a class that accounts for the majority of *R* genes (McHale *et al.*, 2006). In terms of its structure, *R3a* contains an N-terminal coil-coiled (CC) domain followed by the canonical NB-LRR domains (Huang *et al.*, 2005). *R3a* specifically recognises *Avr3a* which is arguably the best studied *P. infestans* effector. Within the *P. infestans* genome, functional *Avr3a* was identified alongside two paralogous sequences referred to as PEX147-2 which is transcribed at low levels (Morales *et al.*, unpublished) and the non-expressed PEX147-3 (Armstrong *et al.*, 2005). The avirulent form of *Avr3a*, *Avr3a*^{KI}, elicits a strong hypersensitive cell death response (HR) upon perception by *R3a* (Armstrong *et al.*, 2005), whereas the virulent allele, *Avr3a*^{EM} evades this recognition.

To elucidate the diversification of Avr3a as a consequence of a closely entwined host and pathogen co-evolution process (Ma & Guttman, 2008; McCann & Guttman, 2008), Armstrong *et al.* (unpublished) have studied the sequence diversity of Avr3a in the Toluca Valley in Mexico, a centre for *Solanum*/*P. infestans* co-evolution (Gruenwald & Flier, 2005; Flier *et al.*, 2003; Niklaus & Wilbert, 2005). *P. infestans* isolates were collected from commercially grown potatoes in field stations, low-input cultivated locally adapted *Solanum* landraces and wild *Solanum* species (Flier *et al.*, 2003). Genomic sequences encoding for Avr3a were amplified from 82 isolates, cloned and then Sanger sequenced (Table 3.1). Intriguingly, every isolate contained Avr3a^{EM} and/or Avr3a^{KI}. The majority (72%) of isolates were homozygous for Avr3a^{EM} whereas Avr3a^{KI} homozygous isolates accounted only for 2.4% of isolates and were found exclusively in *P. infestans* isolates sampled from wild *Solanum* species.

Additional C-terminal variations R124G, Q133H and M139L were identified as permutations of Avr3a^{EM} and Avr3a^{KI} resulting in the novel alleles Avr3a^{EMG124} (Avr3a^{EMG}), Avr3a^{EMH133} (Avr3a^{EMH}) as well as Avr3a^{KIH133} (Avr3a^{KIH}) and Avr3a^{KIL139} (Avr3a^{KIL}) of which only the latter was described previously by Cardenas *et al.*, (2011) (Figure 3.1). The variant Avr3a^{EMG} was found in combination with both Avr3a^{EM} (7.3%) and Avr3a^{KI} (1.2%) in *P. infestans* isolates collected from commercial fields, locally grown potatoes and wild *Solanum* species. Avr3a^{EMH} and Avr3a^{KIH} share the same amino acid substitution (Q133H). However, these alleles have only been identified from *P. infestans* isolates collected from wild *Solanum* species and in conjunction with Avr3a^{EM} (Avr3a^{EM}/Avr3a^{EMH}; 3.7 %) and Avr3a^{KI} (Avr3a^{KI}/Avr3a^{KIH}; 3.7 %) respectively.

Table 3.1: *P. infestans* Avr3a haplotypes of 82 isolates collected from the Toluca Valley. Samples were collected from the valley representing field stations/commercial fields, locally grown potatoes from low-input cultivation and wild *Solanum* species (Flier *et al.*, 2003).

AVR3A GENOTYPE	NUMBER OF <i>P. INFESTANS</i> ISOLATES				
	Valley	Local	Wild	Total	Percentage
$E^{80}M^{103}$	18	10	31	59	72
$E^{80}M^{103}/E^{80}M^{103}H^{133}$	0	0	3	3	3.7
$E^{80}M^{103}/E^{80}M^{103}G^{124}$	0	1	5	6	7.3
$E^{80}M^{103}/K^{80}I^{103}$	6	1	0	7	8.5
$E^{80}M^{103}G^{124}/K^{80}I^{103}$	1	0	0	1	1.2
$E^{80}M^{103}/K^{80}I^{103}L^{139}$	0	1	0	1	1.2
$K^{80}I^{103}/K^{80}I^{103}H^{133}$	0	0	3	3	3.7
$K^{80}I^{103}/K^{80}I^{103}$	0	0	2	2	2.4
Total	25	13	44	82	100

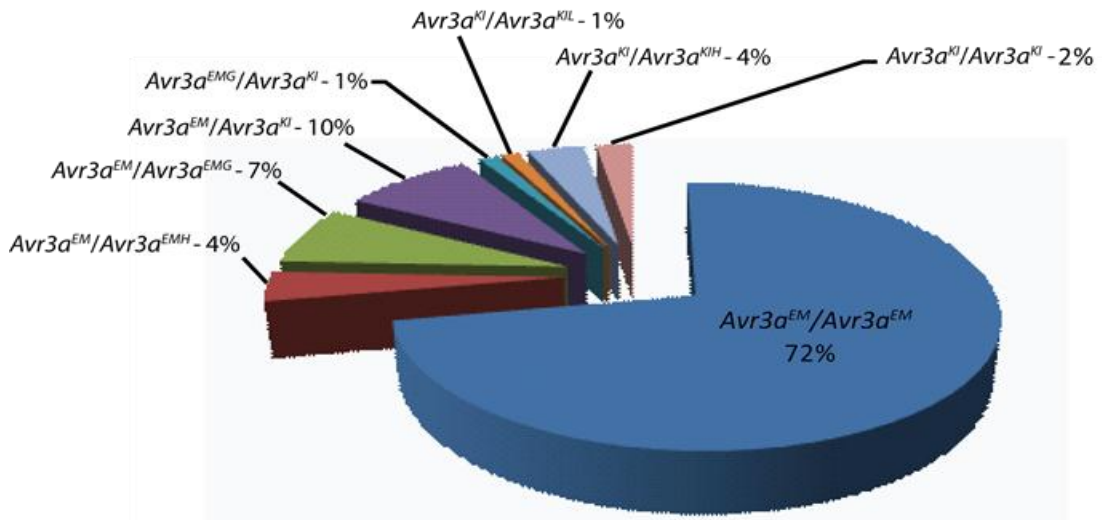


Figure 3.1: Graphical representation of the distribution of Avr3a alleles sampled from the Toluca Valley.

	60	70	80	90	100	110	120	130	140	
Avr3a ^{EM}	APNFNLANLNEEMFNVAALTE ^R RADAKK ^L LAKQLMGNDKLADAAY ^W WQHNRVTL ^D QIDTFLK ^L ASRKT ^Q GAKYN ^Q IYNSYMMHLGLTGY									
Avr3a ^{EMG}	APNFNLANLNEEMFNVAALTE ^R RADAKK ^L LAKQLMGNDKLADAAY ^W WQHNRVTL ^D QIDTFLK ^L AS ^E KT ^Q GAKYN ^Q IYNSYMMHLGLTGY									
Avr3a ^{EMH}	APNFNLANLNEEMFNVAALTE ^R RADAKK ^L LAKQLMGNDKLADAAY ^W WQHNRVTL ^D QIDTFLK ^L ASRKT ^Q GAKYN ^H IYNSYMMHLGLTGY									
Avr3a ^{KI}	APNFNLANLNEEMFNVAALTE ^R RADAKK ^L LAKQLMGNDKLADAAY ^W WQHNRVTL ^D QIDTFLK ^L ASRKT ^Q GAKYN ^Q IYNSYMMHLGLTGY									
Avr3a ^{KIH}	APNFNLANLNEEMFNVAALTE ^R RADAKK ^L LAKQLMGNDKLADAAY ^W WQHNRVTL ^D QIDTFLK ^L ASRKT ^Q GAKYN ^H IYNSYMMHLGLTGY									
Avr3a ^{KIL}	APNFNLANLNEEMFNVAALTE ^R RADAKK ^L LAKQLMGNDKLADAAY ^W WQHNRVTL ^D QIDTFLK ^L ASRKT ^Q GAKYN ^S Y ^M H ^L GLTGY									

— █ — █ — █ — █ —

α1 α2 α3 α4

Figure 3.2: C-terminal *P. infestans* Avr3a sequences from 82 isolates collected in the Toluca Valley. Amino acid positions derived from the full length Avr3a genes are shown on the top. Non-synonymous amino acid substitutions are highlighted in black. The helical regions predicted from the Avr3a crystal structure analysis and the corresponding amino acid positions are shown below the alignment (Yaeno *et al.*, 2011; Boutemy *et al.*, 2011).

Advances in elucidating the protein structure of oomycete RXLR-containing effectors have provided a novel insight into the basis of effector function. So far, the structure of the two *P. capsici* paralogs Avr3a4 (Yaeno *et al.*, 2011) and Avr3a11 as well as the *P. infestans* PEXRD2 (Boutemy *et al.*, 2011) and *Hyaloperonospora arabidopsidis* ATR1 effectors (Chou *et al.*, 2011) have been studied. Based on the structure of the effector domain of *P. capsici* Avr3a4 and Avr3a11 (Yaeno *et al.*, 2011; Boutemy *et al.*, 2011), it is predicted that the effector domain of *P. infestans* Avr3a, which shares 41% amino acid sequence identity with Avr3a11, assumes a four helix bundle fold, which is stabilised by a hydrophobic core. Mutational studies of Avr3a have shown correlations between protein structure, stability and some of the functional aspects (Bos *et al.*, 2009).

3.2 AIM

The aims of the studies detailed in this Chapter were:

- a) To identify the most robust, Gateway® compatible, *Agrobacterium tumefaciens* based transient expression system in *Nicotiana benthamiana* for the functional study of Avr3a alleles and paralogs.
- b) To determine the recognition patterns of Avr3a alleles Avr3a^{KIH}, Avr3a^{KIL}, Avr3a^{EMH}, Avr3a^{EMG} and paralogs PEX147-2 and PEX147-3 by R3a in comparison to Avr3a^{KI} and Avr3a^{EM}.
- c) To elucidate the stability of Avr3a alleles Avr3a^{KIH}, Avr3a^{KIL}, Avr3a^{EMH}, Avr3a^{EMG} and paralogs PEX147-2 and PEX147-3 *in planta* in comparison to Avr3a^{KI} and Avr3a^{EM}.
- d) To determine if Avr3a alleles or paralogs function as dominant/negative targets to suppress R3a dependent recognition of Avr3a^{KI}.

3.3 RESULTS

3.3.1 Establishment of a transient expression system

The model plant *N. benthamiana* has been exploited to characterise the Avr3a-R3a interaction. Co-infiltration of *N. benthamiana* leaves with a mixture of recombinant *Agrobacterium tumefaciens* expressing *R3a* and *Avr3a^{KI}* results in a rapid cell death response that is not observed upon co-infiltration of *R3a* with *Avr3a^{EM}* (Armstrong *et al.*, 2005; Bos *et al.*, 2006). However, the level of transient expression of *P. infestans* effectors via *Agrobacterium tumefaciens* is, amongst other conditions, dependent on the vector background.

R3a, cloned into the binary vector pGRAB, was co-infiltrated with the HR eliciting allele *Avr3a^{KI}* in different gateway compatible vectors into *N. benthamiana* to compare the

levels of expression. Three different gateway compatible binary vectors were used for the experiment and comprised pGRAB[GW] (Whisson *et al.*, 2007), pB7WGC2 (resulting in an N-terminal fusion of constructs with CFP) (Karimi *et al.*, 2002) and pGWB402Ω (Nakagawa *et al.*, 2007).

Expression of recombinant genes in all vectors was driven by a 35S Cauliflower mosaic virus promoter including a TMV leader sequence. The relative levels of *Avr3a^{Kl}* gene expression from each vector were indirectly determined by assessing the strength of R3a dependent cell death at 4 and 5 days post inoculation (dpi) in *N. benthamiana*. A co-infiltration site was only recognised as an HR response when at least 50% of the inoculated area yielded a visual cell death phenotype (Figure 3.3 a, b).

Expression of *Avr3a^{Kl}* with the vector pGWB402Ω yielded the slowest and weakest HR response whereas expression via pGRAB[GW] and pB7WGC2 resulted in almost similar phenotypes although the effect was more pronounced for pGRAB[GW] at 4 dpi. By 5 dpi, co-expression of *R3a* with *Avr3a^{Kl}* in pGRAB[GW] resulted in 100% of cell death elicitation followed by *Avr3a^{Kl}* in pB7WGC2 which yielded a 78% cell death rate. This experiment was repeated three times with five plants per experiment (three leaves per plant and two infiltration sites per leaf) and gave reproducible results.

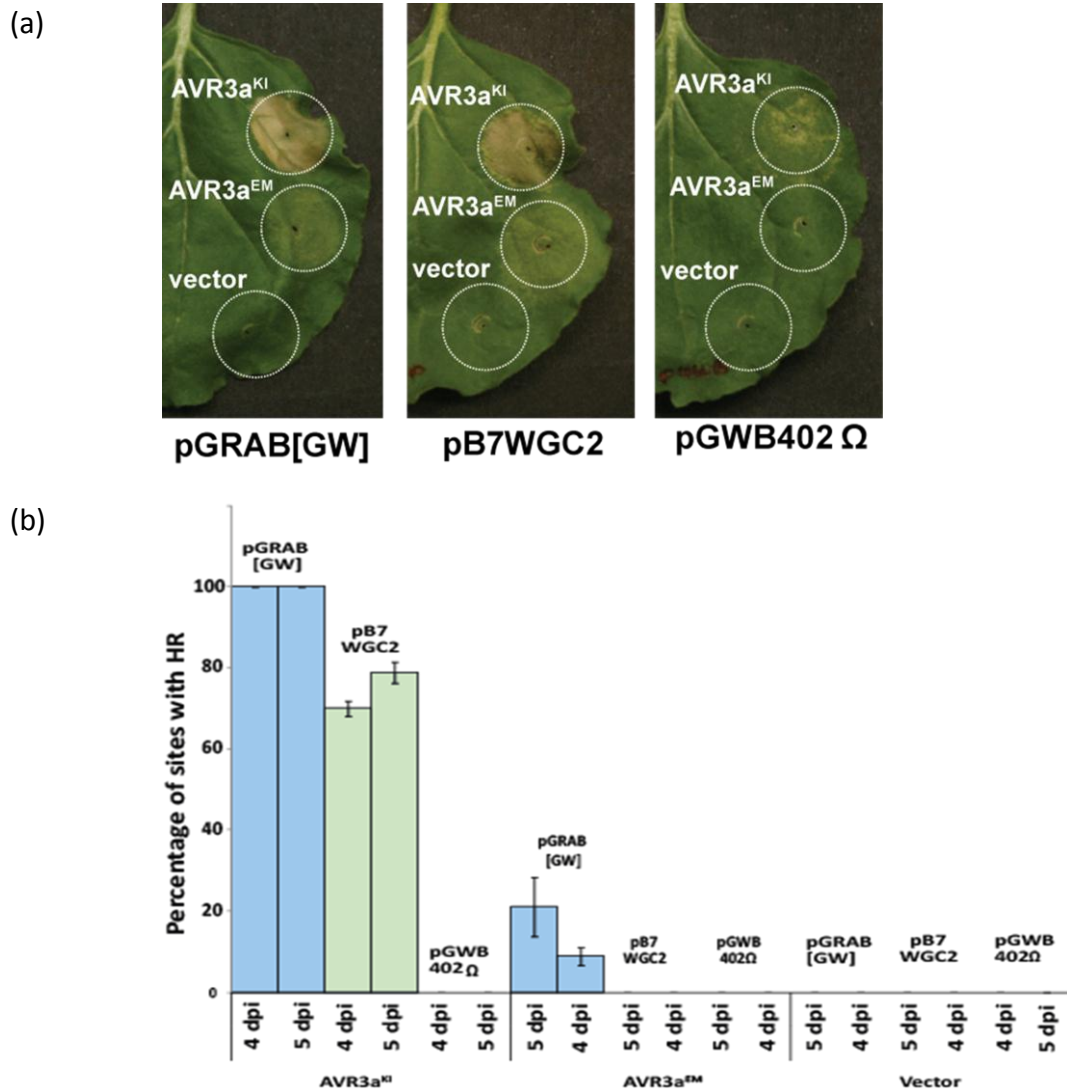


Figure 3.3: (a) Hypersensitive response development in *N. benthamiana* leaves following co-infiltration and transient expression of *R3a* with *Avr3a* alleles and empty vector control in different vector backgrounds. (b) Percentages of infiltration sites resulting in *R3a*-dependent HR. Percentages were calculated based on three independent experiments with 30 infiltration sites per experiment. Error bars indicate the calculated standard error.

It has been reported that in some cases weak recognition responses to virulent alleles can be observed under ultraviolet (UV) light that are not visible to the unaided eye or under natural light (Joosten *et al.*, 1997; Westerink *et al.*, 2004). Hypersensitive cell death responses are typically associated with the accumulation of autofluorescent polyphenolic compounds that can be visualised under UV light (Koga *et al.*, 1988). Indeed, Bos *et al.* (2006) showed that *Avr3a*^{EM} triggers a weak *R3a*-specific response when the co-inoculated sites are viewed under UV light. To investigate whether *Avr3a*^{KI}

and/or Avr3a^{EM} delivered via the various vectors yield a recognition response by R3a, agro-infiltration results obtained after 5 dpi were visualized under UV light (Figure 3.4a). In line with previous findings (Bos *et al.*, 2006), a weak recognition of Avr3a^{EM} in pGRAB[GW] and pB7WGC2 was observed following co-infiltration with R3a in *N. benthamiana*. This recognition appeared significantly weaker if compared to the response elicited by Avr3a^{KI} but much more pronounced if compared to the empty vector control. However, *Avr3a* expression from pGWB402Ω yielded only a visible response under UV light for co-expression of *R3a* with Avr3a^{KI} and not for Avr3a^{EM} or the empty vector control.

The autofluorescence emitted from polyphenolic compounds at 505nm following excitation at 395nm wavelength was quantified using a spectrophotometer (Figure 3.4b). A statistical analysis was carried out using a t-test method for parametric data to examine whether the means between delivery vectors are statistically significantly different (Table 3.2). As described above (Figure 3.3), co-expression of Avr3a^{KI} in pGRAB[GW] with *R3a* resulted in 100% HRs and was used as a maximum, relative value for comparison. The results show a higher level of relative autofluorescence for Avr3a^{KI} and Avr3a^{EM} delivered via pGRAB[GW] if compared to delivery through pB7WGC2. The weakest recognition responses were observed for *Avr3a* alleles expressed via pGWB402Ω.

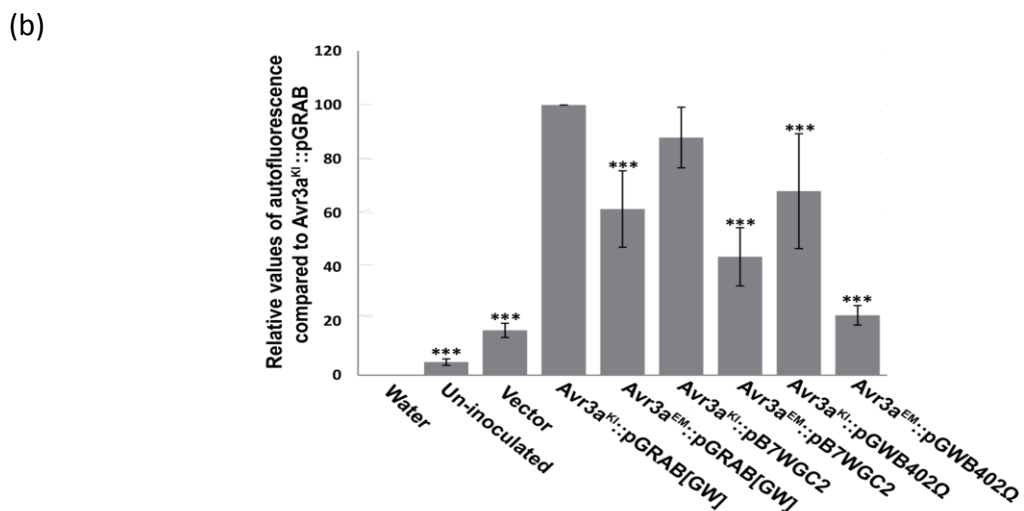
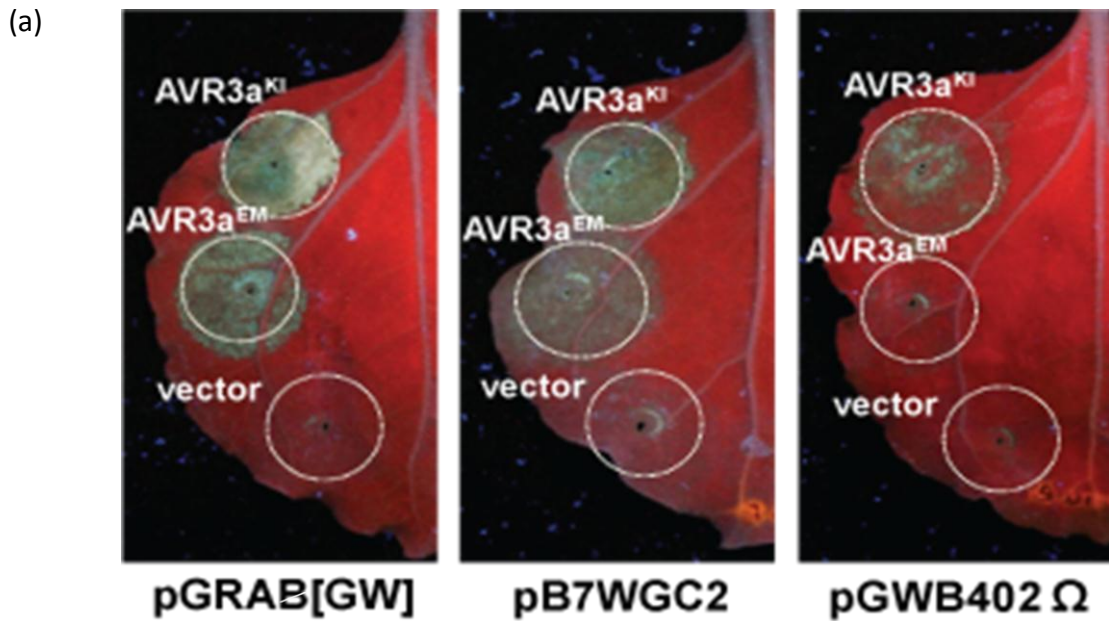


Figure 3.4: Quantification of autofluorescence associated with PCD. (a) Cell death symptoms are visualized under ultra-violet (UV) light at 5 days post infiltration. (b) Relative values of autofluorescence for R3a-mediated recognition of Avr3a^{EM} and Avr3a^{KI} are plotted following delivery via various vectors, in comparison to pGRAB[GW]. Relative values for empty vector control and un-inoculated sites were also measured using a spectrofluorometer at 505nm after excitation at a wavelength of 395nm. The values were calculated based on 3 independent biological replicates, each including 30 infiltrations per experiment. Statistically significant differences are denoted by stars (***) $p < 0.001$ (Table 3.2).

Table 3.2: Statistical analysis of autofluorescence emitted from *A. tumefaciens* co-infiltration sites of *Avr3a^{KI}* and *Avr3a^{EM}* with *R3a* in different vector backgrounds.

Avr3a^{KI} ::pGRAB n=90 Mean; 280.384 Stdev; 96.362 Sterror; 17.593	Avr3a^{EM} ::pGRAB n=90 Mean; 171.742 Stdev; 90.284 Sterror; 16.483	Avr3a^{KI} ::pB7WGC2 n=90 Mean; 246.637 Stdev; 61.326 Sterror; 11.196	Avr3a^{EM} ::pB7WGC2 n=90 Mean; 122.844 Stdev; 59.129 Sterror; 10.795	Avr3a^{KI} ::pGWB402Ω n=90 Mean; 190.961 Stdev; 116.440 Sterror; 21.259	Avr3a^{EM} ::pGWB402Ω n=90 Mean; 62.095 Stdev; 19.901 Sterror; 3.633	Vector n=60 Mean; 46.548 Stdev; 20.252 Sterror; 2.614	Un- inoculated n=60 Mean; 13.514 Stdev; 9.261 Sterror; 1.195	Water n=60 Mean; 0 Stdev; 0 Sterror; 0
Avr3a^{KI} ::pGRAB	<i>p</i> <0.001	0.242	<i>p</i> <0.001	<i>p</i> <0.001	<i>p</i> <0.001	<i>p</i> <0.001	<i>p</i> <0.001	<i>p</i> <0.001
	Avr3a^{EM} ::pGRAB	<i>p</i> <0.001	0.003	0.959	<i>p</i> <0.001	<i>p</i> <0.001	<i>p</i> <0.001	<i>p</i> <0.001
		Avr3a^{KI} ::pB7WGC2	<i>p</i> <0.001	0.004	<i>p</i> <0.001	<i>p</i> <0.001	<i>p</i> <0.001	<i>p</i> <0.001
			Avr3a^{EM} ::pB7WGC2	0.001	<i>p</i> <0.001	<i>p</i> <0.001	<i>p</i> <0.001	<i>p</i> <0.001
				Avr3a^{KI} ::pGWB402 Ω	<i>p</i> <0.001	<i>p</i> <0.001	<i>p</i> <0.001	<i>p</i> <0.001
					Avr3a^{EM} ::pGWB402 Ω	<i>p</i> <0.001	<i>p</i> <0.001	<i>p</i> <0.001
						Vector	<i>p</i> <0.001	<i>p</i> <0.001
							Un- inoculated	<i>p</i> <0.001

Indeed, the autofluorescence levels observed following the co-infiltration of Avr3a^{KI} with R3a in pGWB402Ω were not significantly different if compared to the recognition of Avr3a^{EM} in vectors pGRAB[GW] ($p=0.959$) and pB7WGC2 ($p=0.004$)(Table 3.2). pGRAB[GW] empty control, which represent the effects of *A. tumefaciens* on *N. benthamiana*, displayed a very weak accumulation of autofluorescent compounds that was less than 20% of the amount seen for R3a-dependent recognition of Avr3a^{KI} delivered by pGRAB[GW] and similar to the recognition response elicited following expression of Avr3a^{EM} via pGWB402Ω. Following this study, we determined that the gateway compatible vector pGRAB[GW] gave the most robust expression of *P. infestans* effectors Avr3a^{KI} and Avr3a^{EM} and was subsequently chosen for all downstream functional analyses.

3.3.2 Modelling of Avr3a alleles

Based on the structure of the effector domain of *P. capsici* Avr3a4 and Avr3a11 (Yeano *et al.*, 2011; Boutemy *et al.*, 2011), it is predicted that the effector domain of *P. infestans* Avr3a, which shares 41% sequence identity to Avr3a11 (Figure 3.5), assumes a four helix bundle fold, which is stabilised by a hydrophobic core (Boutemy *et al.*, 2011). Superimposing the *P. infestans* (Pi) Avr3a amino acid changes onto *P. capsici* (Pc) Avr3a11 suggests that Pi_K80E affects Pc_E71 in α helix 1, Pi_I103M affects Pc_Q94 in α helix 2, Pi_R124G resides in the Pc_loop3, Pi_Q133H affects Pc_R120 in α helix 4 and Pi_M139L affects Pc_M126 (Figure 3.5). Based on the crystal structure analysis of Pc_Avr3a11, all amino acid changes observed in Pi_Avr3a reside in side-chains that are surface accessible (Figure 3.6).

PC_Avr3a11 [68-132]	68 70 75 80 85 90 95 100 105 110 115 120 125 130 132 GPTKAAVKKMAKAIMADPSKADDVYQKWADKGYTTLTQLSDFLK--S-KTRG-KYDFVYNGYVITYRDYV SSSSSSSSSSSBSSSSSSSSSSSSSSSSSSSSSSSSSSSSSSSSSSSSSS--S-SSSS-SSSSBSSSBSSSSSSSS
PI_Avr3a [77-147]	77 80 85 90 95 100 105 110 115 120 125 130 135 140 145 ALTEKADAKKLAQQLMGNDKLADAAYVWQHNRVTLTLDQIDTFKLKLSRKTQGAKYNQIYNSYMHLGLTGY * * ** ** * ** * * ** * ** * ** * ** * ** * ** * ** * ** * ** * ** * ** * ** * ** * **
Features of PC_Avr3a11	W-motif Y-motif α1 loop1 α2 loop2 α3 loop3 α4
PI_Avr3a [77-147]	ALTEKADAKKLAQQLMGNDKLADAAYVWQHNRVTLTLDQIDTFKLKLSRKTQGAKYNQIYNSYMHLGLTGY
PI_PEX147-3	ALTEKADAKKLAQQLMGNDKMAKAAYVWQHNGVTPSQIDTFKLKLSGKTQGARYNEIYNS-YLMHLGLTAY
PI_PEX147-2	ALTEKADAKKLAQQLMGNGKLADAAYVWQHNRVTLTLDQIDAFKLKLSRKTQGARYNRIYNSCYMMHLGLTGF ***** ** * **
Features of PC_Avr3a11	W-motif Y-motif α1 loop1 α2 loop2 α3 loop3 α4
Avr3a ^{EM}	ALTEKADAKKLAQQLMGNDKLADAAYVWQHNRVTLTLDQIDTFKLKLSRKTQGAKYNQIYNSYMMHLGLTGY
Avr3a ^{EM} R3a-HR	VG G M V C EAP R G N E H E A R
Avr3a ^{EM} No R3a-HR	K R V L P
Avr3a ^{KI}	ALTEKADAKKLAQQLMGNDKLADAAYVWQHNRVTLTLDQIDTFKLKLSRKTQGAKYNQIYNSYMMHLGLTGY
Avr3a ^{KI} No R3a-HR	W P R P
Avr3a ^{KI} R3a-HR	SA R D S Q I S

Figure 3.5: Amino acid alignments between the C-terminal region of *P. capsici* Avr3a11 [position 70-132], *P. infestans* Avr3a, Avr3a paralogs and Avr3a variants (position 77-147) (Adapted from Boutemy *et al.*, 2011). Amino acid changes in Avr3a are superimposed on to *P. capsici* Avr3a11. Highlighted are the changes Pi_K80E (Pc_E71 [red]), Pi_I103M (Pc_Q94 [green]) Pi_R124G (within loop 3: Pc_K111-Y118 [yellow]), Pi_Q133H (Pc_R120 [blue]) and Pi_M139L (Pc_M126 [purple]). The secondary structure of the Avr3a effector is indicated as previously published (Yaeno *et al.*, 2011). Coloured boxes indicate helical bundles, connected by loops. Structurally important and conserved amino acids are highlighted in grey (Boutemy *et al.*, 2011). Conserved amino acids are marked with a star. The letter B and S indicate buried and surface residues, respectively which were determined based on the PcAvr3a11 crystal structure (Boutemy *et al.*, 2011).

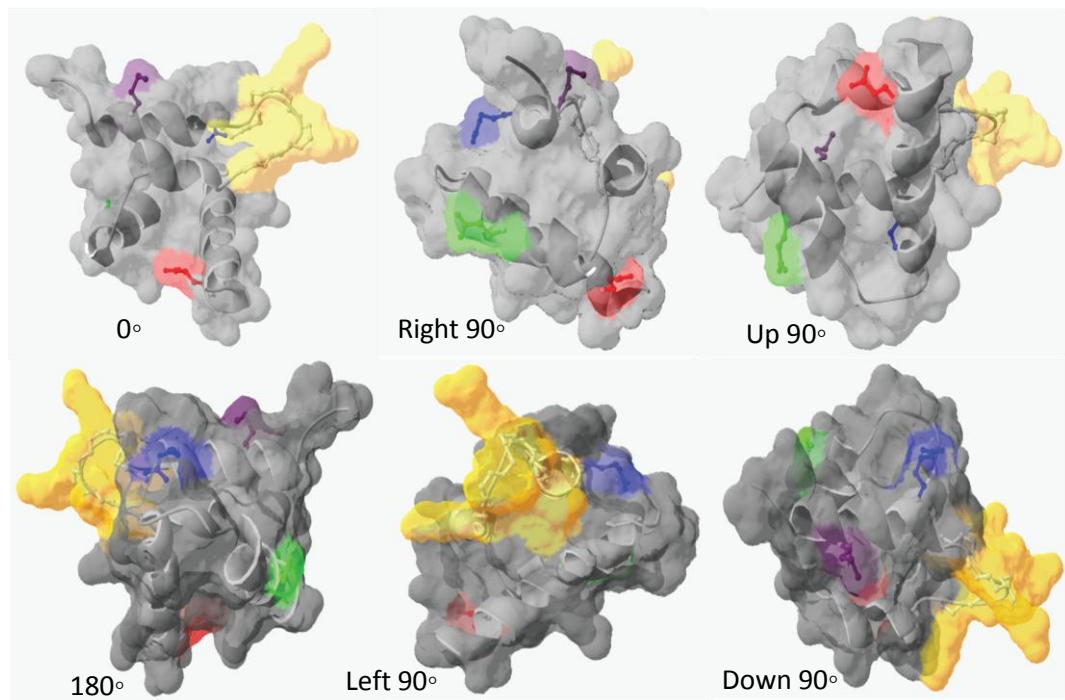









Figure 3.6: Amino acid changes in *P. infestans* Avr3a are superimposed onto the structure of *P. capsici* Avr3a11. Highlighted are the changes Pi_K80E (Pc_E71 [red]), Pi_I103M (Pc_Q94 [green]) Pi_R124G (within loop 3: Pc_K111-Y118 [yellow]), Pi_Q133H (Pc_R120 [blue]) and Pi_M139L (Pc_M126 [purple]). The accessibility of the respective amino acids is shown by colouration of the surface area.

3.3.3 Modelling of *Pi*_PEX147-2

The alignments between the Avr3a alleles and paralogs have highlighted some amino acid changes (Figure 3.5). There are seven amino acids in PEX147-2 which are different if compared to Avr3a and PEX147-3 (Table 3.3). Interestingly, amongst them is one additional amino acid, C138, which has been inserted in Pex147-2 and is located in the α 4 domain. This amino acid substitution displaces a critical key residue (Pc_Avr3a11 Y125) (Boutemy *et al.*, 2011). Based on the crystal structure analysis of Pc_Avr3a11, the remaining six amino acid changes with Pi_PEX147-2 reside in site-chain amino acids that are surface accessible (Figure 3.7).

Table 3.3: Amino acid changes in PEX147-2 compared to Pc_Avr3a11, Pi_Avr3a and Pi_Pex147-3.

Pc_Avr3a11	Pi_Avr3a	Pi_Pex147-3	Pi_Pex147-2	Colour Code
P86	D95	D95	G95	
K99	N108	N108	K108	
Y101	V110	V110	L110	
D108	T117	T117	A117	
-	R124	G124	S124	
R120	Q133	E133	R133	
-	-	-	C138	

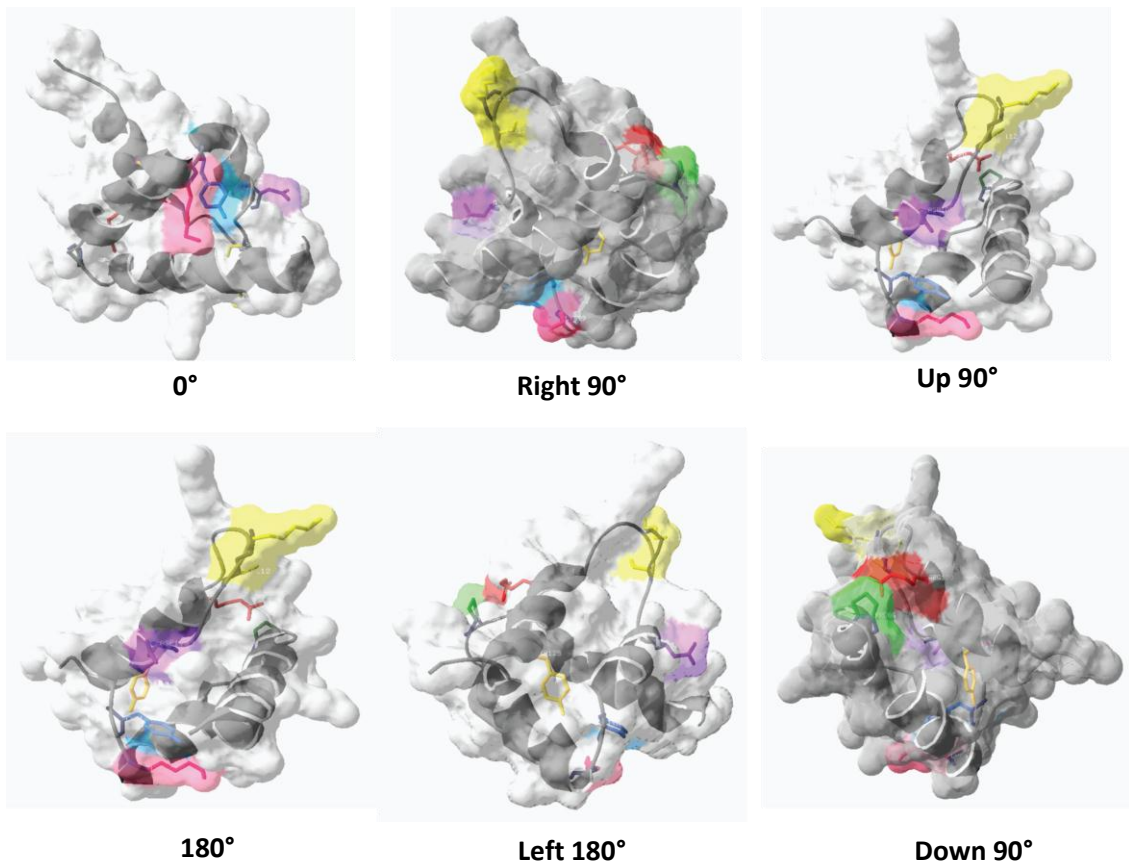


Figure 3.7: Amino acid changes in PEX147-2 compared to Pi_Avr3a which is superimposed on the structure of PcAvr3a11. Highlighted are the changes G95, K108, L110, A117, S124, R133 and the position of the additional amino acid C138. The colour code is according to Table 3.3.

3.3.4 Recognition of Avr3a alleles and paralogs PEX147-2/PEX147-3 by the resistance protein *R3a*

To determine whether the additional alleles and the Avr3a paralogs are recognised by *R3a*, they were cloned into the vector pGRAB[GW] that gave the highest levels of expression (see section 3.3.1 above) and co-expressed with *R3a* in *N. benthamiana*.

Avr3a^{KI} and *Avr3a^{EM}* cloned into this vector (see above) were used as a positive and negative control, respectively. Furthermore, *Avr3a^{KI/Y147del}* (Bos *et al.*, 2009) was included as a control. The terminal amino acid tyrosine has been removed in this mutated form of *Avr3a^{KI}* and it has been shown previously that *Avr3a^{KI/Y147del}* maintains recognition by R3a but is unable to interact and stabilise the *Avr3a* virulence target CMPG1 (Bos *et al.*, 2009; 2010). The *A. tumefaciens* strain Ag11, together with the helper plasmid pSoup and the virulence enhancer VirG were utilised as previously described (Armstrong *et al.*, 2005; Gilroy *et al.*, 2011b).

No visible responses were observed upon expression of these alleles alone in *N. benthamiana*, demonstrating that they do not trigger a cell death response in the absence of the cognate resistance gene (Figure 3.8a). However, strong and very reproducible HRs were elicited within 4–5 dpi upon co-expression of R3a with *Avr3a^{KI}*, *Avr3a^{KI/Y147del}*, *Avr3a^{KIL}*, *Avr3a^{KIH}* and PEX147-3. However, no visible HRs were elicited on the R3a sites co-infiltrated with either *Avr3a^{EM}*, *Avr3a^{EMG}*, *Avr3a^{EMH}* or PEX147-2 (Figure 3.8a, b). Results from 3 independent replicates were analysed and summarised (Figure 3.8c). These results demonstrate that all *Avr3a^{KI}* derived variants are recognised by R3a whereas the variants derived from *Avr3a^{EM}* evade recognition by R3a. In line with previous findings (Bos *et al.*, 2006), the paralog PEX147-3 is recognised by R3a whereas PEX147-2 evades recognition.

To investigate whether the variants *Avr3a^{EMH}*, *Avr3a^{EMG}* and the paralog, PEX147-2 are also weakly recognised by R3a, agro-infiltration results obtained after 5 dpi were visualized under UV light. A weak accumulation of polyphenolic compounds was detectable on co-infiltrated sites of R3a with *Avr3a^{EM}* and *Avr3a^{EMG}* but not with

Avr3a^{EMH} or Pex147-2 (Figure 3.9). These results indicate that, similar to Avr3a^{EM}, R3a also weakly recognises Avr3a^{EMG} but not Avr3a^{EMH} or PEX147-2.

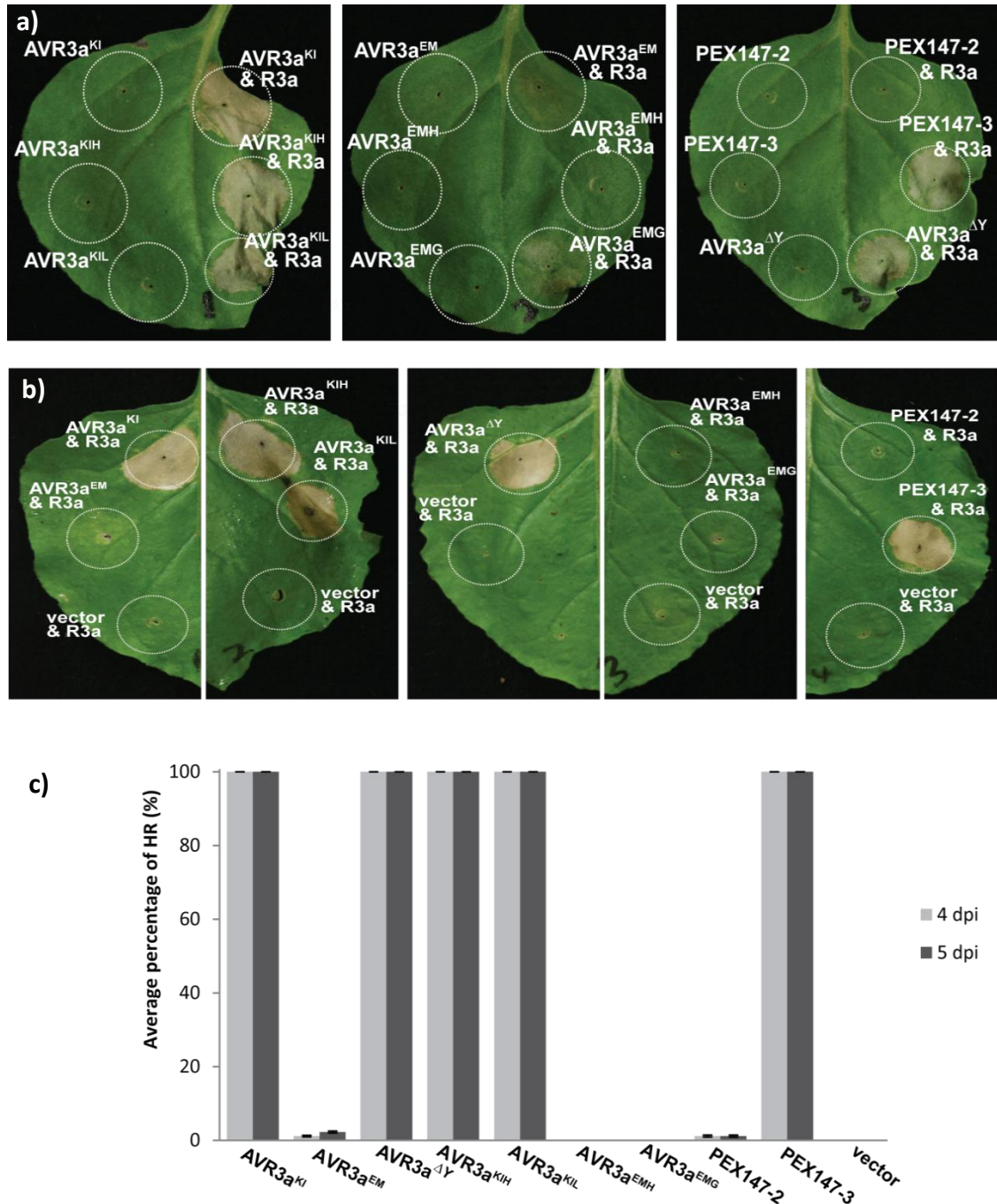


Figure 3.8: Recognition of Avr3a alleles and paralogs by R3a. Expression of *Avr3a* alleles and paralogs does not yield cell death responses in *N. benthamiana* in the absence of R3a. Alleles and paralogs of *Avr3a* were expressed via *A. tumefaciens* (left site of the leaves) and co-infiltrated with R3a (right site of the leaves) (a). The development of phenotypically distinct cell death responses associated with the HR following the recognition of *Avr3a* alleles and paralogs by R3a was compared to empty vector control (b) and recorded visually at 4 and 5 days post inoculation (c). The percentages of sites developing HRs were calculated based on 30 infiltrations per experiment and 3 independent biological replicates.

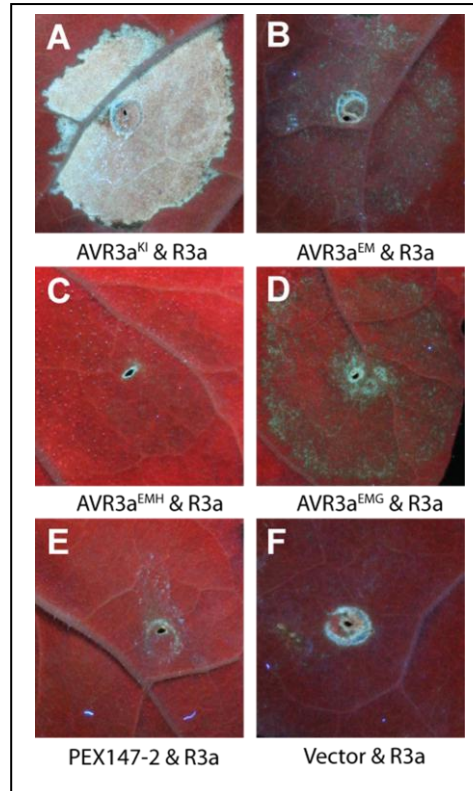


Figure 3.9: Autofluorescence associated with cell death responses in *N. benthamiana*. Avr3a alleles and paralogs were co-infiltrated with R3a and autofluorescence was recorded under UV at 5 days post-infiltration.

As shown above, R3a strongly recognizes Avr3a^{KIH}, Avr3a^{KIL} and PEX147-3 but fails to elicit a phenotypically distinct HR following co-infiltration with Avr3a^{EMH}, Avr3a^{EMG} and PEX147-2. Previous studies have shown that mutations in Avr3a can affect protein stability *in planta* and thus impact on the recognition by the resistance protein R3a (Bos *et al.*, 2009). To address the question whether the differences in recognition of these Avr3a alleles and paralogs is attributed to protein instability *in planta*, N-terminal fusion constructs were constructed. In all subsequent sections it has been assumed that the stability of the native protein is similar to that of the fusion proteins; similar assumptions have been made in previous studies (Bos *et al.*, 2006; 2009; 2010; Oh *et al.*, 2009; Gilroy *et al.*, 2011a).

Gateway technology, the *Avr3a* alleles and paralogs (minus the signal peptide) were cloned in frame to an N-terminal CFP epitope in the vector pB7WGC2 which was assessed in terms of gene expression above (Section 3.3.1). The constructs CFP-*Avr3a*^{KIH}, CFP-*Avr3a*^{KIL}, CFP-*Avr3a*^{EMH}, CFP-*Avr3a*^{EMG}, CFP-PEX147-3 and CFP-PEX147-2 were generated. The positive controls used in this study were *Avr3a*^{KI}, *Avr3a*^{EM} and *Avr3a*^{KI/Y147del} which had already been cloned into pB7WGC2 resulting in the constructs CFP-*Avr3a*^{KI}, CFP-*Avr3a*^{EM} and CFP-*Avr3a*^{KI/Y147del} (Bos *et al.*, 2010). All constructs were initially infiltrated side-by-side on their own and with R3a in *N. benthamiana* leaves to establish if the N-terminal fusions display identical recognition patterns if compared to the un-tagged constructs (Figure 3.10).

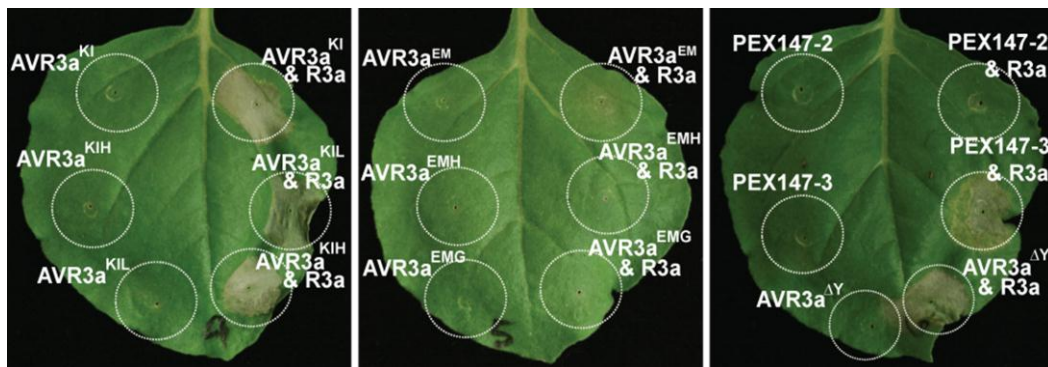


Figure 3.10: Expression of N-terminal CFP tagged *Avr3a* alleles and paralogs in *N. benthamiana*. Tagged alleles and paralogs of *Avr3a* were expressed via *A. tumefaciens* (left side of the leaves) and co-infiltrated with R3a (right side of the leaves). The development of phenotypically distinct cell death responses associated with the HR following the recognition of *Avr3a* alleles/paralogs by R3a was recorded visually at 4 and 5 days post inoculation

As shown in Figure 3.10, expression of CFP-fusions of *Avr3a* alleles and paralogs in the absence of R3a does not elicit a visible plant response. Co-infiltration with R3a triggers an HR response for *Avr3a*^{KIH}, *Avr3a*^{KIL} and PEX147-3 but not for *Avr3a*^{EMH}, *Avr3a*^{EMG} and PEX147-2. Thus, the N-terminal fusions displayed identical recognition patterns if compared to the non-tagged constructs.

A. tumefaciens strains carrying each of the constructs alone were infiltrated in *N. benthamiana* leaves to isolate the corresponding proteins. Following expression for 4–5 dpi, inoculated areas were excised, collected and subjected to western blot analysis using a GFP antibody to detect CFP-fusion products. No cross activity of the GFP antibody was found with other proteins and a strong, single signal of about 40 kDa in size was detected for Avr3a^{KIH}, Avr3a^{KIL}, Avr3a^{EMH}, Avr3a^{EMG} and PEX147-3. The signal strength of these proteins was comparable to the controls Avr3a^{KI}, Avr3a^{EM} and Avr3a^{KI/Y147del} (Figure 3.11). The lack of R3a-specific HRs upon co-infiltration with Avr3a^{EM} derived alleles is not due to instability of these alleles but consistent with their ability to evade recognition by R3a. Interestingly, PEX147-2 yielded no product under these conditions. Variations in the protocol and inclusion of the silencing suppressor p19 in 5 independent experiments did not produce a detectable signal for PEX147-2 (data not shown), suggesting that this Avr3a paralog is not stable *in planta*.

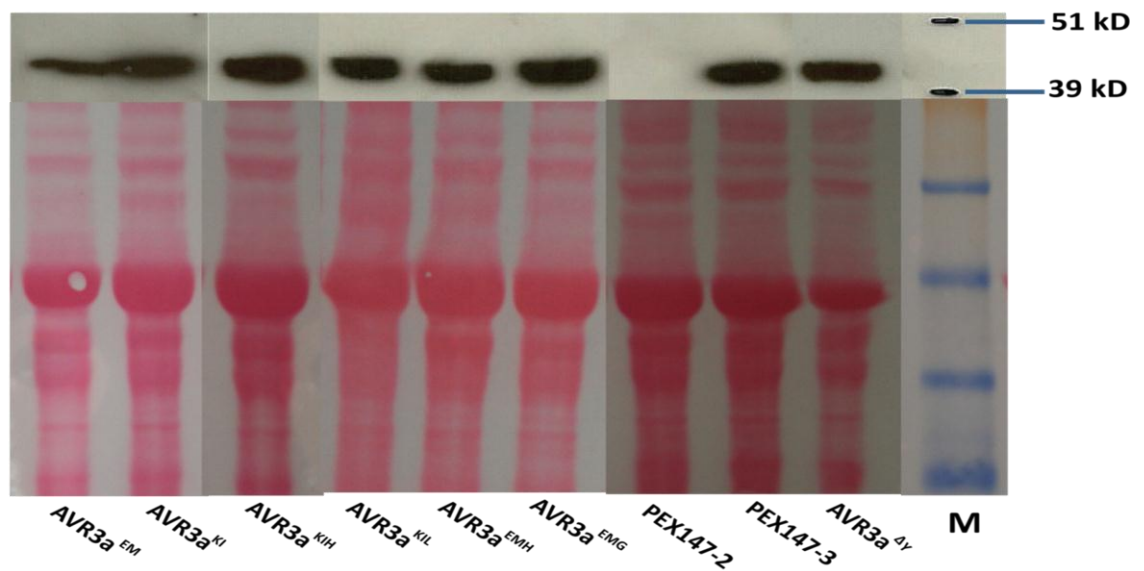


Figure 3.11: N-terminal fusions of the Avr3a alleles with CFP were used to demonstrate stability of the constructs *in planta*. Protein extracts from sites that transiently expressed the CFP-Avr3a alleles were sampled and, following western blotting, probed with an anti-GFP antibody. Equal loading was ensured by visualising protein samples after western blotting with Ponceau staining. Protein sizes are shown in kDa and correspond to a protein size marker (M) that was run alongside the sample.

3.3.5 Inhibition study of R3a-dependent recognition by Avr3a alleles

As mentioned before, adapted pathogens can use multiple mechanisms to evade detection by the host immune system (Vleeshouwers *et al.*, 2011). Recent studies (Chen *et al.*, 2012; Wang *et al.*, 2011) have shown that one of these strategies can involve suppression of HRs following recognition. To rule out potential inhibitory functions of Avr3a^{EM}, Avr3a^{EMG} and Avr3a^{EM} and the paralogs PEX147-2/PEX147-3 on the recognition of Avr3a^{KI} by R3a, untagged version of Avr3a^{EM} variants and paralogs were co-infiltrated in *N. benthamiana* with R3a and untagged Avr3a^{KI}. In all cases, a clear HR developed by 4–5 dpi (Figure 3.12). Thus, the lack of R3a-specific HRs upon co-infiltration with Avr3a^{EM} derived alleles/paralogs is not due to instability of the effector variants or suppression of R3a-dependent recognition but consistent with their ability to evade recognition by R3a.

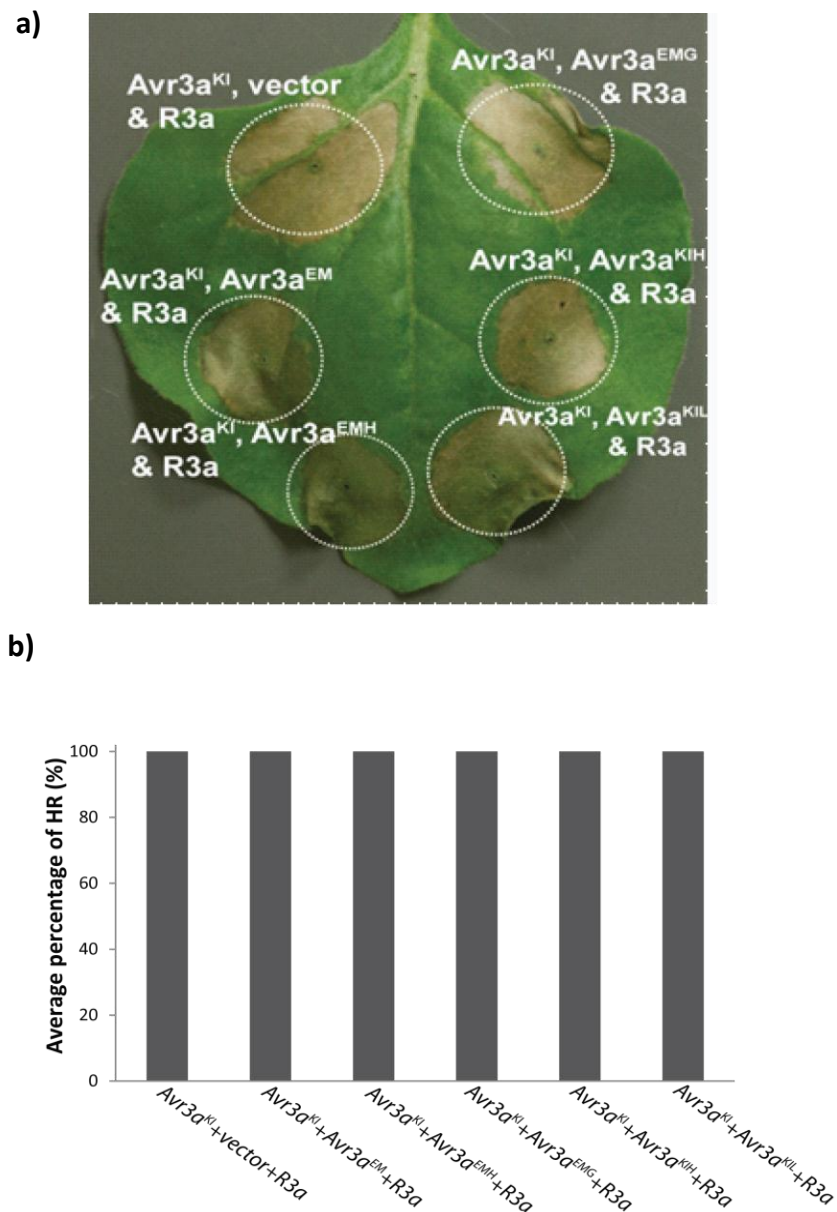


Figure 3.12: Avr3a alleles and paralogs do not inhibit cell death responses elicited by co-infiltration of Avr3a^{KI} and R3a in *N. benthamiana*. (a) Avr3a alleles and paralogs or an empty vector control were co-infiltrated with Avr3a^{KI} and R3a. The development of phenotypically distinct cell death responses associated with the HR following the recognition of Avr3a^{KI} by R3a was recorded visually at 4 days post inoculation. (b) The graph was plotted based on 90 infiltration sites produced from 3 independent experiments. The HRs were scored at 4 dpi.

3.4 DISCUSSION

The first part of this study focused on establishing a robust, transient *Agrobacterium tumefaciens* based effector expression system that is suitable for Gateway cloning and facilitates functional studies of Avr3a alleles and paralogs in *N. benthamiana*. Many *P.*

infestans effectors have been cloned into a Gateway compatible donor vector, pDONR201, which utilizes Kanamycin resistance as a selectable marker. The binary expression vector pGWB402Ω was the initial destination vector of choice for cloning as it contains the selectable antibiotic Spectinomycin and thus allows discrimination against non-recombinant pDONR201 plasmids. Unfortunately, expression with this vector was weak if compared to alternative vectors pGRAB[GW] and pB7WGC2 (Figures 3.3 and 3.4). This was an unexpected result as all vectors utilise the same promoter (CMV 35S) and were delivered via the same *Agrobacterium* strain, Agl1. We speculate that the expression differences are due to differences in the origin of replication or stabilisation of the plasmids as this will impact on plasmid copy-numbers in *Agrobacterium*. The vector pGRAB is based on the vector pGREEN which contains a pCo1E1 *ori* that only functions in *E. coli* (Hellens *et al.*, 2000). Thus, to replicate in *Agrobacterium*, the helper plasmid pSoup is needed which contains the pSa replication locus (Hellens *et al.*, 2000). The pB7WGC2 binary vector is utilising the Co1E1 and pVS1 origins for replication in *E. coli* and *Agrobacterium* respectively (Karimi *et al.*, 2002). The vector pGWB402Ω carries the replication origin Co1E1 for *E. coli* and *rep*, which is described as a broad host range replication origin for *Agrobacterium* (Nakagawa *et al.*, 2007). Regardless of the individual molecular properties of the expression vectors, the vectors pGRAB[GW] and pB7WGC2 yielded the most robust phenotypes and were used for functional studies that require untagged or tagged Avr3a alleles and/or paralogs, respectively.

Avr3a is an essential effector for *P. infestans* (Bos *et al.*, 2010). Previous studies have shown that *Avr3a* is up-regulated during the biotrophic phase of infection and silencing of this gene significantly reduces virulence on normally susceptible hosts (Vetukuri *et*

al., 2011). Bos *et al.*, (2010) have shown that Avr3a^{KI} and Avr3a^{EM} are fully functional in that both alleles can complement loss of Avr3a^{EM} in the *P. infestans* isolate 88069 (please see Chapter 5). Further data provided by Armstrong *et al.* (unpublished) have shown that limited variation of Avr3a exists in the Toluca Valley/Mexico, a region of *Solanum* and *P. infestans* co-evolution (Gruenwald & Flier, 2005). In addition to Avr3a^{EM} and Avr3a^{KI}, the alleles Avr3a^{KIL}, Avr3a^{KIH}, Avr3a^{EMG} and Avr3a^{EMH} were discovered. However, as mentioned before, these alleles were only identified in conjunction with Avr3a^{EM} and/or Avr3a^{KI} (Table 3.1; Figure 3.1). The low frequency of these additional Avr3a alleles in Mexico is consistent with a ‘recent’ selective sweep and has also been observed for European and Southern American *P. infestans* populations (Armstrong *et al.*, 2005; Cardenas *et al.*, 2011; Chapter 1).

In terms of the likely origin of the Avr3a alleles and paralogs, the chief driver in nature to generate new genes with novel function is through gene duplication followed by sequence divergence (Long *et al.*, 2003; Roth *et al.*, 2007). Subsequently, both genetic drift and positive selection play a role to fix duplicated genes in the host–pathogen co-evolution process (Lynch & Conery, 2000). The phenomena is known as gene ‘birth and death’ and is common in gene families (Hughes & Nei, 1989). New genes which are derived from gene duplications are referred to as paralogous genes. It was proposed by Armstrong *et al.* (2005) that Avr3a^{EM} arose from an Avr allele after gene duplication and positive selection. The additional Avr3a alleles which have been studied in this thesis are likely to have arisen from mutations within the Avr3a^{KI} or Avr3a^{EM} background, respectively. Only one amino acid substitution (Q133H) is shared between the additional Avr3a^{KI} and Avr3a^{EM} derived alleles and could be a result of a gene conversion event (Chen *et al.*, 2007).

As outlined below, it is tempting to speculate that the limited diversity of *Avr3a* is directly related to effector function. The *P. infestans* effector *Avr3a* has at least two distinct functions which include suppression of the PTI responses triggered by INF1 perception and inducing a hypersensitive response following recognition by R3a (Bos *et al.*, 2005; 2009; 2010). In terms of plant–pathogen co-evolution, it would be advantageous for *P. infestans* to generate *Avr3a* isoforms that suppress PTI including INF1 cell death but evade recognition by R3a. Interestingly, in a mutational study of *Avr3a^{KI}* and *Avr3a^{EM}*, Bos *et al.* (2009) failed to identify such forms of *Avr3a*, despite screening in excess of 11,000 mutants. Indeed, only four amino acid substitutions in *Avr3a^{KI}* lead to evasion of R3a recognition but failed subsequently to suppress ICD (Figure 3.5). Interestingly, these artificially generated changes in the amino acid sequence of *Avr3a^{KI}* resulted in decreased protein stability *in planta* which was not observed for the naturally occurring *Avr3a^{KI}* and *Avr3a^{EM}* variants from the Toluca Valley (Figure 3.11). In contrast, upon infiltration of N-terminal, CFP-*Avr3a* fusions in the model Solanaceae *N. benthamiana*, the naturally occurring *Avr3a* alleles displayed similar protein accumulation and thus stability if compared to *Avr3a^{KI}* and *Avr3a^{EM}* (Figure 3.11).

The study by Bos *et al.* (2009) has also identified 19 mutations in *Avr3a^{EM}* which repeatedly yield a gain of recognition phenotype upon co-infiltration with R3a (Figure 3.5). This provides evidence that there are limited amino acid positions that can be modified by the pathogen to maintain virulence function whilst evading recognition by R3a. Indeed, the naturally occurring amino acid substitution in the *Avr3a^{KI}* background retained their recognition by R3a whereas those in the *Avr3a^{EM}* background do not elicit R3a-dependent HRs (Figures 3.8; Figure 3.9). In line with this, the naturally

occurring amino acid substitutions do not coincide with changes that resulted in R3a gain-of-recognition mutations described by Bos *et al.* (2009) (Figure 3.5). The finding that Avr3a^{EM} appears to be fully functional as a virulence determinant is consistent with the population data presented by Armstrong *et al.* (Table 3.1; Figure 3.1) which has revealed a high percentage of *P. infestans* isolates containing Avr3a^{EM}.

Surprisingly, despite sharing less than 20% sequence similarity, the *P. capsici* effector Avr3a11 (which is homologous to *P. infestans* Avr3a and *P. sojae* Avr1b) and *P. infestans* effector PexRD2 (a promoter of plant cell death (Oh *et al.*, 2009)), share a similar α -helical fold termed the “WY-domain” (Boutemy *et al.*, 2011). The two motifs that make up the WY-domain, W and Y, have been identified in many RXLR effectors from *Phytophthora* species and led to the hypothesis that, in many cases, RXLR effectors are derived from common ancestors (Jiang *et al.*, 2008). Mutations in the W and Y domain of *P. capsici* Avr1b impacted to various degrees on the ETS function of Avr1b and also the ETI response following perception by the soybean resistance gene RPS1b (Dou *et al.*, 2008). It is estimated that approximately 44% of annotated *Phytophthora* RXLR containing effectors share the WY-domain and that in many cases important structural as well as polymorphic surface exposed residues are harboured within this domain (Boutemy *et al.*, 2011). In this context, it has been shown that Avr3a amino acid 80 (E/K) and 103 (M/I) reside as surface exposed amino acids on α helix 1 and 2, respectively (Boutemy *et al.*, 2011; Yaeno *et al.*, 2011; Figure 3.6).

The additional C-terminal variations R124G, Q133H and M139L identified in Avr3a^{EMG124} (Avr3a^{EMG}), Avr3a^{EMH133} (Avr3a^{EMH}) as well as Avr3a^{KIH133} (Avr3a^{KIH}) and Avr3a^{KIL139} (Avr3a^{KIL}) are, with the exception of Avr3a^{EMG} which resides in loop 3,

located in the Y-domain of the $\alpha 4$ helical region and are all surface exposed (Figure 3.5). Therefore, all naturally occurring variations of Avr3a are within the WY-domain. In addition, Bos *et al.* (2009) have shown that Avr3a^{EM} gain of R3a recognition mutations are found throughout Avr3a^{EM} but not within the $\alpha 4$ helical region (Bos *et al.*, 2009; Figure 3.5). With the exception of the mutation S123C in loop 3, the majority of gain of recognition mutations did not significantly boost INF1-cell death suppression function (Bos *et al.*, 2009). This is consistent with dual function for the Avr3a effector (Bos *et al.*, 2005; 2009) and the subject of the studies in Chapter 4 and 5. Boutemy *et al.* (2011) has proposed a model for the structure/function relationship in Avr3a and has shown that the amino acids K/E80 and I/M103 of Avr3a map to E71 and Q94 in Pc_Avr3a11. These residues locate to the same face of the four-helix bundle. Interestingly, the additional changes (Pi_Q133H equivalent to Pc_R120 and Pi_M139L representing Pc_M126) are located on helix 4. The face of helix 4 is distinct from the protein face in which K/E80 and I/M103 reside. The amino acid substitution Pi_R124G resides within the loop 3 of *P. capsici* (Pc_K111-Y118) and is also surface exposed (Figure 3.6).

Amino acid replacement in surface residues is one of the proposed models for the evolution of RXLR effectors (Boutemy *et al.*, 2011; Win *et al.*, 2012). In this context, and in line with a dual function of Avr3a, the amino acid substitutions did not impact on R3a recognition. Avr3a^{KI}, Avr3a^{KIH} and Avr3a^{KIL} maintained their recognition by R3a whereas Avr3a^{EM}, Avr3a^{EMH} and Avr3a^{EMG} avoided recognition (Figure 3.8). However, under UV light Avr3a^{EM} and Avr3a^{EMG} displayed an accumulation of phenolic compounds that is typically associated with recognition responses whereas Avr3a^{EMH} did not display the same weak recognition phenotype (Figure 3.9). As Avr3a^{EMH} is stable *in planta* (Figure 3.10) it is tempting to speculate that Avr3a^{EMH} has either lost its

virulence function, modifies a guarded virulence target in a way that is no longer detected by R3a (assuming an indirect interaction) or evades direct interaction with R3a.

Gain of additional virulence functions that enables Avr3a^{EMH} to suppress recognition by R3a could be ruled out. Using co-infiltration of Avr3a^{KI} and R3a in the presence of the additional Avr3a alleles, a strong HR response was detectable in all combinations (Figure 3.12) which provides evidence that the Avr3a^{EM} derived alleles do not function as dominant/negative repressors or have gained additional virulence function that would enable them to suppress R3a specific PCD. However, in other pathogen systems, some effectors have been found that can suppress hypersensitive cell death induced by another effector even in the presence of its cognate R proteins (Dodds & Rathjen, 2010). Resistance mediated by the tomato *I-2* and *I-3* genes can be suppressed by Avr1 from *Fusarium oxysporum* f.sp. *lycopersici* (Houterman *et al.*, 2008). In recent studies, IPI-O4 was shown to function as a repressor and perturbs the HR elicited by IPI-O1 recognition by Rpi-blb1 (Halterman *et al.*, 2010; Chen *et al.*, 2012). In addition, Wang *et al.* (2011) have reported on 'immediate-early effectors' from *P. sojae* that can suppress PCD triggered by many 'early' effectors as well as PAMPS. The authors proposed an interesting model by which the pathogen evades or even pre-empts recognition by the host plant (Wang *et al.*, 2011).

When discovered, Avr3a^{KI} was flanked by two paralogous genes, *Pex147-2* and *Pex147-3*, and one pseudogene (*Pex147p*) which contained a frameshift within the coding sequence (Armstrong *et al.*, 2005). According to Armstrong *et al.* (2005) *Pex147-2* is weakly expressed in *P. infestans* whereas *Pex147-3* is not expressed. As shown in this

study, PEX147-3 is recognised by R3a whereas PEX147-2 is not. However, Pex147-2 is not stable *in planta*, suggesting that the failure of recognition of Pex147-2 by R3a is due to instability of this protein. A similar scenario was reported for Avr3a^{KI} R3a-loss-of-function mutants (Figure 3.5), whereby these mutants were not recognised by R3a due to protein instability *in planta* (Bos *et al.*, 2009). Alignment between Avr3a and the paralogs have identified 7 amino acids in Pex147-2 which are different if compared to Avr3a and Pex147-3 which were shown to be stable *in planta* (Figure 3.5; Figure 3.11; Table 3.3).

The involvement of these amino acids on the stability of Pex147-2 *in planta* has been determined by superimposing the Pex147-2 amino acid changes onto Pi_Avr3a and Pc_Avr3a11. With the exception of Pi_Pex147-2C138, which represents an insertion of an amino acid, the remaining polymorphisms are located on surface residues of the protein that are unlikely to contribute to protein stability *in planta* (Bos *et al.*, 2009; Boutemy *et al.*, 2011) (Figure 3.5; Figure 3.7). Interestingly, the amino acid C138 in PEX147-2 is a unique insertion and displaces the buried amino acid Y139 (Pi_Avr3aY139) that has been shown to be important for protein integrity (Boutemy *et al.*, 2011)(Figure 3.5; Figure 3.7). Thus, insertion of C138 and the subsequently predicted structure disruption is the most likely cause for protein instability of PEX147-2 *in planta*.

Based on this result, Pex147-2 represents an additional pseudomolecule in addition to *Pex147p*. Win *et al.* (2007) suggested that detection of pseudogenes among RXLR effectors could be seen as further evidence for host/pathogen co-evolution. However, the reason why *P. infestans* retains PEX147-2 expression remains to be elucidated.

Conversely, albeit amino acid substitutions also occur in PEX147-3, the stability of this protein is retained *in planta*. However, PEX147-3 has been shown to be recognised by R3a, suggesting that the expression of PEX147-3 might be lost in *P. infestans* as a consequence of this recognition (Armstrong *et al.*, 2005). This strategy by the pathogen is not unprecedented as, for example, the expression of *P. infestans* effector *Avr4* can also be lost to most likely evade recognition by the potato resistance protein R4 (Van Poppel *et al.*, 2008).

CHAPTER 4

4 SUPPRESSION STUDY OF CMPG1-MEDIATED CELL DEATH RESPONSES BY Avr3a ALLELES AND THE PARALOGS PEX147-2 and PEX147-3

4.1 INTRODUCTION

Suppression of host PTI responses upon infection is a prerequisite for adapted pathogens to successfully establish disease. Some of the utilised mechanisms are emerging for bacterial pathogens and have been determined as a primary function of T3SS effectors from plant pathogenic bacteria (Abramovich *et al.*, 2006; Block & Alfano, 2008; Chisholm *et al.*, 2006; Jones & Dangl, 2006; Zhou & Chai, 2008).

As alluded to in Chapter 1, it has been shown that effectors from fungal and oomycete pathogens also actively suppress plant innate immunity (Dodds *et al.*, 2009; Hein *et al.*, 2009). For example, delivery of *H. arabidopsidis* (*Hpa*) ATR1 and ATR13 proteins via the *Pseudomonas syringae* T3SS yields enhanced growth of bacteria on susceptible *Arabidopsis* plants (Sohn *et al.*, 2007). This is linked to the ability of ATR13 to suppress callose deposition and the production of reactive oxygen species in an allele dependent manner following bacterial PAMP recognition (Sohn *et al.*, 2007). A similar activity was observed for the *Hpa* effector RXLR 29 (Cabral *et al.*, 2011). Effectors utilise diverse modes of action and some prevent PTI initiation, function downstream of PAMP perception or prevent ETI responses. For example, the *Cladosporium fulvum* effector ECP6 contains LysM domain and prevents PTI by sequestering chitin oligosaccharides that are released from the fungal hyphae (de Jong *et al.*, 2010). The *P. sojae* effector AVR1b is able to suppress PCD mediated by the proapoptotic protein BAX, a function that has also been shown for many bacterial

effectors (Dou *et al.*, 2008a; Jamir *et al.*, 2004). *P. infestans* AvrBlb2, on the other hand, prevents secretion of the host defence associated papain-like cysteine protease C14 into the host apoplast and thus promotes virulence (Bozkurt *et al.*, 2011). As mentioned before, *P. infestans* AvrBlb1 allele IPI-04 prevents ETI following recognition of IPI-01 and IPI-02 by the cognate potato resistance gene Rpi_BLB1 (also known as RB) (Chen *et al.*, 2012; Champouret *et al.*, 2009). A similar suppression of ETI responses has also been shown for a number of *P. sojae* effectors that prevent HRs following expression of Avh241 and Avh238 (Wang *et al.*, 2011).

P. infestans Avr3a is an essential effector and has been shown to interact with 13 host proteins in yeast-2-hybrid assays including the host U-box E3 ligase CMPG1 (Bos *et al.*, 2010). An important function of Avr3a^{KI} and Avr3a^{EM} is to interact with and stabilize CMPG1 to suppress CMPG1-dependant cell death responses including ICD and CF-4/AVR4 mediated cell death (Bos *et al.*, 2010; Gilroy *et al.*, 2011a; Chapter 1).

4.2 AIM

The aims of the studies presented in this Chapter were to:

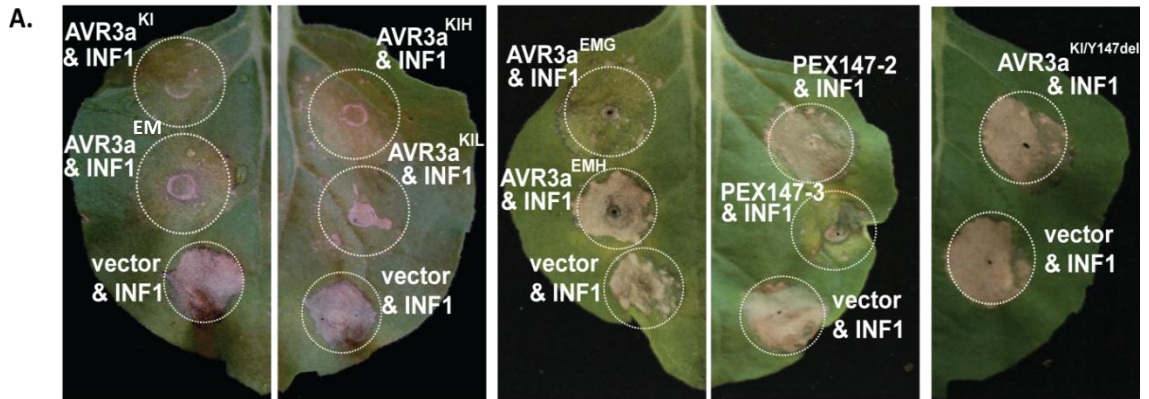
- a) determine the ability of the Avr3a alleles and paralogs to suppress INF1 and CF-4/Avr4 mediated cell death.
- b) assess the ability of the Avr3a alleles and paralogs to interact with and stabilise CMPG1 *in planta*.
- c) identify common virulence targets for Avr3a alleles and paralogs via yeast-2-hybrid analysis.

4.3 RESULTS

4.3.1 Suppression study of INF1 and CF-4/Avr4 mediated cell death by Avr3a alleles and paralogs

The ability of the Avr3a alleles Avr3a^{EMG}, Avr3a^{EMH}, Avr3a^{KIH}, Avr3a^{KIL} and paralogs PEX147-2 and PEX147-3 to suppress CMPG1-dependent cell death responses in *N. benthamiana* following transient, *A. tumefaciens* based expression of *Inf1* and *C. fulvum* *Avr4* co-infiltration with the cognate tomato receptor *CF-4*, was assessed as shown by Gilroy *et al.* (2011a). Co-infiltration of INF1 or CF-4/Avr4 with Avr3a^{KI/Y147del} was used as a negative control as previous data have shown that the tyrosine in position 147 is required for ICD and CF-4/Avr4 suppression (Bos *et al.*, 2009; 2010; Gilroy *et al.*, 2011a). The results from three independent experiments, totalling 90 individual inoculations per variant and elicitor, are shown in Figures 4.1 and 4.2. Statistical analysis was carried out using a Mann-Whitney U test method for non-parametric data (Tables 4.1; Table 4.2).

Consistent with previous results, compared to Avr3a^{KI/Y147del}, Avr3a^{EM} and Avr3a^{KI} very highly significantly ($p < 0.001$) suppress ICD responses with Avr3a^{KI} displaying the strongest ICD suppression ability. Similarly, Avr3a^{KIH}, Avr3a^{KIL} and Avr3a^{EMG} very highly significantly ($p < 0.001$) suppress ICD whereas Avr3a^{EMH} displays limited suppression function that is comparable and statistically not significantly different ($p = 0.455$) to Avr3a^{KI/Y147del} (Figure 4.1; Table 4.1). Interestingly, the Avr3a paralog PEX147-3 could very highly significantly ($p < 0.001$) suppress ICD if compared to Avr3a^{KI/Y147del} whereas the unstable paralog PEX147-2 was unable to suppress ICD and yielded a slightly higher, statistically significant ($p = 0.037$) rate of ICD if compared to Avr3a^{KI/Y147del} (Figure 4.1; Table 4.1).



B.

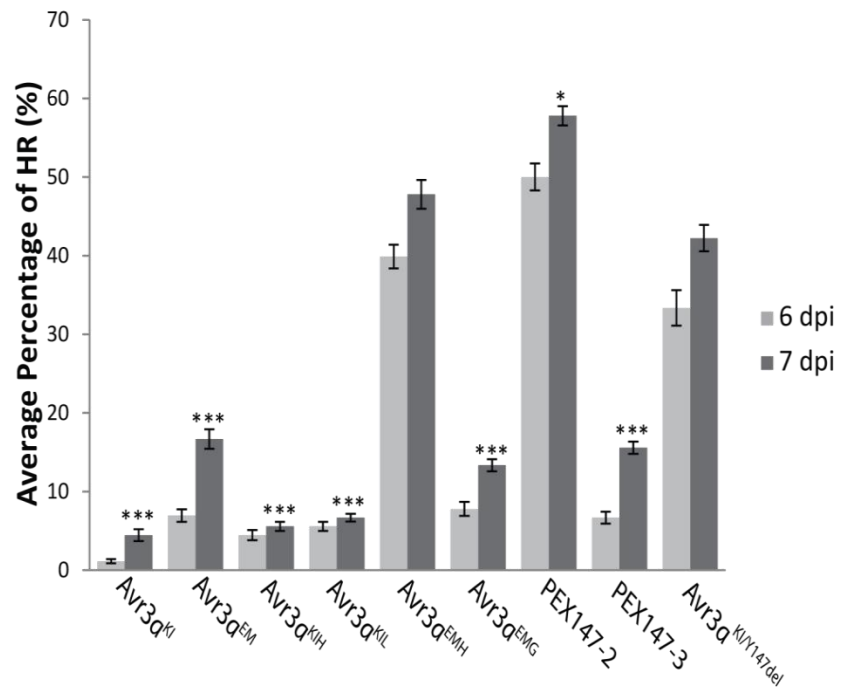


Figure 4.1: Effects of the co-expression of Avr3a alleles and paralogs on CMPG1-dependent cell death responses triggered by transient expression of INF1 in *N. benthamiana*. A) INF1 was co-infiltrated with un-tagged Avr3a alleles and paralogs. Development of phenotypically distinct INF1-mediated cell death responses was recorded visually at 6 and 7 days post inoculation. B) The percentages of cell death responses were calculated based on three independent experiments with 30 infiltrations per experiment. Statistically significant differences at 7 dpi are denoted by stars (***)*p*-value of <0.001, **p*-value of <0.05).

Table 4.1: Statistical analysis (Mann-Whitney U-test method) of INF1 cell death suppression activity of Avr3a alleles and paralogs.

Avr3a^{KI} n=90 Mean; 4.44444 Stdev; 7.24355 Stderror; 0.76353	Avr3a^{EM} n=90 Mean; 16.66666 Stdev; 11.78511 Stderror; 1.24226	Avr3a^{KIH} n=90 Mean; 5.55555 Stdev; 5.55555 Stderror; 0.58560	Avr3a^{KIL} n=90 Mean; 6.66666 Stdev; 4.64811 Stderror; 0.48995	Avr3a^{EMH} n=90 Mean; 47.77777 Stdev; 17.39164 Stderror; 1.83324	Avr3a^{EMG} n=90 Mean; 13.33333 Stdev; 7.45356 Stderror; 0.78567	PEX147-2 n=90 Mean; 57.77777 Stdev; 11.52026 Stderror; 1.21434	PEX147-3 n=90 Mean; 15.55555 Stdev; 7.24355 Stderror; 0.76353	Avr3a^{KI/AY} n=90 Mean; 42.22222 Stdev; 16.0054 Stderror; 1.68711
Avr3a^{KI} n=90	U = 3555 $p=0.008$	U = 3960 $p=0.516$	U = 3960 $p=0.516$	U = 2295 $p<0.001$	U = 3690 $p=0.037$	U=1890 $p<0.001$	U=3645 $p=0.022$	U=2520 $p<0.001$
	Avr3a^{EM} n=90	U=3645 $p=0.037$	U=3645 $p=0.037$	U=2790 $p<0.001$	U=3915 $p=0.532$	U=2385 $p<0.001$	U=3960 $p=0.682$	U=3015 $p<0.001$
		Avr3a^{KIH} n=90	U=4050 $p=1.000$	U=2385 $p<0.001$	U=3780 $p=0.137$	U=1980 $p<0.001$	U=3735 $p=0.090$	U=2610 $p<0.001$
			Avr3a^{KIL} n=90	U=2385 $p<0.001$	U=3780 $p=0.137$	U=1980 $p<0.001$	U=3735 $p=0.090$	U=2610 $p<0.001$
				Avr3a^{EMH} n=90	U=2655 $p<0.001$	U=3645 $p=0.180$	U=2700 $p<0.001$	U=3825 $p=0.455$
					Avr3a^{EMG} n=90	U=2250 $p<0.001$	U=4005 $p=0.830$	U=2880 $p<0.001$
						PEX147-2 n=90	U=2295 $p<0.001$	U=3420 $p=0.037$
							PEX147-3 n=90	U=2925 $p<0.001$

In agreement with ICD suppression function, the Avr3a variants displayed a somewhat similar ability to perturb CF-4/Avr4 elicited PCD (Figure 4.2; Table 4.2). Compared to Avr3a^{KI/Y147del}, the alleles Avr3a^{KI}, Avr3a^{EM}, Avr3a^{KIH}, Avr3a^{KIL} and Avr3a^{EMG} all very highly significantly ($p < 0.001$) suppressed the HR induced by CF-4/Avr4. In contrast, Avr3a^{EMH} failed to statistically significantly ($p = 1.000$) impact on this HR development (Figure 4.2).

Interestingly, compared to Avr3a^{KI/Y147del}, PEX147-3 could ($p < 0.001$) suppress INF1 mediated cell death (Figure 4.1; Table 4.1) but could not significantly suppress CF-4/Avr4 mediated cell death ($p = 0.448$) (Figure 4.2; Table 4.2). Similarly, the unstable PEX147-2 failed to significantly suppress the PCD response elicited by CF-4/Avr4 ($p = 0.682$) (Figure 4.2; Table 4.2).

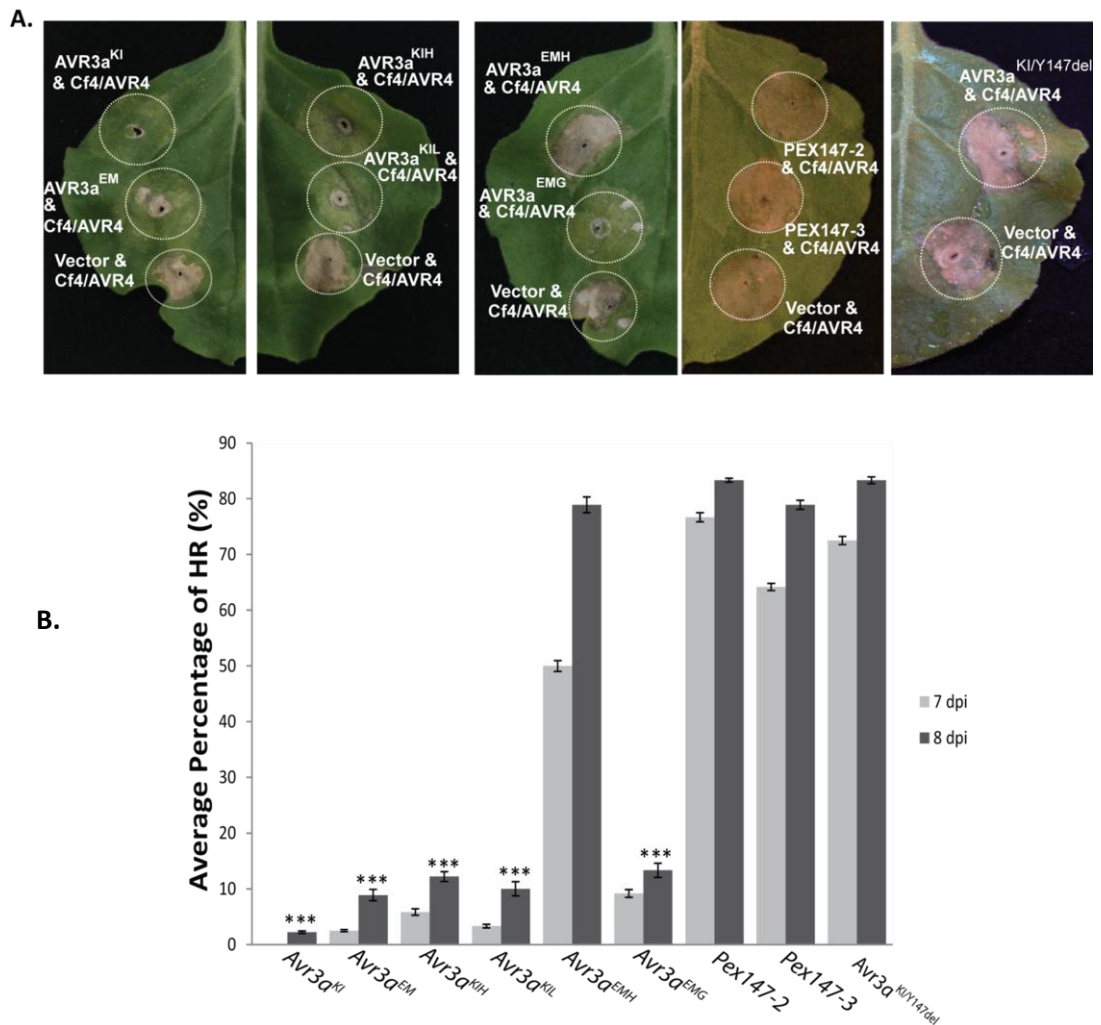


Figure 4.2: Effects of Avr3a alleles and paralogs on CMPG1-dependent cell death responses triggered by transient expression of CF-4/Avr4 in *N. benthamiana*. A) CF-4 and Avr4 were co-infiltrated with un-tagged Avr3a alleles and paralogs. Development of phenotypically distinct cell death responses was recorded visually at 6 and 7 days post inoculation. B) The percentages of cell death responses were calculated based on three independent experiments with 30 infiltrations per experiment. Statistically significant differences at 8 dpi are denoted by stars (***) p -value of <0.001).

Table 4.2: Statistical analysis (Mann-Whitney U-test method) of CF-4/Avr4 cell death suppression activity of Avr3a alleles and paralogs.

Avr3a^{KI} n=90 Mean; 1.66666 Stdev; 2.28217 Stderror; 0.20833	Avr3a^{EM} n=90 Mean; 6.66666 Stdev; 4.75073 Stderror; 0.43368	Avr3a^{KIH} n=90 Mean; 11.66666 Stdev; 3.48608 Stderror; 0.31823	Avr3a^{KIL} n=90 Mean; 9.16666 Stdev; 7.45355 Stderror; 0.68041	Avr3a^{EMH} n=90 Mean; 72.4 Stdev; 9.12870 Stderror; 0.83333	Avr3a^{EMG} n=90 Mean; 12.49999 Stdev; 8.33333 Stderror; 0.76072	PEX147-2 n=90 Mean; 85 Stdev; 4.75073 Stderror; 0.43368	PEX147-3 n=90 Mean; 65 Stdev; 6.97216 Stderror; 0.63646	Avr3a^{KI/AY} n=90 Mean; 84.16666 Stdev; 10.78515 Stderror; 0.98454
Avr3a^{KI} n=90	U = 3780 $p=0.052$	U =3645 $p=0.010$	U =3735 $p=0.030$	U =765 $p<0.001$	U = 3600 $p=0.006$	U=675 $p<0.001$	U=945 $p<0.001$	U=765 $p<0.001$
	Avr3a^{EM} n=90	U=3915 $p=0.468$	U=4005 $p=0.799$	U=1035 $p<0.001$	U=3870 $p=0.344$	U=945 $p<0.001$	U=1215 $p<0.001$	U=1035 $p<0.001$
		Avr3a^{KIH} n=90	U=3960 $p=0.636$	U=1170 $p<0.001$	U=4005 $p=0.824$	U=1080 $p<0.001$	U=1350 $p<0.001$	U=1170 $p<0.001$
			Avr3a^{KIL} n=90	U=1080 $p<0.001$	U=3915 $p=0.487$	U=990 $p<0.001$	U=1260 $p<0.001$	U=1080 $p<0.001$
				Avr3a^{EMH} n=90	U=1215 $p<0.001$	U=3960 $p=0.682$	U=3870 $p=0.448$	U=4050 $p=1.000$
					Avr3a^{EMG} n=90	U=1125 $p<0.001$	U=1395 $p<0.001$	U=1215 $p<0.001$
						PEX147-2 n=90	U=3780 $p=0.243$	U=3960 $p=0.682$
							PEX147-3 n=90	U=3870 $p=0.448$

4.3.2 *In planta* stabilisation of CMPG1 by Avr3a alleles and paralogs

The ability of the *Avr3a* alleles and paralogs to stabilise CMPG1 *in planta* was assessed using both Western blot analysis and confocal microscopy (Bos *et al.*, 2010). To observe the stabilisation of CMPG1 by Westerns, N-terminal myc tagged CMPG1 (4x-myc-ΔN-STCMPG1) was co-infiltrated with the *Avr3a* alleles and paralogs as well as with *Avr3a*^{KI/Y147del} and empty vector as negative controls in *N. benthamiana*.

In planta stabilisation of CMPG1 was assessed at three days post inoculation by extracting total protein samples from the co-infiltrated areas and probing the resulting western blots with an anti-myc antibody as shown by Bos *et al.* (2010). No product was detected in lanes representing co-expression of myc tagged CMPG1 with *Avr3a*^{KI/Y147del} or empty vector. This is consistent with CMPG1 being degraded *in planta* as described previously (Bos *et al.*, 2010). All untagged *Avr3a* alleles stabilised CMPG1 by 3 dpi albeit AVR3^{EMH} produced the faintest CMPG1 product (Figure 4.3A). However, all *Avr3a* paralogs co-expressed with myc tagged CMPG1 produced no signals, indicating that PEX147-2 and PEX147-3 are unable to stabilize CMPG1 *in planta* (Figure 4.3A).

C-terminal fusions of CMPG1 with YFP (StCMPG1-YFP) were used to corroborate the western data and to quantify the levels of CMPG1 stabilisation *in planta* using confocal microscopy. *Avr3a* alleles and paralogs were co-infiltrated with StCMPG1b-YFP (Bos *et al.*, 2010) in *N. benthamiana* and imaged at 2 dpi with the help of Dr Petra Boevink. Accumulation of YFP fluorescence in the plant nuclei, as evidence for CMPG1 stabilisation (Bos *et al.*, 2010), was readily observed for *Avr3a*^{KI}, *Avr3a*^{KIH}, *Avr3a*^{KIL}, *Avr3a*^{EM}, *Avr3a*^{EMG} and *Avr3a*^{EMH}. Consistent with the western blot analysis (Figure 4.3A), faint YFP fluorescence was also observed for *Avr3a*^{EMH} but not for PEX147-2,

PEX147-3, AVR3^{KI/Y147del} and empty vector control (Figure 4.3B). The YFP fluorescence intensity was measured and compared from independent experiments (Figure 4.3C). All Avr3a alleles yielded YFP fluorescence levels that were very significantly higher ($p < 0.001$; Avr3a^{KI}, Avr3a^{KIH}, Avr3a^{KIL}, Avr3a^{EMG}, Avr3a^{EMH} and Avr3a^{EM}) if compared to AVR3^{KI/Y147del} and empty vector controls. Both PEX147-2 and PEX147-3 did not yield any measurable YFP fluorescence which is in accordance with their western data and also the instability observed for PEX147-2 *in planta* (Figure 3.11). Statistically, the latter two were not significantly different if compared to the empty vector control ($p = 0.704$ [Pex147-2]; $p = 0.215$ [Pex147-3]).

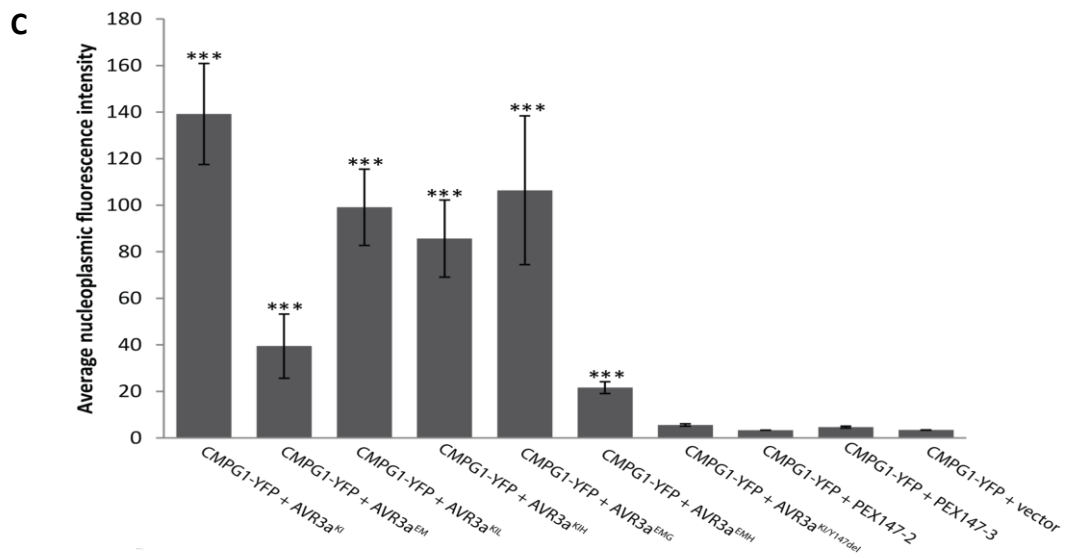
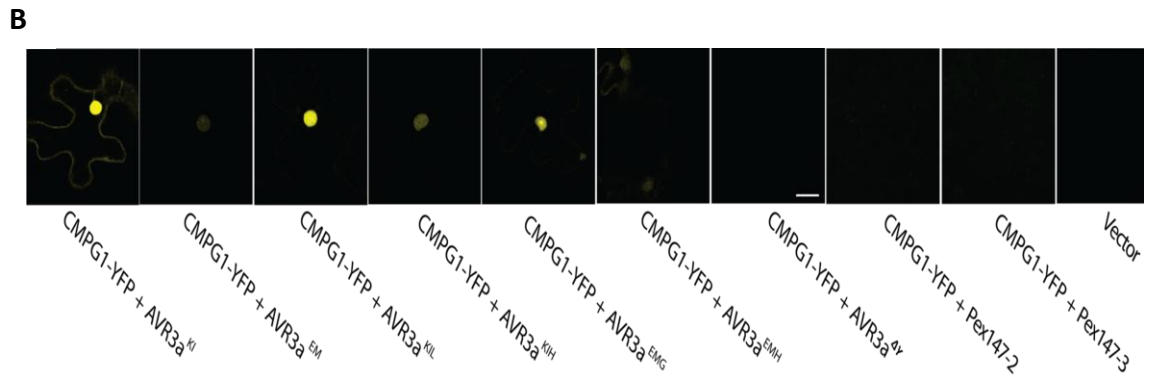
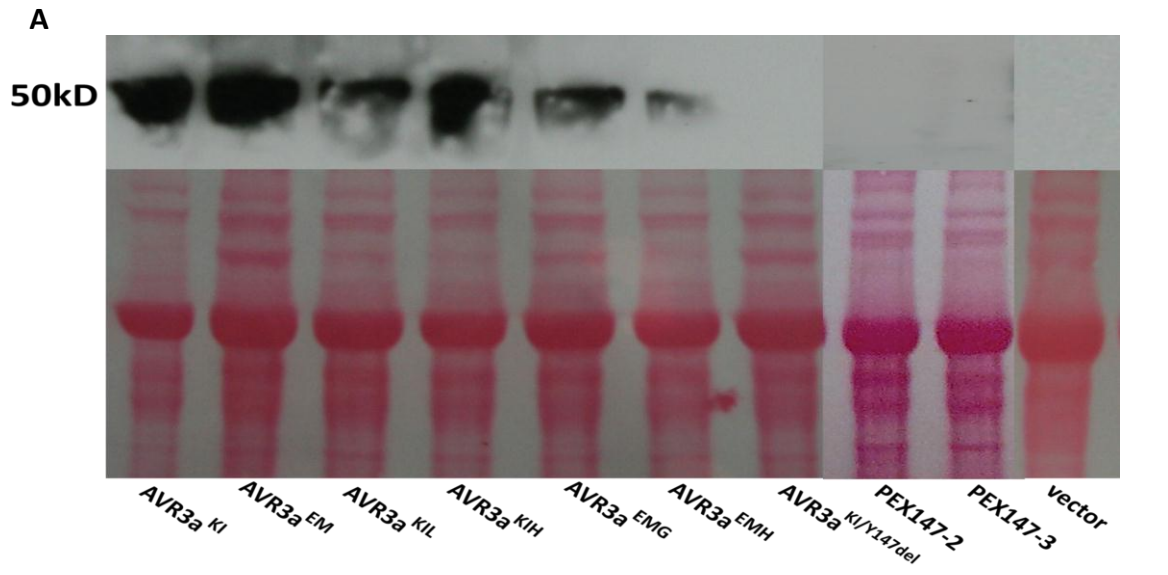


Figure 4.3: The ability of Avr3a alleles and paralogs to stabilise CMPG1 *in planta*. (A) Avr3a alleles and paralogs were co-infiltrated with 4x-myc-ΔN-StCMPG1 in *N. benthamiana*. The presence/absence of stabilised CMPG1 was assessed at 3 dpi by probing protein blots with an anti-myc antibody. Equal loading was ensured by visualising protein samples after Western blotting with Ponceau staining. Protein sizes are indicated. (B) C-terminal fusions of CMPG1 with YFP (StCMPG1b::YFP) were co-infiltrated with Avr3a alleles and paralogs in *N. benthamiana* to quantify the levels of CMPG1 stabilisation *in planta* using confocal microscopy at 2 days post infiltration. With the help of Dr. Petra Boevink, representative images were taken with the same gain and magnification. The scale bar measures 20 μm. (C) The YFP fluorescence intensity from independent experiments was measured and is represented graphically. Statistically significant differences are denoted by stars (***) $p < 0.001$.

Table 4.3: Statistical analysis (t-Test) of the recorded levels of YFP fluorescence following co-expression of C-terminal fusions of CMPG1 to YFP (StCMPG1b::YFP) with Avr3a alleles and paralogs in *N. benthamiana*

Avr3a ^{KI} n;17 Mean; 139.18 Stdev; 89.57 Stderror; 21.72	Avr3a ^{EM} n=16 Mean; 60.71 Stdev; 73.07 Stderror; 18.27	Avr3a ^{KIH} n=19 Mean; 85.6 Stdev; 79.40 Stderror; 18.21	Avr3a ^{KIL} n=12 Mean; 115.8 Stdev; 68.95 Stderror; 19.91	Avr3a ^{EMH} n=17 Mean; 16.93 Stdev; 13.57 Stderror; 3.29	Avr3a ^{EMG} n=23 Mean; 107.0 Stdev; 152.9 Stderror; 31.89	PEX147-2 n=31 Mean; 3.33 Stdev; 0.11 Stderror; 0.02	PEX147-3 n=18 Mean; 5.40 Stdev; 2.06 Stderror; 0.48	Avr3a ^{KI/ΔY} n=21 Mean; 6.40 Stdev; 3.73 Stderror; 0.81	Vector n= 24 Mean; 3.38 Stdev; 0.13 Stderror; 0.03
Avr3a ^{KI} n=17	$p < 0.001$	$p = 0.067$	$p = 0.454$	$p < 0.001$	$p = 0.410$	$p < 0.001$	$p < 0.001$	$p < 0.001$	$p < 0.001$
	Avr3a ^{EM} n=34	$p = 0.032$	$p = 0.005$	$p = 0.089$	$p = 0.055$	$p < 0.001$	$p < 0.001$	$p < 0.001$	$p < 0.001$
		Avr3a ^{KIH} n=19	$p = 0.289$	$p = 0.002$	$p = 0.577$	$p < 0.001$	$p < 0.001$	$p < 0.001$	$p < 0.001$
			Avr3a ^{KIL} n=12	$p < 0.001$	$p = 0.840$	$p < 0.001$	$p < 0.001$	$p < 0.001$	$p < 0.001$
				Avr3a ^{EMH} n=11	$p < 0.001$	$p < 0.001$	$p < 0.001$	$p < 0.001$	$p < 0.001$
					Avr3a ^{EMG} n=23	$p < 0.001$	$p < 0.001$	$p < 0.001$	$p < 0.001$
						PEX147-2 n=31	$p = 0.010$	$p = 0.033$	$p = 0.704$
							PEX147-3 n=14	$p = 0.793$	$p = 0.215$
								Avr3a ^{KI/ΔY} n=34	$p = 0.191$

4.3.3 Identification of common virulence targets for Avr3a alleles and paralogs using yeast-2-hybrid assays

Through a yeast two-hybrid assay, CMPG1 has been identified, alongside 12 further host proteins, as potential targets that interact with Avr3a^{KI} and/or Avr3a^{EM} (Bos *et al.*, 2010). Interacting proteins that had initially been identified in Y2H screens involving AVR3^{KI} as a bait have been denoted KIPI (Avr3a^{KI} from *P. infestans*) and comprise: KIPI-2 (Acyl-ACP thioesterase [FatA]), KIPI-5 (unknown protein), KIPI-7 (Sec3), KIPI-25 (unknown protein), KIPI-26 (TPR containing protein), KIPI-29 (putative DEAD box helicase), KIPI-30 (pyruvate kinase family protein), KIPI-34 (unknown protein) and KIPI-43 (PH domain containing). Similarly, interacting proteins that have been initially identified with AVR3^{EM} are referred to as EMPI and comprise: EMPI-1 (unknown protein), EMPI-2 (CMPG1), EMPI-9 (Sec5/ExoC2) and EMPI-32 (3-methyl-2-oxobutanoate hydroxyl transferase) (Bos *et al.*, 2010). The Avr3a alleles and paralogs were cloned into the Y2H compatible bait vector pDEST and used in a targeted Y2H screen to assess their interaction with KIPI and EMPI host proteins. The afore mentioned host targets had already been cloned into a suitable Y2H vector (Bos *et al.*, 2010) and were used in this study as preys. Recombinant yeast cells that had been transformed with the baits and all possible combination of preys were grown on plates lacking the reporter gene histidine and compared to the controls to assess potential interactions. Furthermore, recombinant yeast cells that indicated protein–protein interactions were confirmed in triplicates with a β -galactosidase assay to visualise the strength of the interactions.

Interestingly, in the yeast system, all recombinants involving PEX147-2 did not interact with any of the host virulence targets identified for Avr3a^{KI} or Avr3a^{EM} (Figure 4.4). In contrast to PEX147-2, PEX147-3 interacted with four previously identified host targets which were KIP1-25, KIP1-30, EMPI-1 and EMPI-9 but not with CMPG1 (EMPI-2) (Figure 4.4).

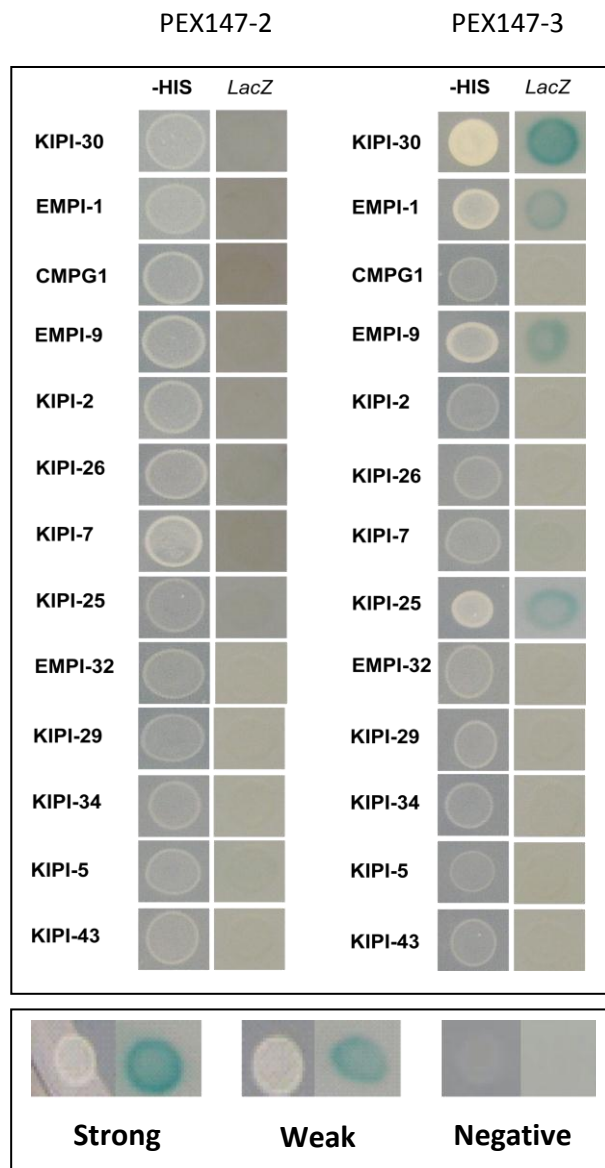


Figure 4.4: Yeast-two-hybrid based protein-protein interaction study involving 13 potential Avr3a host virulence targets and PEX147-2 and PEX147-3. The β -galactosidase assay (LacZ) (right) and a Histidine-based reporter assay (-HIS) (left) were used to show the strength of the interactions. Results for the Avr3a paralogs PEX147-2 (A) and PEX147-3 (B) are shown. The control interactions are indicated in the bottom panel.

In yeast, Avr3a^{KIH} interacted with 11 of the previously described Avr3a^{KI} and Avr3a^{EM} host targets including CMPG1 (Figure 4.5A). Avr3a^{KIH} did not interact with KIPI-5 or KIPI-34, both of which interacted with Avr3a^{KI}, but interacted with EMPI-32 which did not elicit reporter gene activation upon co-infiltration with Avr3a^{KI} (Table 4.4).

Avr3a^{KIL} interacted with 10 of the Avr3a^{KI} and Avr3a^{EM} targets but not with CMPG1, KIPI-5, or KIPI-26. Thus, compared to Avr3a^{KIH}, the interaction with CMPG1 and KIPI-26 was lost whilst the interaction with KIPI-34 was gained (Figure 4.5B).

Intriguingly, in general, alleles derived from Avr3a^{EM} interacted with fewer of the Avr3a^{KI} and Avr3a^{EM} host targets in yeast (Figure 4.5C; Figure 4.5D). Avr3a^{EMH} interacted with seven proteins and Avr3a^{EMG} with two, EMPI-1 and KIPI-25, which were shared with Avr3a^{EMH}. Only EMPI-1 was a common host target for Avr3a^{EM} derived alleles in the yeast system. Surprisingly, the Y2H analysis supported a strong interaction between CMPG1 and Avr3a^{EMH}, which failed to suppress ICD and CF-4/Avr4 mediated PCD and resulted in the weakest stabilisation of CMPG1 *in planta* (Figure 4.1; Figure 4.2; Figure 4.3). No such interaction was observed in yeast for Avr3a^{EMG} which suppressed CMPG1-dependent cell death responses and stabilised CMPG1 *in planta* (Figure 4.1; Figure 4.2; Figure 4.3).

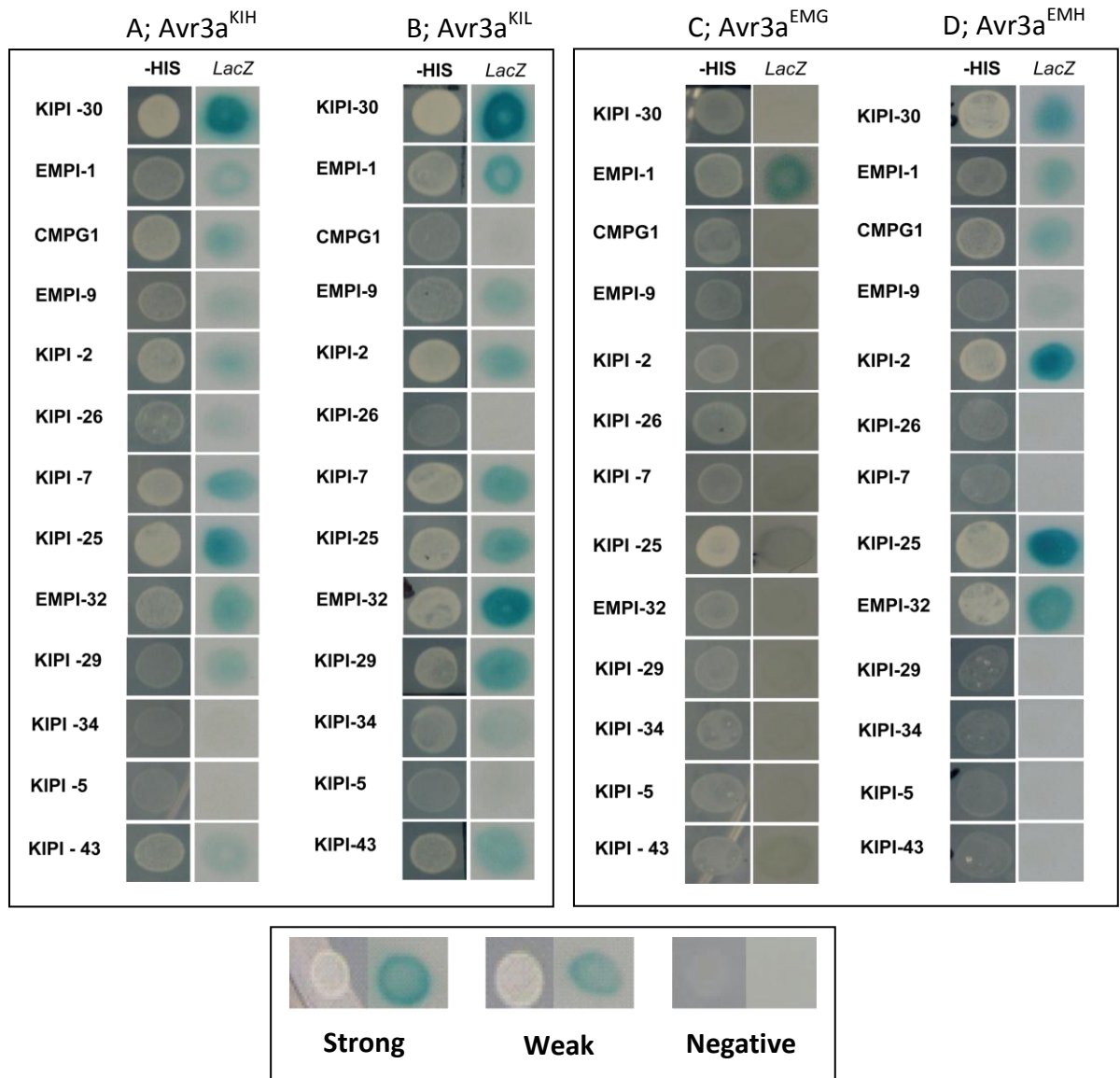


Figure 4.5: Yeast-two-hybrid based protein–protein interaction study involving 13 potential Avr3a host virulence targets and Avr3a^{KI} and Avr3a^{EM} derived alleles. The β -galactosidase assay (LacZ) (right) and a Histidine-based reporter assay (-HIS) (left) were used to show the strength of the interactions. Results for the Avr3a alleles Avr3a^{KIH} (A), Avr3a^{KIL} (B), Avr3a^{EMG} (C) and Avr3a^{EMH} (D) are shown. Control interactions are indicated in the bottom panel.

To rule out effects of protein instability in yeast, the stability of Avr3a alleles and paralogs were determined by western blot analysis as described by Bos *et al.* (2010). Yeast recombinants carrying Avr3a alleles and paralogs were grown overnight, the total protein was extracted and separated by gel electrophoresis and blotted onto suitable membranes. An antibody that was raised against the DNA binding domain

fused to the *Avr3a* alleles and paralogs in the respective bait vectors was used to probe the membranes (Bos *et al.*, 2010). All *Avr3a* alleles yielded a band of somewhat equal intensity and of the expected size of 37kD (Figure 4.6). A similar band was observed for the *Avr3a* paralogs PEX147-3 but not for PEX147-2, which suggest that the latter is not stable in yeast (Figure 4.6).

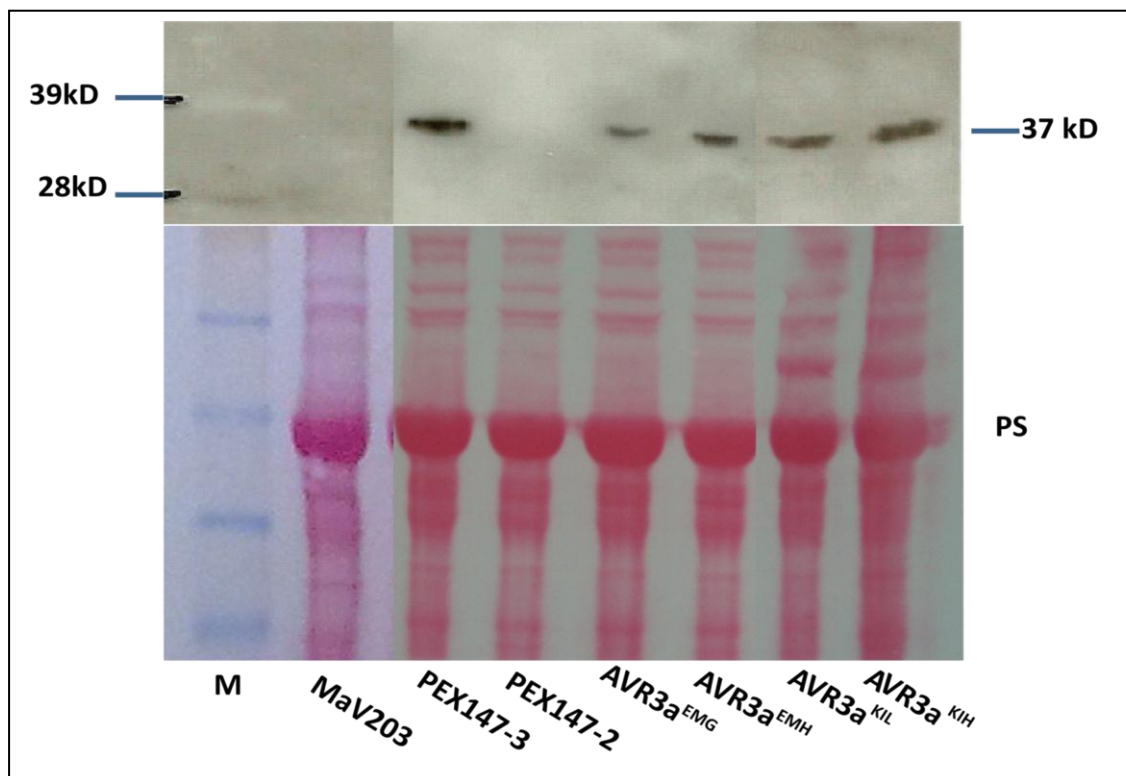


Figure 4.6: N-terminal fusions of the *Avr3a* alleles and paralogs with the DNA-binding domain were used to demonstrate stability of the constructs in yeast. Protein extracts from recombinant yeast cells were sampled and, following western blotting, probed with an anti-DNA-binding domain antibody. Equal loading was ensured by visualising protein samples after Western blotting with Ponceau staining. Protein sizes are shown in kDa and correspond to a protein size marker (M) that was run alongside the samples. Empty yeast cells, MaV203, were used as a negative control.

The results of the Y2H screening and the complementary CMPG1 stabilisation data obtained following the western and confocal microscopy studies (Figure 4.3), have summarised in Table 4.4.

Table 4.4: Summary of observed interactions of the Avr3a alleles and paralogs in Y2H, Western and Confocal imaging analysis. Y2H data for Avr3a^{KI} and Avr3a^{EM} were published in Bos *et al.* (2010) and Avr3a interactors and their predicted gene ontology are shown as Avr3aPI-x. The denotations are as follows: (+++) strong interaction yielding histidine and strong x-gal activation; (++) the interaction was strong enough to activate histidine reporter and x-gal weakly; (+) weak interaction – only the histidine reporter was activated; (-) no reporter gene activation.

	Yeast-Two-Hybrid													Western Analysis CMPG1-YFP	Confocal Imaging CMPG1-YFP
	KIP1-2 (Avr3a-PI-5) (Acyl-ACP thioesterase [FataA])	KIP1-5 (Avr3a-PI-9) (Unknown protein)	KIP1-7 (Avr3a-PI-7) (Sec3)	KIP1-25 (Avr3a-PI-8) (Unknown protein)	KIP1-26 (Avr3a-PI-6) (TPR containing protein)	KIP1-29 (Avr3a-PI-10) putative DEAD box helicase)	KIP1-30 (Avr3a-PI-1) (pyruvate kinase family protein)	KIP1-34 (Avr3a-PI-11) (Unknown protein)	KIP1-43 (Avr3a-PI-12) (PH domain containing)	EMPI-1 (Avr3a-PI-2) (Unknown Protein)	EMPI-2 (Avr3a-PI-3) (CMPG1)	EMPI-9 (Avr3a-PI-4) (Sec5 /Exoc2)	EMPI-32 (3-methyl-2-oxobutanoate hydroxyl transferase)		
Avr3a ^{KI}	+/++	++	++	++	++	++	+++	++	++	++	++	++	-	+++	+++
Avr3a ^{EM}	++	-	-	++	+	-	+++	-	-	++	++	+++	++	+++	+
Avr3a ^{KIH}	+	-	++	++	+	+	+++	-	+	+	+	+	++	++	++
Avr3a ^{KIL}	+	-	++	++	-	++	+++	+	+	++	-	+	+++	++	+++
Avr3a ^{EMH}	+++	-	-	+++	-	-	++	-	-	++	++	+	+++	+	+
Avr3a ^{EMG}	-	-	-	+	-	-	-	-	-	++	-	-	-	++	+++
PEX147-2	-	-	-	-	-	-	-	-	-	-	-	-	-	-	-
PEX147-3	-	-	-	+	-	-	+++	-	-	+	-	++	-	-	-
Avr3a ^{KI/ΔY}															

4.4 DISCUSSION

The identification of pathogen effectors, in particular those delivered via the bacterial T3SS and oomycete effectors carrying the canonical RXLR or LFLAK domains, has given an unprecedented insight into the mechanisms employed by pathogens to manipulate host defences (Deslandes & Rivas, 2012, Oh *et al.*, 2009, van Damme *et al.*, 2012). Many research groups have evaluated candidate effectors by transient expression *in planta* and by measuring the impact on disease resistance/susceptible (e.g. Sohn *et al.*, 2007) or their ability to suppress PTI responses including cell death development or

callose deposition (Anderson *et al.*, 2012; Cabral *et al.*, 2011; Fabro *et al.*, 2011;; Wang *et al.*, 2011).

In agreement with previous data (Bos *et al.*, 2010; Gilroy *et al.*, 2011a), in comparison to Avr3a^{KI/Y147del}, both Avr3a^{KI} and Avr3a^{EM} highly significantly suppressed CMPG1-dependent INF1 and CF-4/Avr4 mediated cell death responses (Figure 4.1; Figure 4.2). The same observation was recorded for Avr3a^{KIL}, Avr3a^{KIH} and Avr3a^{EMG} but not for Avr3a^{EMH} or PEX147-2 which has shown to be unstable *in planta* (Figure 3.11). Interestingly, PEX147-3 highly significantly suppressed ICD but not CF-4/Avr4 mediated PCD.

The ICD suppression activity of Avr3a^{EM} and PEX147-3 contradicts earlier studies conducted by Bos *et al.* (2006; 2009) and Oh *et al.* (2009) which suggested that Avr3a^{EM} (then referred to as PexRD7) and PEX147-3 are unable to suppress ICD and that, in addition to Avr3a^{KI}, only PexRD8 and PexRD36 could suppress ICD. In this context, it should however, be pointed out that the ICD experiments described by Bos *et al.* (2006; 2009) and Oh *et al.* (2009) are different in their setup if compared to the studies described here and by Gilroy *et al.* (2011a) as well as Bos *et al.* (2010). In Bos *et al.* (2006; 2009) and Oh *et al.* (2009), effector expression and INF1 delivery were conducted sequentially (INF1 was delivered 24 hours after effector delivery) whereas in Gilroy *et al.* (2011a), Bos *et al.* (2010) and in this study, the effectors were simultaneously co-infiltrated with INF1.

A recent study in which *P. sojae* effectors were tested in their ability to suppress BAX-triggered cell death (Wang *et al.*, 2011) demonstrated that the timing of effector

delivery can, indeed, influence the effectiveness of suppressing PCD responses. Interestingly, the strongest PCD suppression responses have been recorded in samples where the effectors were expressed prior to BAX delivery and not upon co-infiltration (Wang *et al.*, 2011). However, it is conceivable that *Agrobacterium* mediated delivery of effectors triggers a PTI response which impacts negatively on the subsequent delivery of PCD triggers. Thus, the observed potential of effectors to perturb PCDs could be overestimated in experiments that use sequential delivery.

Avr3a^{EMH} and Avr3a^{KIH} share the same amino acid substitution (Q133H) which locates to the helix 4 of the Avr3a protein (Figure 3.5). This amino acid resides in a different surface plane if compared to the K80E and I103M changes which are found in helix 1 and 2, respectively (Figures 3.5 and 3.6). Although Avr3a^{EMH} and Avr3a^{KIH} are equally stable *in planta* (Figure 3.11), the ICD and CF-4/Avr4 PCD suppression capability of these two proteins differ significantly and Avr3a^{EMH} is unable to perturb responses that Avr3a^{KIH} suppresses. It is conceivable that the Q133H change impacts negatively on Avr3a function but that the effect manifests itself stronger in the AVR3^{EM} background if compared to the AVR3^{KI} background. Indeed, in line with observations from Bos *et al.* (2010) and Gilroy *et al.* (2011a), if compared to Avr3a^{EM}, Avr3a^{KI} appears to be able to suppress ICD and CF-4/Avr4 PCD more strongly and highly significantly so for INF1 cell death responses (Table 4.1). Similarly, Avr3a^{KI} suppresses CF-4/Avr4 responses more strongly and are statistically significant if compared to Avr3a^{KIH} and Avr3a^{KIL} (Figure 4.2; Table 4.2). The same trend was observed for ICD suppression but the data did not support a significant effect. A model that could be drawn from these observations is that Avr3a^{KI} is the most effective suppressor of the PCD responses studied so far and

that subsequent changes reduce the functionality. Beyond a certain activity threshold, effector function is significantly impaired.

Recent studies by Bos *et al.* (2010) and Gilroy *et al.* (2011a) have shown that Avr3a is essential for *P. infestans* virulence and suppresses PCD responses by stabilising the host E3-ligase CMPG1. In terms of their function, E3-ligases ensure specificity within the ubiquitination of proteins which subsequently target proteins for proteasomal degradation or alter their localisation and/or activity (Schnell & Hicke, 2003). The attachment of Ubiquitin, a 76-amino acid peptide, to the target proteins involves an ubiquitin-activating enzyme (E1), a conjugating enzyme (E2) and a ubiquitin ligase (E3) (Glickman & Ciechanover, 2002; Chapter 1).

CMPG1 was initially identified in parsley suspension cultures following treatment with the *P. sojae* oligopeptide elicitor Pep25 derived from a 42-kDA cell wall protein (Kirsch *et al.*, 2001). A Solanaceae homolog was identified as an Avr9/CF-9 rapidly elicited (ACRE) gene in CF-9-expressing tobacco cells (Durrant *et al.*, 2000; Rowland *et al.*, 2005). Out of three ACRE genes required for Avr9/CF-9 cell death, two encoded for E3 ligases including ACRE74, a U-box protein with homology to parsley CMPG1 and Arabidopsis PUB (Plant U-Box) 20 and PUB21 (González-Lamothe *et al.*, 2006). ACRE74, also known as *Nicotiana tabacum* (Nt) CMPG1, was subsequently shown to be involved in cell death responses triggered by the perception of diverse molecules such as *Cladosporium fulvum* Avr9, *P. infestans* INF1 and *Pst*, AvrPto (González-Lamothe *et al.*, 2006).

In accordance with previous data, Avr3a^{KI} and Avr3a^{EM} both successfully stabilize CMPG1 whereas a deletion of the last amino acid at position 147 (tyrosine [y]) in Avr3a^{KI/Y147del} is impaired in this activity (Figure 4.3; Bos *et al.*, 2009). However, deletion of the terminal tyrosine in Avr3a^{KI} does not impact on the recognition by R3a, which is in line with previous findings suggesting that the avirulence and cell-death suppression activity of Avr3a are uncoupled (Figure 3.8; Bos *et al.*, 2009).

To determine if the functional diversity of the Avr3a alleles and paralogs is linked to their respective ability to stabilise CMPG1, two complementary assays, western blot analysis and confocal microscopy, were utilised (Bos *et al.*, 2010). Both systems take advantage of the instability of CMPG1 which is normally rapidly degraded by the 26s proteasome (Bos *et al.*, 2010). The western blot analysis was used to determine the accumulation of 4xmyc tagged StCMPG1 upon co-expression of Avr3a alleles and paralogs in *N. benthamiana* (Figure 4.3A). The complementary approach utilised CMPG1 C-terminally fused to YFP (CMPG1-YFP) to demonstrate accumulation of YFP fluorescence in the plant nucleus (Figure 4.3B) and quantified the fluorescence intensity using confocal microscopy fluorescence (Figure 4.3C). The data obtained are very consistent between the different assays and tied in with previous data for the controls Avr3a^{KI/Y147del} and empty vector as well as for Avr3a^{KI} and Avr3a^{EM} (Bos *et al.*, 2010). Consistent with their ability to suppress ICD and CF-4/Avr4 PCD, the Avr3a alleles Avr3a^{KI}, Avr3a^{EM}, Avr3a^{KIH}, Avr3a^{KIL} and Avr3a^{EMG} all stabilised CMPG1. Avr3a^{EMH}, which failed to suppress ICD and CF-4/Avr4 PCD (Figures 4.1; Figure 4.2), very weakly stabilised CMPG1, albeit statistically very highly significantly if compared to the negative controls. This finding further supports the hypothesis from above that Avr3a effector function decreases with certain, deleterious, mutations. In the interaction

with CMPG1 this effect could be quantitative. According to this hypothesis, an Avr3a allele has to maintain a certain threshold of CMPG1 perturbation to compromise CMPG1-dependent cell death responses. Beyond the required level of CMPG1 interference (e.g. stabilisation), the functionality of CMPG1 is maintained and subsequent cell death responses are executed.

The fact that the Avr3a paralogs PEX147-3 could not suppress all CMPG1-dependent PCDs analysed in this study could suggest that PEX147-3 acts downstream of CMPG1 in a pathway that is specific for ICD suppression but not required for CF-4/Avr4 mediated PCD. Alternatively, it is conceivable that PEX147-3 impacts differently on CMPG1 and does not bring about stabilisation but modifies CMPG1 in a way that is specific to ICD. Future biochemical and proteomics studies are required to elucidate the exact mechanisms of perturbation by these molecules.

Despite the good correlation between the CMPG1 western analysis and the confocal microscopy study to observe stabilisation of CMPG1 in the nucleus (Figure 4.3), the Y2H study did not produce coherent data to support a direct link between CMPG1 interaction and stabilisation. However, the Y2H screen failed to detect interactions between CMPG1 and Avr3a^{KIL} as well as Avr3a^{EMG} whilst suggesting a strong interaction between CMPG1 and Avr3a^{EMH}. As all products, with the exception of PEX147-2, were stable in the yeast strain used (Figure 4.6).

These problems, which have been reported as some of the limitations of the technology, can occur as a consequence of a) protein misfolding or (lack of) post-translational modification, b) fusion with the transcription factor domains, which could

potentially impact to the binding affinity and c) protein toxicity (Coates & Hall, 2003; Causier & Davies, 2002).

However, the Y2H system has been described as the most sensitive method to study protein–protein interaction *in vivo* (Causier & Davies, 2002). Consequently, most of the identified protein–protein interactions thus far have been detected using this system (Bruckner *et al.*, 2009). In the case of oomycete effector studies, this system has, for example, been used by Chen *et al.* (2012) to determine the function of IPI-O4 in suppressing R gene mediated cell death.

It is therefore possible that Y2H systems other than the one used in this study would have picked up some of the expected interactions. Furthermore, alternative approaches such as bimolecular fluorescence complementation (BiFC), or Split-YFP, which is a widely used and established approach to analyse and localise protein–protein interactions in plant cells (Walter *et al.*, 2004; Bos *et al.*, 2010), could be used to demonstrate a direct interaction between the Avr3a alleles or paralogs and CMPG1 (or other potential host virulence targets) *in planta*. However, it is also conceivable that the stabilisation of CMPG1 can occur by a mechanism that does not require a direct interaction between the Avr3a alleles and CMPG1 which is reminiscent of the ability of PEX147-3 to suppress ICD whilst not stabilising CMPG1. *Vice versa*, it is apparent that a strong interaction in Y2H, as for example observed for Avr3^{EMH} and CMPG1, does not necessarily yield a strong CMPG1 stabilisation *in planta*.

CHAPTER 5

5 *IN PLANTA* COMPLEMENTATION STUDY

5.1 INTRODUCTION

To enable parasitic colonization and reproduction, plant pathogenic bacteria, fungi, oomycetes and nematodes deliver a repertoire of effectors into the host apoplast (Song *et al.*, 2009) and inside the cells where they localise to various internal compartments (Boevink *et al.*, 2011; Caillaud *et al.*, 2012; Chapter 1). Amongst other functions, these effectors suppress host defence responses via diverse mechanisms (Chisholm *et al.*, 2006; Jones & Dangl, 2006; Mukhtar *et al.*, 2011). To date, seven protein secretion systems have been described for Gram positive and negative bacteria (reviewed by Tseng *et al.*, 2009) although often mainly the type II and III secretion systems (T2SS, T3SS) are associated with effector delivery (McCann & Guttman, 2008; Zhou & Chai, 2008; Collmer *et al.*, 2009). In contrast, biotrophic fungi and oomycetes utilise specialized structures known as haustoria (Panstruga, 2003; Whisson *et al.*, 2007) for effector delivery albeit the mechanism of RXLR effector delivery remains controversial (Ellis & Dodds, 2011).

Bacterial effectors that are secreted via the T3SS have given us an unprecedented insight into the diversity and redundancy of effector complements. For example, the tomato and Arabidopsis pathogen *Pseudomonas syringae* pv. tomato (*Pst*) causes bacterial speck disease. Two strains of *Pst*, DC3000 that infects both tomato and Arabidopsis and T1, which only effects tomato, have been compared. The study revealed that of the 30+ currently known T3SS effectors from DC3000 about 50% are

missing in T1 (Almeida *et al.*, 2009). A recent review on bacterial T3SS effectors concluded that effector repertoires are not only very variable but also highly redundant and employ various mechanisms to compromise the plant's defences (Collmer *et al.*, 2009). Indeed, bacterial mutagenesis screens combined with plant infection assays for *Ralstonia solanacearum* GMI1000 in tomato and *Pst* DC3000 in *Arabidopsis* have shown that only two of the over 70 *R. solanacearum* effectors, when mutated, produced a slight loss of virulence phenotype in tomato (Cunnac *et al.*, 2004; Poueymiro & Genin, 2009) and only one affected lesion formation for *Pst* DC3000 in tomato (Badel *et al.*, 2006).

This is in stark contrast to *P. infestans* where sequencing of the genome has identified in excess of 500 RXLR encoding effectors and almost 200 Crinklers (Haas *et al.*, 2009). Reverse genetic tools, including gene silencing, have shown that multiple effectors are indeed essential for pathogenicity (Vetukuri *et al.*, 2011; Bos *et al.*, 2010). Amongst these effectors is Avr3a which was shown to be highly up-regulated during infection in diverse isolates including T30-4, 88069 and 3928A (Genotype A2-Blue13) at 2–3 days post infection (dpi) (Bos *et al.*, 2010; Cooke *et al.*, 2012).

Avr3a contains a signal peptide to facilitate transport from *P. infestans* haustoria into the extracellular matrix. From there, Avr3a is translocated into the host cytoplasm in a process that requires the canonical RXLR and EER amino acid motifs (Armstrong *et al.*, 2005; Whisson *et al.*, 2007). Stable silencing of *Avr3a* in the *P. infestans* isolate 88069 significantly reduces virulence *in planta* compared to wild type levels (Bos *et al.*, 2010; Vetukuri *et al.*, 2011), which suggests that Avr3a effector function is non-redundant and essential for pathogenicity in the isolate 88069 (Figure 5.1). The isolate 88069 is

homozygous for $Avr3a^{EM}$ and the corresponding silenced line, CS12, has shown similar growth and sporulation *in vitro* (Bos *et al.*, 2010; Vetukuri *et al.*, 2011) compared to wild type 88069. The cytoplasmic localization of $Avr3a$ in host cells has enabled complementation assays for the loss of virulence in CS12 by transiently expressing $Avr3a^{KI}$ and $Avr3a^{EM}$ via *A. tumefaciens* in *N. benthamiana* prior to pathogen infection. However, the $Avr3a$ mutation, $Avr3a^{KI/Y147del}$, failed to exhibit the same complementation ability (Bos *et al.*, 2010).

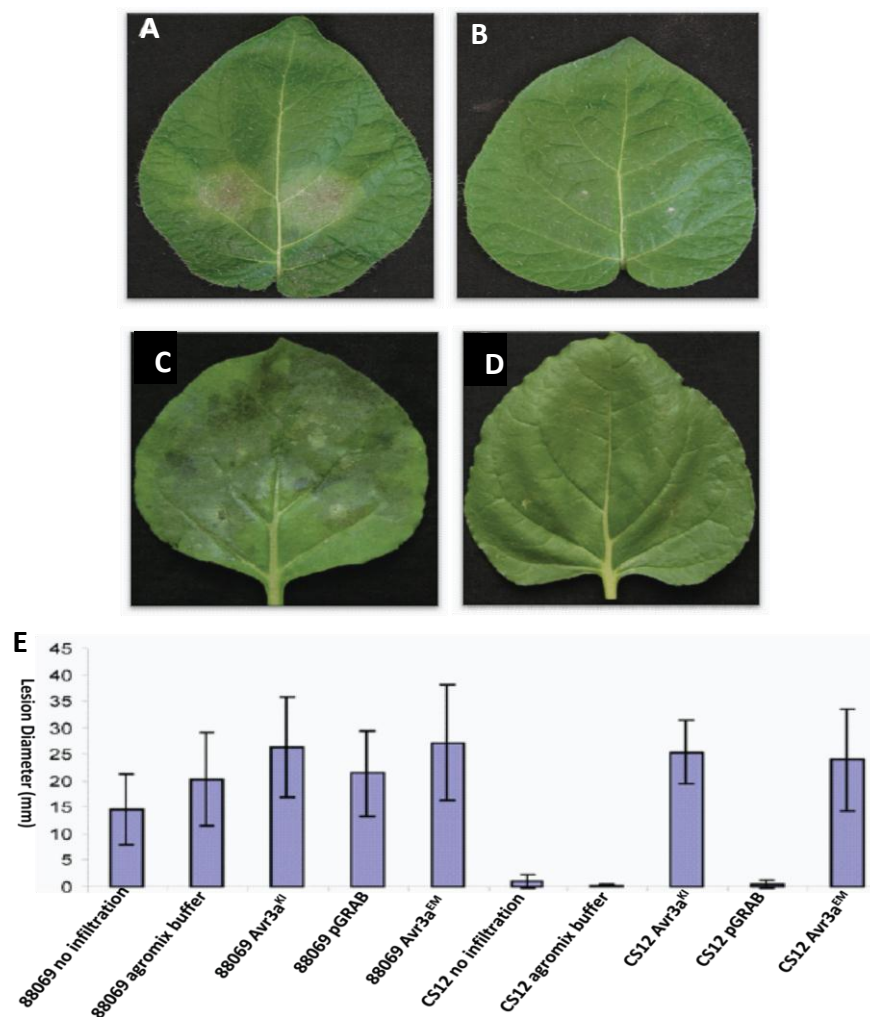


Figure 5.1: Avr3a-silenced line CS12 has lost its ability to infect the plants (A) Infection of potato cultivar Bintje by wild-type *P. infestans* isolate 88069 and (B) Avr3a-silenced line CS12 at 4 dpi. (C) Infection of *N. benthamiana* by wild-type *P. infestans* isolate 88069 at 6 dpi. (D) Infection of *N. benthamiana* by Avr3a-silenced line CS12 at 6 dpi. (E) Measurements of lesion sizes at 6 dpi (mm) upon infection of isolate 88069 or silenced line CS12 on leaves that were uninfiltrated, infiltrated with agromix, agroinfiltrated to express $AVR3a^{KI}$, $Avr3a^{EM}$, or empty pGRAB vector (Bos *et al.*, 2010).

5.2 AIM

The aim of this study was to determine the capability of the Avr3a alleles and paralogs PEX147-2 and PEX14-7 to complement the *Avr3a*^{EM} silenced line, CS12. The underlying question being asked was whether these additional *P. infestans* alleles and paralogs are fully functional in restoring virulence or if their virulence function is stronger or weaker if compared to *Avr3a*^{EM} and *Avr3a*^{KI}.

5.3 RESULTS

The ability of Avr3a alleles and paralogs to restore CS12 virulence in *N. benthamiana* was determined by transient, *in planta* effector expression prior to *P. infestans* infection. Recombinant *A. tumefaciens* containing empty vector and *Avr3a*^{KI/Y147del} were used as negative controls while *Avr3a*^{KI} and *Avr3a*^{EM} functioned as positive controls. The growth of CS12 on the pre-inoculated areas was assessed and Trypan blue staining was performed for representative leaves to visualize the observed phenotypes (Figure 5.1). In total, four independent experiments were carried out and the growth of CS12 was assessed based on 72 inoculation sites per construct. Data were recorded and subjected to a Mann-Whitney U test to determine statistical differences between the samples (Figure 5.2; Table 5.1). The Mann-Whitney U test (also known as Mann–Whitney–Wilcoxon test) was the most suitable statistical analysis for the comparison of the non-parametric sample data.

Compared to the empty vector control, which was duplicated on every leaf, expression of *Avr3a*^{KI/Y147del} yielded only a moderate, but statistically significant ($p= 0.026$) gain in virulence for the *Avr3a* silenced line CS12. Growth of CS12 was observed on approximately 28% of the *Avr3a*^{KI/Y147del} inoculated sites (Figure 5.1). Similarly, CS12

growth on sites expressing PEX147-2 and PEX147-3 was not statistically different to $Avr3a^{KI/Y147del}$ (PEX147-2; $p=0.443$; PEX147-3; $p=0.115$) although PEX147-3 expression prior to CS12 inoculation yielded statistically highly significant levels of increased virulence if compared to the empty vector control ($p \leq 0.005$). A somewhat comparable trend was also observed for the expression of $Avr3a^{EMH}$ and $Avr3a^{EMG}$ which yielded low levels of complementation that were not statistically significant ($Avr3a^{EMH}$; $p=0.215$; $Avr3a^{EMG}$; $p=0.159$) if compared to $Avr3a^{KI/Y147del}$, but were nevertheless significant compared to the empty vector control ($Avr3a^{EMH}$; $p \leq 0.005$; $Avr3a^{EMG}$; $p \leq 0.005$).

Intriguingly, the only allele that could restore *P. infestans* infectivity to the same level as the avirulent form $Avr3a^{KI}$ whilst evading recognition by R3a was $Avr3a^{EM}$. Indeed, there were no statistically significant differences between $Avr3a^{EM}$, $Avr3a^{KI}$, $Avr3a^{KIH}$ and $Avr3a^{KIL}$ in restoring virulence for CS12 (Table 5.1). The average lesion development in the areas transiently expressing these alleles ranged from 60–70 inoculated sites and were significantly ($p \leq 0.005$) different to $Avr3a^{EMH}$, $Avr3a^{EMG}$ as well as PEX147-2, PEX147-3, $Avr3a^{KI/Y147del}$ and empty vector controls which restored pathogenicity in only 14% of the inoculated and infected areas.

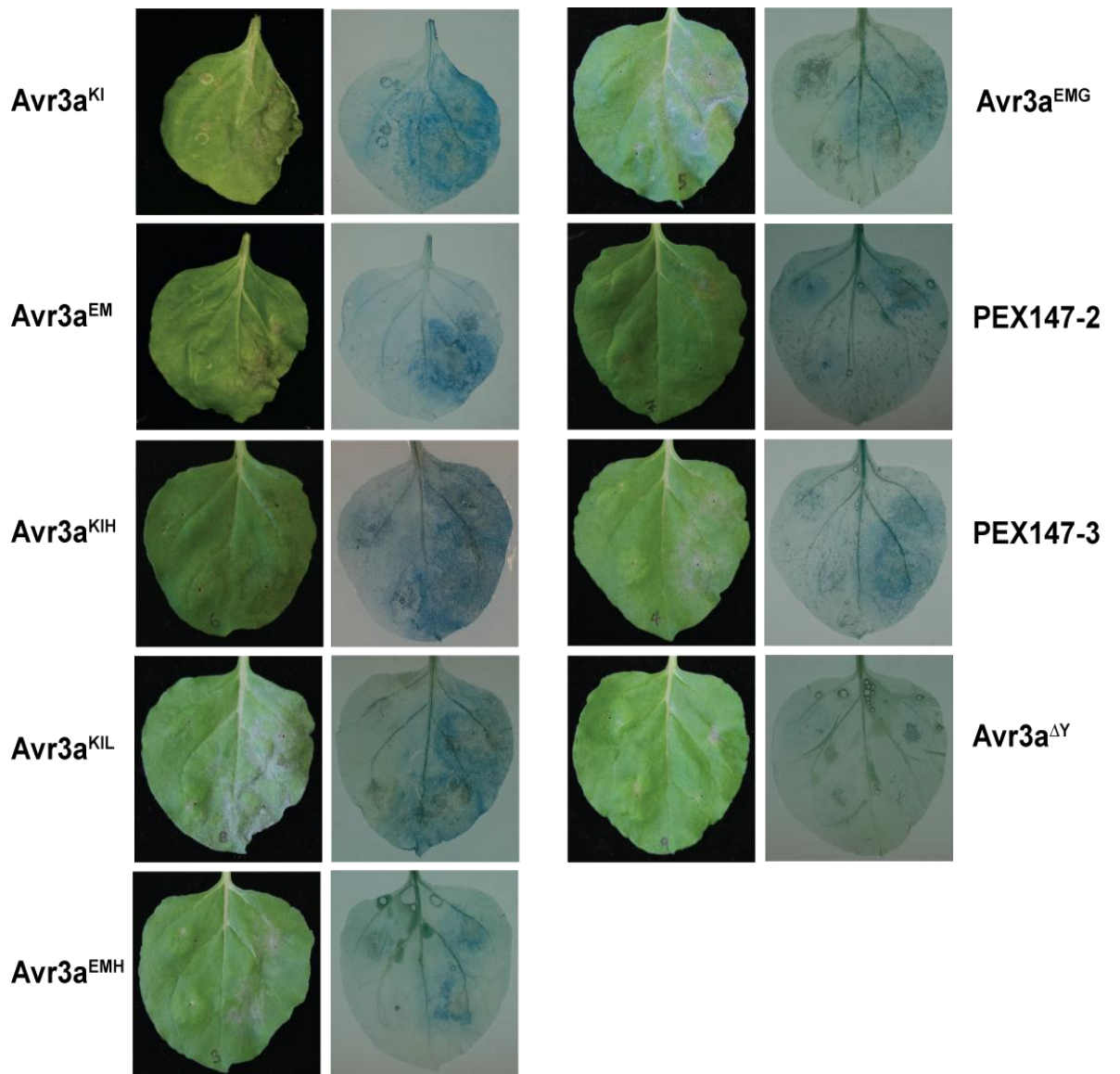


Figure 5.2: Complementation study of *Avr3a*^{EM} silenced *P. infestans* line, CS12. *P. infestans* disease development in *N. benthamiana* is shown at 6 days post CS12 infection (5.1A). Leaves were infiltrated with recombinant *Agrobacterium tumefaciens* carrying empty vector control (left) and *Avr3a* alleles and paralogs (right) 2 days prior to pathogen challenge. Images on the left show *P. infestans* ingress and images on the right display the same leaves after Trypan blue staining to visualise more clearly dead plant tissue and pathogen mycelium.

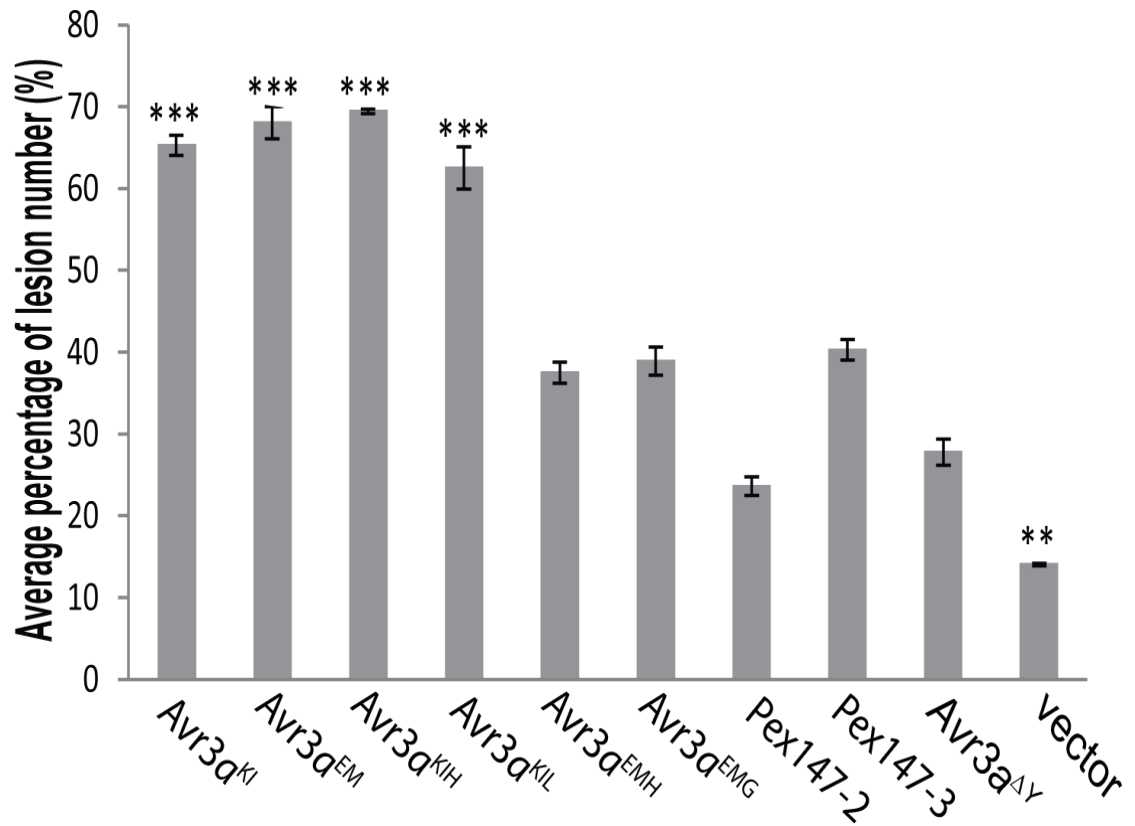


Figure 5.3: Complementation study of Avr3a^{EM} silenced *P. infestans* line, CS12. Data from four independent experiments are represented graphically (5.1B). Statistical significant differences of the samples and vector control compared to Avr3a^{KI}/Δ147Y are denoted by stars (*** $p < 0.005$, ** $p < 0.05$).

Table 5.1: Statistical analysis (Mann-Whitney U-test method) of *Avr3a*^{EM} silenced *P. infestans* line, CS12, complementation study by the *Avr3a* alleles and paralogs. Mann-Whitney U tests were used to determine statistical differences between the samples. The value n represents the total number of inoculated sites.

Avr3a^{KI} n=72 Mean; 65.27778 Stdev; 10.48588 Stderror; 1.235773	Avr3a^{EM} n=72 Mean; 68.05555 Stdev; 16.83938 Stderror; 1.984541	Avr3a^{KIH} n=72 Mean; 69.44444 Stdev; 2.405628 Stderror; 0.283506	Avr3a^{KIL} n=72 Mean; 62.5 Stdev; 22.04792 Stderror; 2.598373	Avr3a^{EMH} n=72 Mean; 37.5 Stdev; 11.02397 Stderror; 1.299187	Avr3a^{EMG} n=72 Mean; 38.88889 Stdev; 14.63285 Stderror; 1.724498	PEX147-2 n=72 Mean; 23.61111 Stdev; 9.622501 Stderror; 1.134023	PEX147-3 n=72 Mean; 40.27777 Stdev; 10.48588 Stderror; 1.235773	Avr3a^{KI/ΔY} n=72 Mean; 27.77778 Stdev; 13.39396 Stderror; 1.578493	Vector n=648 Mean; 14.0432 Stdev; 3.474796 Stderror; 0.136503
Avr3a^{KI}	U = 2520 <i>p</i> =0.725	U = 2484 <i>p</i> =0.595	U = 2520 <i>p</i> =0.730	U = 1872 <i>p</i> <0.005	U = 1908 <i>p</i> < 0.005	U=1476 <i>p</i> <0.005	U=1944 <i>p</i> < 0.005	U=1620 <i>p</i> <0.005	U=12096 <i>p</i> <0.005
	Avr3a^{EM}	U=2556 <i>p</i> =0.858	U=2448 <i>p</i> =0.485	U=1800 <i>p</i> < 0.005	U=1836 <i>p</i> <0.005	U=1404 <i>p</i> <0.005	U=1872 <i>p</i> <0.005	U=1548 <i>p</i> <0.005	U=11448 <i>p</i> <0.005
		Avr3a^{KIH}	U=2412 <i>p</i> =0.381	U=1764 <i>p</i> <0.005	U=1800 <i>p</i> < 0.005	U=1368 <i>p</i> <0.005	U=1836 <i>p</i> < 0.005	U=1512 <i>p</i> <0.005	U=11124 <i>p</i> <0.005
			Avr3a^{KIL}	U=1944 <i>p</i> <0.005	U=1980 <i>p</i> <0.005	U=1548 <i>p</i> <0.005	U=2016 <i>p</i> <0.005	U=1692 <i>p</i> <0.005	U=12774 <i>p</i> <0.005
				Avr3a^{EMH}	U=2556 <i>p</i> =0.864	U=2196 <i>p</i> =0.046	U=2520 <i>p</i> =0.733	U=2340 <i>p</i> =0.215	U=18576 <i>p</i> <0.005
					Avr3a^{EMG}	U=2160 <i>p</i> = 0.031	U=2556 <i>p</i> =0.865	U=2304 <i>p</i> =0.159	U=18252 <i>p</i> <0.005
						PEX147-2	U=2124 <i>p</i> =0.020	U=2448 <i>p</i> =0.443	U=22140 <i>p</i> =0.282
							PEX147-3	U=2268 <i>p</i> =0.115	U=17928 <i>p</i> <0.005
								Avr3a^{KI/ΔY}	U=20844 <i>p</i> =0.026

5.4 DISCUSSION

To date, four *Phytophthora* genomes have been sequenced and annotated and include *P. sojae*, *P. ramorum* (Tyler *et al.*, 2006), *P. infestans* (Haas *et al.*, 2009) and *P. capsici* (Lamour *et al.*, 2011). Furthermore, the closely related species to *P. infestans*, *P. ipomoeae*, *P. mirabilis* and *P. phaseoli*, have also been studied (Raffaele *et al.*, 2010). Effectors of the RXLR class are highly abundant in these *Phytophthora* genomes and current predictions estimate over 350 such genes in these various genomes (Jiang *et al.*, 2008; Haas *et al.*, 2009; Lamour *et al.*, 2011). The RXLR motif is also found in effectors from the oomycete *Hyaloperonospora arabidopsidis* (Baxter *et al.*, 2010) which belongs, like *P. infestans*, *P. ramorum* and *P. sojae*, to the Peronosporales. In addition, RXLR-like effectors have been found in *Saprolegnia parasitica* (Wawra *et al.*, 2012b) but not in the oomycetes *Pythium ultimum* (Levesque *et al.*, 2010) or *Albugo labachii* (Kemen *et al.*, 2011).

In addition to RXLR-containing effectors, a second group of effectors termed crinklers (CRNs) has been described in *Phytophthora* species (Haas *et al.*, 2009; Schornack *et al.*, 2010). The name crinkler describes the leaf crinkling and cell death phenotype associated with the expression of some CRNs *in planta*. Approximately 196 CRNs have been identified in *P. infestans*, 100 in *P. sojae* and 19 in *P. ramorum* (Haas *et al.*, 2009). Like RXLR effectors, CRNs are bi-modular and contain a canonical N-terminal domain which harbours the conserved LXLFLAK motif that is required for translocation into the host plant (Schornack *et al.*, 2010) and diverse C-terminal sequences that are thought to promote virulence (Haas *et al.*, 2009). Interestingly, CRNs have also been found in the oomycete pathogens *P. ultimum* and *Aphanomyces euteiches* which form no haustoria (Jiang *et al.*, 2008; Gaulin *et al.*, 2008; Schornack *et al.*, 2010). Considering

the large number of RXLR and CRN effectors in *P. infestans*, it is surprising that single effectors such as Avr3a appear to be essential for pathogenicity in oomycete pathogens. Indeed, as mentioned before, this finding is in stark contrast to bacterial T3SS effectors which are less abundant yet highly redundant (Collmer *et al.*, 2009). Nevertheless, *Avr3a* is not the only essential *P. infestans* effector for which silencing yields a significant reduced virulence phenotype (Bos *et al.*, 2010; Ventukuri *et al.*, 2011) and about 20 additional RXLRs have generated similar phenotypes (Whisson *et al.*, unpublished). Similarly, two CRN effectors from *P. sojae* have shown to be essential for pathogenesis by suppressing host defence responses including suppression of host-cell death responses and callose deposition (Liu *et al.*, 2011).

Bos *et al.* (2010) has shown that both *P. infestans* Avr3a^{KI} and Avr3a^{EM} can complement CS12 and are essential for *P. infestans* pathogenicity whereas Avr3a^{KI/Y147del} fails to restore pathogenicity. The data presented in this study are in good agreement with the previous findings (Figure 5.1). Furthermore, the data presented here demonstrate that Avr3a^{KIH} and Avr3a^{KIL} also restore virulence of CS12, whereas Avr3a^{EMH} and AVR3^{EMG} as well as PEX147-2 and PEX147-3 do not complement CS12 to statistically significant levels (Figure 5.2).

The inability of PEX147-2 to complement CS12 is not surprising considering that the protein product is unstable *in planta* (Figure 3.11). Therefore, PEX147-2 could be seen as a control alongside empty vector and Avr3a^{KI/Y147del}. Indeed, expression of *Pex147-2* did not yield a statistically significant growth rate for CS12 if compared to empty vector control ($p=0.282$) and Avr3a^{KI/147del} ($p=0.443$).

It is, however, surprising that whilst Avr3a^{KIH} could restore virulence of CS12, Avr3a^{EMH} could not, despite sharing the same amino acid substitution. Based on the low frequency of the change Q133H in the Avr3a^{KI} and Avr3a^{EM} background (Table 3.1; Figure 3.1), it is tempting to speculate that this change is slightly detrimental to Avr3a function. In previous functional studies, Avr3a^{KI} appeared to be slightly superior (statistically significant in some cases) if compared to Avr3a^{EM} in suppressing CMPG1-dependent cell death responses including ICD, CF-9/Avr9, CF-4/Avr4, cellulose-binding elicitor lectin (CBEL) recognition, Pto/AvrPto interaction and *Erwinia amylovora* (*Eam*) nonhost response in *N. benthamiana* (Bos *et al.*, 2006; 2009; 2010; Gilroy *et al.*, 2011a). The same observation was made in this study (Chapter 4) where Avr3a^{KI} had a stronger, yet not statistically significant cell death suppression activity if compared to Avr3a^{EM} (Figure 4.1). Thus, if the Q133H has a slightly negative impact on functionality, Avr3a^{KIH} remains potentially above the required activity threshold for functionality whereas Avr3a^{EMH} is below the required threshold. Indeed, unlike Avr3a^{KIH}, Avr3a^{EMH} did not suppress ICD or the recognition response following co-infiltration of CF-4 with Avr4 and only weakly stabilized CMPG1 *in planta* (Figure 4.1; Figure 4.2; Figure 4.3) which is in line with the compromised functionality hypothesis presented here.

In this context, it is also feasible that the function of Avr3a^{EMG} has been compromised and is below the threshold required for restoring full virulence of CS12, whereas Avr3a^{KIH} and Avr3a^{KIL} remain above this boundary. It is interesting to note that nevertheless, Avr3a^{EMG} suppresses CMPG1-dependent cell death responses including ICD and CF-4/Avr4 (Figure 4.1; Figure 4.2). Albeit that a lack of concrete evidence exists at this stage to support the molecular basis of the phenotype, the outcome could be explained in at least two ways: A) the mode of action by which Avr3a^{EMG} (and

potentially also Avr3a^{EMH}) interacts with and stabilizes CMPG1 is different to Avr3a^{EM} or quantitatively not as efficient or as effective. B) CMPG1 is an important virulence target for Avr3a but not the only essential target and Avr3a^{EMH} is compromised in effectively modifying the additional (unknown) host target(s). In support of these hypotheses is the fact that, in yeast-2-hybrid assays, Avr3a^{EMG} interacts only with three of the eight interactors identified for Avr3a^{EM}. However, CMPG1 was not amongst the Y2H interactors of Avr3a^{EMG} which is in contrast to the western and confocal analyses (Figures 4.3; Figure 4.5C) and could potentially point towards a false-negative result.

The low frequency by which the additional alleles are found in nature and the fact that *Pex147-3* is not expressed in *P. infestans* is in good agreement with the mutation studies conducted by Bos *et al.* (2009). It appears that Avr3a tolerates relatively few mutations to retain functionality and, in the case of Avr3a^{EM}, to continue to evade recognition by R3a. *Pex147-3*, which is more closely related to Avr3a than *Pex147-2* (Armstrong *et al.*, 2005), can be distinguished from Avr3a by 8 synonymous and 20 nonsynonymous polymorphisms (Armstrong *et al.*, 2005). It appears that *Pex147-3* can suppress ICD independently of stabilizing CMPG1 (Figure 4.1) but that Avr3a has acquired additional functions that are required to restore virulence in CS12 that are missing in *Pex147-3*.

The data presented here provide clear evidence that ICD suppression alone is not the only (essential) virulence function for Avr3a. Albeit Bos *et al.* (2009; 2010) demonstrated that the C-terminal tyrosine in position 147 in Avr3a^{KI} is crucial for suppressing ICD and deletion of this amino acid fails to restore virulence of C12, Avr3a^{EMG} and *PEX147-3* could suppress ICD but were unable to restore virulence of

CS12. Indeed, ICD suppression appears to be redundant in *P. infestans* as at least two additional RXLR effectors, PexRD8 and PexRD3645-1, also suppress ICD (Oh *et al.*, 2009).

CHAPTER 6

6 GENERAL DISCUSSION AND FUTURE WORK

6.1 GENERAL DISCUSSION

Due to the socioeconomic importance of potato as a crop and the impact of late blight disease on food security, there is a need to secure potato production worldwide. Approaches that are currently being implemented to reduce losses to pathogens whilst increasing yield include integrated disease management which aims to provide the most suitable growing and storing conditions for pathogen free production. However, the use of environmentally harmful fungicides (up to 20 applications per growing season) remains an integral part of current potato production methods (Hansen *et al.*, 2007). The identification and deployment into cultivars of broad spectrum disease resistance genes offer an opportunity to substantially reduce the amount of pesticide applications.

However, traditional breeding methods have not taken advantage of the emerging knowledge of pathogen infection mechanisms and the role of effectors to identify and/or engineer durable *R* genes (Vleeshouwers *et al.*, 2011). In a paradigm shift from conventional breeding, the use of universally expressed and essential pathogen effectors (also known as core effectors) as the chief drivers to identify more durable resistances provides a unique opportunity to realize durability (Birch *et al.*, 2008). This approach relies, however, on a detailed knowledge of effector diversity and their mode of action and functional redundancy (Vleeshouwers *et al.*, 2008).

The focus of this study was the *P. infestans* effector Avr3a and the recently discovered limited naturally occurring diversity. Importantly, I have shown that this restriction of Avr3a diversity is most likely a result of the pathogen's need to maintain Avr3a function to promote virulence.

Chapter Three of this thesis expands on the findings of Armstrong *et al.* (2005) who demonstrated that two major haplotypes, Avr3a^{KI} and Avr3a^{EM}, explain avirulence and virulence, respectively in potato plants carrying the cognate *R3a* gene. Sequence diversity of Avr3a was established in the Toluca Valley in Mexico, a centre for *Solanum/P. infestans* co-evolution (Gruenwald & Flier, 2005) by Armstrong *et al.* (unpublished). Additional alleles, Avr3a^{KIL}, Avr3a^{KIH}, Avr3a^{EMG} and Avr3a^{EMH}, were identified. These allelic variations were found within the C-terminal domain of the effector. Win *et al.* (2007) demonstrated that typically this part of effectors exhibits increased levels of polymorphism compared to the N-terminal domain which contains the signal peptide and RXLR (EER) domain(s) which are associated with effector secretion and translocation, respectively. This trend seems to be true for Avr3a. In addition to the here described amino acid substitutions, further C-terminal amino acid polymorphisms N77T, N74D, R81K, C95G have been reported alongside K80E and I103M in *P. infestans* isolates collected in the Northern Andean region (Cardenas *et al.*, 2011). N-terminal amino acid changes in Avr3a include N15Y and S19C, the latter which was also found in the Toluca Valley (Cardenas *et al.*, 2011; Armstrong *et al.*, unpublished) but not the subject of this study. It was proposed by Armstrong *et al.* (2005) that Avr3a^{EM} arose from an avirulent allele (e.g. Avr3a^{KI}) in a process that involved gene duplication and was driven by positive selection. The additional Avr3a alleles which have been studied in this thesis are likely to have arisen from mutations

within the Avr3a^{KI} or Avr3a^{EM} background, respectively. Only one amino acid substitution is shared between Avr3a^{KI} and Avr3a^{EM} (Q133H) and could be a result of a gene conversion event (Chen *et al.*, 2007).

The frequency of these newer alleles is, however, very low (Table 3.1; Figure 3.1) and Avr3a^{KIL}, Avr3a^{KIH}, Avr3a^{EMG} and Avr3a^{EMH} exist only in conjunction with either Avr3a^{KI} and/or Avr3a^{EM}. The limited diversity found for Avr3a in naturally occurring isolates is in line with laboratory studies described by Bos *et al.* (2009) where mutagenesis of Avr3a often yielded unstable proteins, gain of recognition by R3a or loss of virulence function. By threading the amino acid substitutions onto the established protein structure of *P. capsici* effector Avr3a11, a homolog of *P. infestans* Avr3a, it was demonstrated that the polymorphic amino acids locate to surface exposed residues (Boutemy *et al.*, 2011). Using the same approach for PEX147-2, it was shown that an amino acid insertion displaces a buried tyrosine that is key to the protein structure. Subsequently, it was shown that, indeed, PEX147-2 is unstable *in planta* and upon expression in yeast.

It is often thought that effector proteins and their cognate host resistance genes rapidly co-evolve (Ma & Guttman, 2008; McCann & Gutmann, 2008). Therefore, it was initially predicted that Avr3a should be highly mutable and diverse in *P. infestans* populations as isolates that could overcome R3a emerged quickly following the deployment of this resistance into potato cultivars in the 1950s (Fry 2008; Vleeshouwers *et al.*, 2011). However, the conservation of Avr3a is in stark contrast to the diversity of the *R* genes within the locus of the cognate potato resistance gene *R3a*. The *R3* locus is the second largest NB-LRR gene cluster in potato and contains 24

members on chromosome 11 (Jupe *et al.*, 2012). Nevertheless, Avr3a is not the only effector recognised by genes from the R3 locus and, in addition to R3a (Huang *et al.*, 2005), the functionally validated potato and tomato *R* genes *R3b* which recognised the *P. infestans* effector AVR3b (Li *et al.*, 2011b), and the *Fusarium oxysporum* resistance gene *I2*, reside in this group (Ori *et al.*, 1997). Unlike the *H. arabidopsidis* effector ATR13 and the cognate Arabidopsis resistance gene RPP13, which show very close co-evolution and an almost matching diversity (Allen *et al.*, 2004), Avr3a and R3a appear to display contrasting evolution. Indeed, ATR13 and RPP13 display balancing selection, (also known as trench warfare) where long-lived *R* genes and effector variants are stably maintained within populations (Bakker *et al.*, 2006). R3 genes display a somewhat similar balancing selection whereas Avr3a shows hallmarks associated with an 'arms race' where selective sweeps result in rapid turnover of Avr alleles and yield loci with few, relatively young alleles (Bakker *et al.*, 2006).

In addition to the low diversity, the naturally occurring alleles that were tested in this study were recognised by R3a if they contained the amino acids K80 and I103. The paralog PEX147-3, which shares the amino acid K80 but displays an I103V substitution, is also recognised by R3a whereas PEX147-2 was found to be unstable *in planta*. These results are in line with the analysis conducted by Bos *et al.* (2006; 2009), which showed that regardless of the polymorphism at position 103, the amino acid residue K80 is critical for R3a recognition. Importantly, this also suggests that the naturally occurring Avr3a^{KI} derived variants do not offer an advantage over Avr3a^{KI} in plants that contain R3a. A role as dominant-negative effectors that suppress Avr3a-R3a recognition could be ruled out for all alleles and paralogs (Figure 3.12). To elucidate the functionality of the naturally occurring Avr3a alleles and the paralogs PEX147-3 and PEX147-2, their

ability to suppress host immunity, an activity typically associated with pathogen effectors (Block & Alfano, 2008), was assessed.

In Chapter Four, the focus was initially on the well established virulence role of Avr3a, to interact with and perturb CMPG1-dependent cell death responses (Bos *et al.*, 2010; Gilroy *et al.*, 2011b). Both Avr3a^{KI} and Avr3a^{EM} have been shown to suppress host immunity induced by INF1 by interacting with and stabilizing CMPG1 (Bos *et al.*, 2010). Naturally occurring variants derived from Avr3a^{KI} are functionally similar to Avr3a^{KI} in that they interact with and stabilise CMPG1 *in planta* and suppress ICD and CF-4/Avr4 cell death responses. In contrast, only Avr3a^{EMG} stabilises CMPG1 *in planta* to a level that is comparable with Avr3a^{EM} albeit not as efficiently as Avr3a^{KI} (summarised in Figure 6.1). Upon co-infiltration with CMPG1 *in planta*, Avr3a^{EMH} produced the weakest CMPG1 stabilisation product in western and confocal microscopy analysis. In line with this, Avr3a^{EMH} is unable to perturb ICD or CF-4/Avr4 cell death elicitation in the model plant *N. benthamiana* (Figure 4.3A). Intriguingly, PEX147-3, which did also not interact with or stabilise CMPG1 *in planta*, suppresses INF1 but not CF-4/Avr4 mediated cell death. This suggests that PEX147-3 functions either downstream or independently of CMPG1. Interestingly, the *P. infestans* effector RD8 also suppresses ICD (Oh *et al.*, 2009) and interacts, like PEX147-3, with KIPI-25 but not with CMPG1 (Armstrong *et al.*, unpublished). Armstrong *et al.* (unpublished) have further shown that in Y2H assays, KIPI-25 weakly interacts with CMPG1 and it is therefore tempting to speculate that this interaction could indirectly perturb CMPG1.

In Chapter Five the Avr3a silenced line CS12 was used to assess if CMPG1 stabilisation is the only essential virulence function of Avr3a. Using the mutant Avr3a^{KI/Y147del}, which

is recognised by R3a yet unable to interact with and stabilise CMPG1 *in planta* and does not restore virulence of CS12 upon transient expression in *N. benthamiana*, Bos *et al.* (2010) have shown that CMPG1 modification is an important virulence function. However, in addition to CMPG1, a further 12 host proteins interact with Avr3a^{KI} and/or Avr3^{EM} in the Y2H system (Bos *et al.*, 2010). Albeit the Y2H analysis for the naturally occurring *Avr3a* alleles in Chapter 4 was somewhat inconclusive due to the presence of false negatives and false positive interactions (e.g. the failure of Avr3a^{KIL} and Avr3a^{EMG} to interact with CMPG1 whereas Avr3a^{EMH} did interact; Table 4.4), with the exception of KIP1-5, these interactions were confirmed in various combinations.

The complementation assay is one of the most informative functional assessment tools. Standard virulence tests often focus on simple readouts such as perturbation of callose deposition, ICD suppression or other forms of PCD suppression (e.g. Wang *et al.*, 2011; Anderson *et al.*, 2012) whereas the *in planta* complementation assay allows study of effector function in a holistic approach. It is thus remarkable that only Avr3a^{KI}, Avr3a^{KIL}, Avr3a^{KIH} and Avr3a^{EM} restore virulence of CS12 whereas Avr3a^{EMH} and Avr3a^{EMG}, the latter two which interacted and stabilised CMPG1, do not. It should, however, be pointed out that we know very little about the exact molecular modifications of CMPG1 *in planta* and it is conceivable that Avr3a not only stabilises CMPG1 but also modifies it in an hitherto unknown way. The latter function could, for example, be compromised in Avr3a^{EMH} and Avr3a^{EMG}. Alternatively, in the case of Avr3a^{EMH} where CMPG1 stabilisation was weakest, sufficient endogenous CMPG1 could escape stabilisation and thus yield a resistance response that is sufficient to stop development of CS12. Nevertheless, Avr3a^{EMH} and Avr3a^{EMG} restore virulence to levels that are only comparable to Avr3a^{KI/Y147del}, PEX147-2 and PEX147-3. There is thus

evidence, that CMPG1 stabilisation is unlikely the only essential virulence function of Avr3a (Figure 6.1).

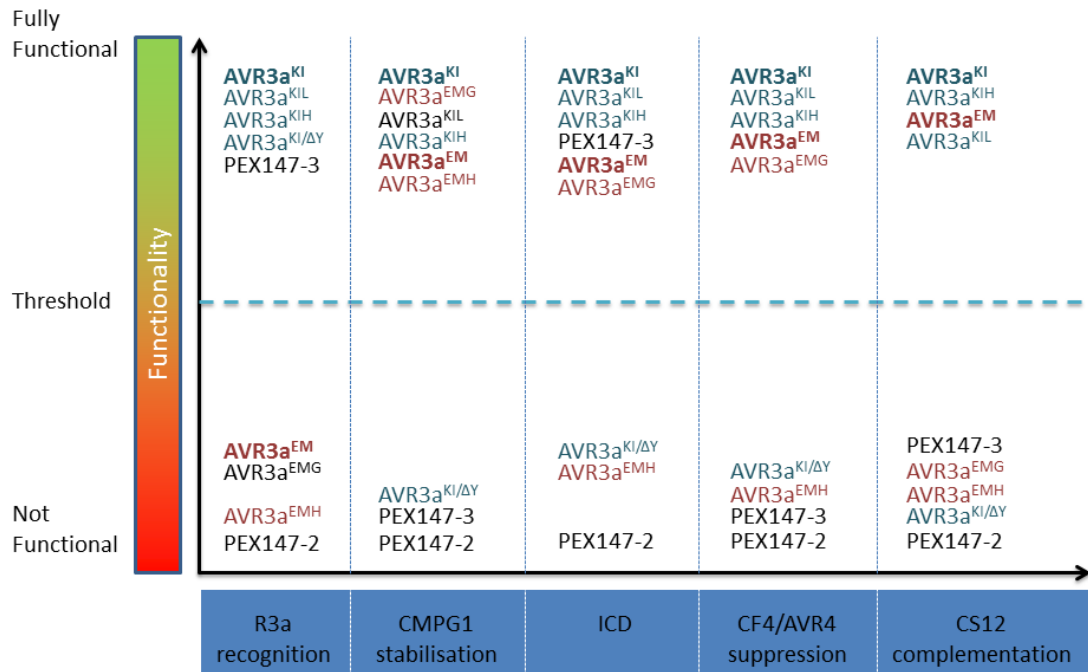


Figure 6.1: Activity of Avr3a^{KI} and Avr3a^{EM} (both in bold) together with their allelic variants (blue for Avr3a^{KI} and red for AVR3^{EM}-derived alleles) and paralogs, PEX147-2 and PEX147-3. Recognition by R3a is shown alongside their ability to interact with and stabilise CMPG1, suppression of INF1 and CF-4/AVR4 cell death as well as restoring pathogenicity of CS12. Tightly grouped effectors were shown not to be statistically different if compared to the appropriate experimental control. The order of effectors within tightly linked groups is indicative of their relative activity in the individual assays but does not necessary reflect statistically significant differences. The Figure summarises the following data: R3a recognition – Figures 3.8 and 3.9; CMPG1 stabilisation – Figure 4.3; INF1 cell death suppression – Figure 4.1; AVR4/CF-4 cell death suppression – Figure 4.2; CS12 complementation – Figure 5.2.

An interesting concept in evolutionary biology is the idea of a cost-of-virulence. This cost is typically associated with adaptation of pathogens following a gene-for-gene model and suggests that adaptations to e.g. host resistances incur a cost for the pathogen (Vanderplank, 1984). The cost of virulence is often associated with a decrease in fitness which could be defined as the ability of an organism to survive and reproduce (Frank, 1993). In Vanderplank's model (Vanderplank, 1984) it is assumed that, in the absence of the resistance gene, isolates that would otherwise be avirulent

have higher fitness than those that are virulent. Bahri *et al.* (2009) showed that, in the absence of the cognate resistance genes, near isogenic genotypes of the fungal wheat pathogen *Puccinia striiformis* f.sp. *tritici*, that differed in the expression of single virulence factors, vir4 and vir6, suffered significant fitness costs on wheat. However, in the same study, the authors demonstrated that expression of vir9 provided an advantage to the yellow rust fungus *P. striiformis* f.sp. *tritici*. Unfortunately, however, the near-isogenic lines were determined based on AFLP markers, and variations in multiple genes (and effectors) could not be ruled out. Furthermore, the virulence genes were inferred based on infection assays on differential wheat cultivars and not by a detailed knowledge of the effectors (Bahri *et al.*, 2009).

With the knowledge of effectors in mind, the cost of virulence model suggests that diversity (sequence or expression) within effector genes that determine the change from avirulence to virulence is often associated with a decrease in fitness. If thought through for Avr3a^{KI} (Avirulent) and Avr3a^{EM} (Virulent) this hypothesis has two implications:

a) if accepting this hypothesis, one would predict a widespread recognition of Avr3a^{KI} in wild Solanaceae hosts of *P. infestans* either through R3a or other, not yet identified *R* genes. Indeed, R3a is predicted to be an ancient gene that originates from central Mexico, is widely deployed in potato cultivars and functional homologs have been identified within wild species such as *S. stoloniferum* (*Rpi-sto2*) (Vleeshouwers *et al.*, 2011). Taking the dominance of Avr3a^{EM} in *P. infestans* populations into consideration, this would also rule out that other *P. infestans* effectors could perturb the recognition of Avr3a^{KI} or at least that these inhibiting effectors are not frequently found which could again be associated with pathogen virulence costs.

b) if the above hypothesis is dismissed, then there is no cost of virulence associated with $Avr3a^{EM}$. Support for this comes from a recent *P. infestans* sequencing project. Cooke *et al.* (2012) sequenced one of the most aggressive contemporary *P. infestans* isolates of cultivated potato. If compared to the reference genome of T30-4 (Haas *et al.*, 2009), the isolate 06_3928A of the lineage 13_A2 displays extensive sequence and expression polymorphisms throughout the genome and within effector genes. The isolate expresses *Avrblb1*, *Avrblb2* and *Avrvnt1* that are recognised by Rpi_blb1, Rpi_blb2 and Rpi_vnt1, respectively (Hein *et al.*, 2009). However, 06_3928A is homozygous for $Avr3a^{EM}$ and, by expressing *Avr2*-like instead of *Avr2* (Gilroy *et al.*, 2011a) and not expressing *Avr4* (Van Poppel *et al.*, 2008) evades recognition by R3a, R2 and R4 respectively. A transgenic line of 06_3928A that stably expresses *Avr2* to demonstrate that *Avr2* is specifically recognised by R2 (Gilroy *et al.*, 2011a) did not yield a growth advantage on susceptible potato cultivar Craigs Royal. Subjectively, the wild type isolate grew more vigorously although effects from the transformation procedure cannot be ruled out. As already mentioned for *Avr4*, mutations, deletion or lack of expression in other *P. infestans* isolates does not interfere with pathogen fitness, which explains why virulent races have evolved rapidly and are found at high frequencies (Vleeshouwers *et al.*, 2011). It is highly likely that in such cases functional redundancy in the effector complement can compensate for the loss of an effector gene to maintain the pathogen's fitness (Birch *et al.*, 2008).

Avr3a is, however, an essential effector and, at least in the silenced *P. infestans* isolate 88069, not functionally redundant. In the conducted complementation assays shown in Figures 5.1, Figure 5.2 and Table 5.1, there was no statistically significant difference in restoring virulence between $Avr3a^{EM}$, $Avr3a^{KI}$, $Avr3a^{KIL}$ and $Avr3a^{KIH}$ and thus no

obvious cost of virulence in the traditional sense. However, a new definition of the cost of virulence is conceivable that could be termed 'cost of dependency'. In order to maintain virulence, *P. infestans* requires Avr3a and to evade recognition by R3a, the pathogen relies on Avr3a^{EM}. Naturally occurring diversity of Avr3a^{KI} remains recognised by R3a whereas diversification of Avr3a^{EM} yields a loss of virulence. Thus, *P. infestans* might be vulnerable to resistances that recognise Avr3a^{EM} unless hitherto unknown suppressers have been co-evolved that prevent events downstream of recognition.

The concept of multiple effectors acting together to protect effector function is not unprecedented (e.g. Hogenhout *et al.*, 2009; Wang *et al.*, 2011). For example, recent studies on the *P. infestans* effector IPI-O, supports this synergy concept (Chen *et al.*, 2012). The alleles IPI-O1 and IPI-O2 elicit Rpi_blb1 (RB) dependent resistance in potato (Champouret *et al.*, 2009). However, isolates that in addition to IPI-O1 contain IPI-O4 variants can infect plants containing *Rpi_blb1* by suppressing *R* gene activity (Halterman *et al.*, 2010).

Without evidence of effectors that could interfere with Avr3a^{KI} and Avr3a^{EM} recognition, Avr3a fulfils all the criteria required to find more durable resistance. Indeed, following the research outlined in this thesis, concerted efforts are underway to identify NB-LRRs that recognise all functional Avr3a forms or Avr3a^{EM} specifically and which could then be deployed together with R3a. Approaches include searches for naturally occurring resistances (Bryan & Hein, 2008) and engineering R3a based gain of recognition forms (Stevens *et al.*, unpublished; Vleeshouwers *et al.*, 2011).

The main conclusions of this study can be summarised as follows:

- Limited Avr3a diversity is associated with the need for the effector to promote virulence whilst retaining protein stability *in planta*.
- Only Avr3a^{EM} evades recognition by R3a whilst providing full virulence function
- CMPG1 stabilisation is not necessarily the only essential function of Avr3a
- There is potentially a cost associated with effector dependency as all studied isolates of *P. infestans* contain Avr3a^{KI} and/or Avr3a^{EM}. Loss of Avr3a yields significantly reduced pathogenicity and only limited amino acid changes are permitted to retain functionality
- Identification or engineering of a resistance gene(s) that recognises Avr3a^{EM} or Avr3a^{EM} and Avr3a^{KI} could provide more durable resistance.

6.2 FUTURE WORK

As is typical for scientific studies, by answering the question if the naturally occurring Avr3 variants are functional, additional questions have been raised:

1. What is the role of KIPI-25?

Pex147-3 suppresses ICD but fails to suppress cell death mediated by CF-4/Avr4. Similarly, RD8 also suppresses ICD (Oh *et al.*, 2009) and, like PEX147-3, does not interact with CMPG1 in yeast. However, both PEX147-3 and RD8 have been shown to interact with KIPI-25 in Y2H assays. In turn, KIPI-25 interacts with CMPG1 in yeast (Armstrong *et al.*, unpublished). It is conceivable that this host virulence target functions down-stream of CMPG1 or, alternatively, functions independently of CMPG1 to suppress INF1 mediated cell death. Thus, follow up experiments could involve the

generation of VIGS construct to silence KIPI-25 transiently in *N. benthamiana* and to then study the effects on ICD, CMPG1 stabilisation and pathogen virulence.

2. Do effectors from other oomycetes also target KIPI-25 or CMPG1 and do they suppress ICD?

The importance of KIPI-25 in suppressing ICD could be further investigated by using the *H. parasitica* effector ATR1^{Emoy3} that has been shown to interact with KIPI-25 but not with CMPG1 (Armstrong, unpublished). ATR1 variants ATR1^{Noks1}, which does not interact with either KIPI-25 or CMPG1, could be used as a control to establish if ATR1^{Emoy3} but not ATR1^{Noks1} suppresses ICD.

3. What is the nature of the CMPG1 stabilisation?

CMPG1 has been shown to be an essential virulence target for Avr3a and is stabilised by Avr3a^{KI} and Avr3a^{EM} (Bos *et al.*, 2010). Interestingly, Avr3a^{EMG} also interacts with CMPG1 to suppress CMPG1-mediated cell deaths including ICD and CF-4/Avr4 but fails to restore pathogenicity of CS12. Similarly, Avr3a^{EMH} stabilises CMPG1 somewhat *in planta* but does not suppress ICD and CF-4/Avr4 mediated cell death. Thus, future studies to elucidate the molecular mechanisms of CMPG1 perturbation could be conducted.

4. Is Avr3a a promiscuous effector with many essential host virulence functions?

In addition to CMPG1, Avr3a interacts with numerous host virulence targets (Bos *et al.*, 2010). Their role remains yet to be discovered and could involve VIGS studies to assess their impact on pathogenicity.

5. Is Avr3a function conserved across oomycetes?

Avr3a homologs have been identified in *P. capsici* (Yeano *et al.*, 2011; Boutemy *et al.*, 2011). The *P. infestans* Avr3a^{EM} silenced line CS12 could be used to assess if the *P. capsici* effectors are true orthologues and if, as such, they can reconstitute virulence of CS12 in *N. benthamiana*.

6. Can we find durable host resistance?

Avr3a^{EM} has been identified in this study as a strong candidate for more durable potato resistance breeding. Thus, the next step is to generate potato plants with an enhanced resistance spectrum and durability by incorporating naturally occurring NB-LRRs or engineered, synthetic *R* genes with expanded pathogen recognition specificities that includes recognition of Avr3a^{EM}. Gain-of-function variants of R3a (R3a^{*}) have already been engineered by an iterative process of random mutagenesis and shuffling of the leucine rich repeat (LRR)-encoding region of R3a which is associated with Avr3a recognition (Stevens *et al.*, unpublished).

7. Does Avr3a play a role in non-host resistance in closely related Solanaceae species?

Non-host resistance is a form of defence found in plants outside the pathogen's host range. Non-host resistance provides protection to all isolates of a given pathogen and is thought to be more durable (Schulze-Lefert & Panstruga, 2011). It has been speculated that the contribution of PTI and ETI to non-host resistance is relative to the phylogenetic distance between host and non-host species (Schulze-Lefert & Panstruga, 2011). According to this hypothesis, for a given pathogen, if the phylogenetic distance between host and non-host plants increases, the non-host resistance to this pathogen is more likely based on PTI. On the other hand, if the phylogenetic distance between

host and non-host plants decreases, ETI is expected to be the main constituent of the non-host resistance. As an essential effector from *P. infestans*, it is conceivable that recognition of Avr3a triggers a non-host HR in other Solanaceae plants such as pepper or *Nicotiana* species (e.g. *Nicotiana sylvestris*). This could be assessed by expressing Avr3 alleles transiently via *A. tumefaciens* in non-host species and assessing recognition specificities.

CHAPTER 7

7 REFERENCES

- Abramovitch R. B., Janjusevic, R., Stebbins, C. E. and Martin G. B.** (2006) Type III effector *AvrPtoB* requires intrinsic E3 ubiquitin ligase activity to suppress plant cell death and immunity. *Proceedings of the National Academy of Sciences, USA*, 103, 2851–2856.
- Agrios, G. N. and Beckerman, J.** (2011) *Plant Pathology*. New York: Academic Press. 922 pp. 6th ed.
- Allen, R. L., Bittner-Eddy, P. D., Grenville-Briggs, L. J., Meitz, J. C., Rehmany, A. P., Rose, L. E. and Beynon, J. L.** (2004) Host-parasite co-evolutionary conflict between *Arabidopsis* and downy mildew. *Science*, 306, 1957–1960.
- Almeida, N. F., Yan, S., Lindeberg, M., Studholme, D. J., Schneider, D.J., Condon, B., Liu, H., Viana, C. J., Warren, A., Evans, C., Kemen, E., MacLean, D., Angot, A., Martin, G. B., Jones, J. D., Collmer, A., Setubal, J. C. and Vinatzer, B. A.** (2009) A draft genome sequence of *Pseudomonas syringae* pv. *tomato* strain T1 reveals a repertoire of Type III related genes significantly divergent from that of *Pseudomonas syringae* pv. *tomato* strain DC3000. *Molecular Plant–Microbe Interactions*, 22, 52–62.
- Anderson, R. G., Casady, M. S., Fee, R. A., Vaughan, M. M., Deb, D., Fedkenheuer, K., Huffaker, A., Schmelz, E. A., Tyler, B. M., McDowell, J. M.** (2012) Homologous RXLR effectors from *Hyaloperonospora arabidopsidis* and *Phytophthora sojae* suppress immunity in distantly related plants. *The Plant Journal*, 72, 882–893. doi: 10.1111/j.1365-313X.2012.05079.x.
- Armstrong, M. R., Whisson, S. C., Pritchard, L., Bos, J. I. B., Venter, E., Avrova, A. O., Rehmany, A. P., Böhme, U., Brooks, K., Cherevach, I., Hamlin, N., White, B., Fraser, A., Lord, A., Quail, M. A., Churcher, C., Hall, N., Berriman, M., Huang, S., Kamoun, S., Beynon, J. L. and Birch, P. R. J.** (2005) An ancestral oomycete locus contains late blight avirulence gene *Avr3a*, encoding a protein that is recognised in the host cytoplasm. *Proceedings of the National Academy of Sciences, USA*, 102, 7766–7771.
- Ausubel, F. M.** (2005) Are innate immune signalling pathways in plants and animals conserved? *Nature Immunology*, 6, 973–979.
- Badel, J. L., Shimizu, R., Oh, H. S. and Collmer, A.** (2006) A *Pseudomonas syringae* pv. *tomato* *AvrE1/hopM1* mutant is severely reduced in growth and lesion formation in tomato. *Molecular Plant–Microbe Interactions*, 19, 99–111.
- Bahri, B., Kaltz, O., Leconte, M., de Vallavieille-Pope, C. and Enjalbert, J.** (2009) Tracking costs of virulence in natural populations of the wheat pathogen, *Puccinia striiformis* f.sp. *tritici*. *BMC Evolutionary Biology*, 9, 26. doi:10.1186/1471-2148-9-26.

- Bakker, E. G., Toomajian, C., Kreitman, M. and Bergelson J.** (2006) A genome-wide survey of *R* gene polymorphisms in *Arabidopsis*. *The Plant Cell*, 18, 1803–1818.
- Ballvora, A., Ercolano, M. R., Weiss, J., Meksem, K., Bormann, C. A., Oberhagemann, P., Salamini, F. and Gebhardt, C.** (2002) The R1 gene for potato resistance to late blight (*Phytophthora infestans*) belongs to the leucine zipper/NBS/LRR class of plant resistance genes. *The Plant Journal*, 30, 361–371.
- Baxter, L., Tripathy, S., Ishaque, N., Boot, N., Cabral, A., Kemen, E., Thines, M., Ah-Fong, A., Anderson, R., Badejoko, W., Bittner-Eddy, P., Boore, J. L., Chibucos, M. C., Coates, M., Dehal, P., Delehaunty, K., Dong, S., Downton, P., Dumas, B., Fabro, G., Fronick, C., Fuerstenberg, S. I., Fulton, L., Gaulin, E., Govers, F., Hughes, L., Humphray, S., Jiang, R. H., Judelson, H., Kamoun, S., Kyung, K., Meijer, H., Minx, P., Morris, P., Nelson, J., Phuntumart, V., Qutob, D., Rehmany, A., Rougon-Cardoso, A., Ryden, P., Torto-Alalibo, T., Studholme, D., Wang, Y., Win, J., Wood, J., Clifton, S. W., Rogers, J., Van den Ackerveken, G., Jones, J. D., McDowell, J. M., Beynon, J. and Tyler, B. M.** (2010) Signatures of adaptation to obligate biotrophy in the *Hyaloperonospora arabidopsidis* genome. *Science*, 330, 1549–1551.
- Bhattacharjee, S., Stahelin, R. V., Speicher, K. D., Speicher, D. W., Haldar, K.** (2012) Endoplasmic reticulum PI(3)P lipid binding targets malaria proteins to the host cell. *Cell*, 148, 201–212.
- Birch, P. R. J. and Whisson, S. C.** (2001) *Phytophthora infestans* enters the genomics era. *Molecular Plant Pathology*, 2, 257–263.
- Birch, P. R. J., Boevink, P. C., Gilroy, E. M., Hein, I., Pritchard, L. and Whisson, S. C.** (2008) Oomycete RXLR effectors: delivery, functional redundancy and durable disease resistance. *Current Opinion in Plant Biology*, 11, 373–379.
- Birch, P. R. J., Rehmany, A. P., Pritchard, L., Kamoun, S. and Beynon, J. L.** (2006) Trafficking arms: oomycete effectors enter host plant cells. *Trends in Microbiology*, 14, 8–11.
- Block, A. and Alfano, J. R.** (2008) Plant targets for *Pseudomonas syringae* type III effectors: virulence targets or guarded decoys? *Current Opinion in Microbiology*, 14, 39–46.
- Boevink, P. C., Birch, P. R. J. and Whisson, S. C.** (2011) Imaging fluorescently tagged *Phytophthora* effector proteins inside infected plant tissue. *Methods in Molecular Biology*, 712, 195–209.
- Boller, T. and Felix, G.** (2009) A renaissance of elicitors: perception of microbe-associated molecular patterns and danger signals by pattern-recognition receptors. *Annual Review of Plant Biology*, 60, 379–406.
- Bos, J. I. B., Chaparro-Garcia, A., Quesada-Ocampo, L. M., McSpadden Gardener, B. B. and Kamoun, S.** (2009) Distinct amino acids of the *Phytophthora infestans* effector Avr3a condition activation of R3a hypersensitivity and suppression of cell death. *Molecular Plant–Microbe Interactions*, 22, 269–281.

Bos, J. I. B., Kanneganti, T.-D., Young, C., Cakir, C., Huitema, E., Win, J., Armstrong, M. R., Birch, P. R. J. and Kamoun, S. (2006) The C-terminal half of *Phytophthora infestans* RXLR effector Avr3a is sufficient to trigger R3a-mediated hypersensitivity and suppress INF1-induced cell death in *Nicotiana benthamiana*. *The Plant Journal*, 48, 165–176.

Bos, J. I. B., Armstrong, M. R., Gilroy, E. M., Boevink, P. C., Hein, I., Taylor, R. M., Tian, Z., Engelhardt, S., Vetukuri, R. R., Harrower, B., Dixelius, C., Bryan, J., Sadanandom, A., Whisson, S. C., Kamoun, S. and Birch, P. R. J. (2010) *Phytophthora infestans* effector Avr3a is essential for virulence and manipulates plant immunity by stabilizing host E3 ligase CMPG1. *Proceedings of the National Academy of Sciences, USA*, 107, 9909–9914.

Boutemy, L. S., King, S. R., Win, J., Hughes, R. K., Clarke, T. A., Blumenschein, T. M., Kamoun, S. and Banfield, M. J. (2011) Structures of *Phytophthora* RXLR effector proteins: a conserved but adaptable fold underpins functional diversity. *Journal of Biological Chemistry*, 286, 35834–35842.

Bozkurt, T. O., Schornack, S., Win, J., Shindo, T., Ilyas, M., Oliva, R., Cano, M. L., Jones, A. M. E., Huitema, E., van der Hoorn, R. A. L. and Kamoun, S. (2011) *Phytophthora infestans* effector AVRblb2 prevents secretion of a plant immune protease at the haustorial interface. *Proceedings of the National Academy of Sciences, USA*, 108, 20832–20837.

Brasier, C. M. (1992) Evolutionary biology of *Phytophthora* part I: Genetic system, sexuality and the generation of variation. *Annual Review of Phytopathology*, 30, 153–171.

Brückner, A., Polge, C., Lentze, N., Auerbach, D. and Schlattner, U. (2009) Yeast Two-Hybrid, a Powerful Tool for Systems Biology. *International Journal of Molecular Sciences*, 10, 2763–2788.

Bryan, G. J. and Hein, I. (2008) Genomic resources and tools for gene functional analysis in potato. *International Journal of Plant Genomics*, doi:10.1155/2008/216513

Cabral, A., Stassen, J. H., Seidl, M. F., Bautor, J., Parker, J. E., Van den Ackerveken, G. (2011) Identification of *Hyaloperonospora arabidopsidis* transcript sequences expressed during infection reveals isolate-specific effectors. *PLoS ONE* 6 (5): e19328.

Caillaud, M. C., Piquerez, S. J. and Jones, J. D. (2012) Characterization of the membrane-associated HaRxL17 Hpa effector candidate. *Plant Signalling & Behavior*, 7, 145–149.

Cárdenas, M., Grajales, A., Sierra, R., Rojas, A., González-Almario, A., Vargas, A., Marín, M., Fermín, G., Lagos, L. E., Grünwald, N. J., Bernal, A., Salazar, C. and Restrepo, S. (2011) Genetic diversity of *Phytophthora infestans* in the Northern Andean region. *BMC Genetics*, 12, 23. doi:10.1186/1471-2156-12-23

Catanzariti, A. M., Dodds, P. N. and Ellis, J. G. (2007) Avirulence proteins from haustoria forming pathogens. *FEMS Microbiol Letters*, 269, 181–188.

Causier, B. and Davies, B. (2002) Analysing protein-protein interactions with the yeast two-hybrid system. *Plant Molecular Biology*, 50, 855–870.

- Champouret, N., Bouwmeester, K., Rietman, H., van der Lee, T., Maliepaard, C., Heupink, A., van de Vondervoort, P. J. I., Jacobsen, E., Visser, R. G. F., van der Vossen, E. A. G., Govers, F. and Vleeshouwers, V. G. A. A.** (2009) *Phytophthora infestans* isolates lacking class I ipiO variants are virulent on Rpi-blb1 potato. *Molecular Plant–Microbe Interactions*, 22, 1535–1545.
- Chaparro-Garcia, A., Wilkinson, R. C., Gimenez-Ibanez, S., Findlay, K., Coffey, M. D., Zipfel, C., Rathjen, J. P., Kamoun, S. and Schornack, S.** (2011) The Receptor-Like Kinase SERK3/BAK1 Is Required for Basal Resistance against the Late Blight Pathogen *Phytophthora infestans* in *Nicotiana benthamiana*. *PLoS ONE* 6: e16608. doi:10.1371/journal.pone.0016608.
- Chen, J-M., Cooper, N.D., Chuzhanova, N., Ferec, C. and Patrinos P.G.** (2007) Gene conversion: mechanisms, evolution and human disease. *Nature Reviews Genetics*, 8, 762–775.
- Chen, Y., Liu, Z. and Halterman, D. A.** (2012) Molecular Determinants of Resistance Activation and Suppression by *Phytophthora infestans* Effector IPI-O. *PLoS Pathology*, 8, e1002595. doi:10.1371/journal.ppat.1002595.
- Chisholm, S. T., Coaker, G., Day, B. and Staskawicz, B. J.** (2006) Host–microbe interactions: Shaping the evolution of the plant immune response. *Cell*, 124, 803–814.
- Chou, S., Krasileva, K. V., Holton, J. M., Steinbrenner, A. D., Alber, T. and Staskawicz, B. J.** (2011) *Hyaloperonospora arabidopsidis* ATR1 effector is a repeat protein with distributed recognition surfaces. *Proceedings of the National Academy of Sciences, USA*, 108, 13323–13328.
- Coates, P. J. and Hall, P. A.** (2003) The yeast two-hybrid system for identifying protein–protein interactions. *Journal of Pathology*, 199, 4–7.
- Collmer, A., Schneider, D. J. and Lindeberg, M.** (2009) Lifestyles of the Effector Rich: Genome-Enabled Characterization of Bacterial Plant Pathogens. *Plant Physiology*, 50, 1623–1630.
- Cooke, D. E. L., Cano, L. M., Raffaele, S., Bain, R. A., Cooke, L. R., Etherington, G. J., Deahl, K. L., Farrer, R. A., Gilroy, E. M., Goss, E. M., Grünwald, N. J., Hein, I., MacLean, D., McNicol, J. W., Randall, E., Oliva, R. F., Pel, M. A., Shaw, D. S., Squires, J. N., Taylor, M. C., Vleeshouwers, V. G. A. A., Birch, P. R. J., Lees, A. K. and Kamoun, S.** (2012) Genome analyses of an aggressive and invasive lineage of the Irish potato famine pathogen. *PLoS Pathogens* 8(10), e1002940. doi:10.1371/journal.ppat.10
- Cunnac, S., Occhialini, A., Barberis, P., Boucher, C. and Genin, S.** (2004) Inventory and functional analysis of the large Hrp regulon in *Ralstonia solanacearum*: identification of novel effector proteins translocated to plant host cells through the type III secretion system. *Molecular Microbiology*, 53, 115–128.
- Damasceno, C. M., Bishop, J. G., Ripoll, D. R., Win, J., Kamoun, S., and Rose, J. K.** (2008) Structure of the glucanase inhibitor protein (GIP) family from *Phytophthora* species suggests co-evolution with plant endo- β -1,3-glucanases. *Molecular Plant–Microbe Interactions*, 21, 820–830.

Dangl, J. L. and Jones, J. D. G. (2001) Plant pathogens and integrated defence responses to infection. *Nature*, 411, 826–833.

de Jonge, R., van Esse, H. P., Kombrink, A., Shinya, T., Desaki, Y., Bours, R., van der Krol, S., Shibuya, N., Joosten, M. H. A. J. and Thomma, B. P. H. J. (2010) Conserved fungal LysM effector Ecp6 prevents chitin-triggered immunity in plants. *Science*, 329, 953–955.

DebRoy, S., Thilmony, R., Kwack, Y. B., Nomura, K., He, S. Y. (2004) A family of conserved bacterial effectors inhibits salicylic acid-mediated basal immunity and promotes disease necrosis in plants. *Proceedings of the National Academy of Sciences, USA*, 101, 9927–9932.

Deslandes, L. and Rivas, S. (2012) Catch me if you can: bacterial effectors and plant targets. *Trends in Plant Science*, 17, 644–655.

Dodds, P. N., Lawrence, G. J., Catanzariti, A. M., Teh, T., Wang, C. I., Ayliffe, M. A., Kobe, B. and Ellis, J. G. (2006) Direct protein interaction underlies gene-for-gene specificity and co-evolution of the flax resistance genes and flax rust avirulence genes. *Proceedings of the National Academy of Sciences, USA*, 103, 8888–8893.

Dodds, P. N., Rafiqi, M., Gan, P. H., Hardham, A. R., Jones, D. A. and Ellis, J. G. (2009) Effectors of biotrophic fungi and oomycetes: pathogenicity factors and triggers of host resistance. *New Phytologist*, 183, 993–1000.

Dodds, P. N. and Rathjen, J. P. (2010) Plant immunity: towards an integrated view of plant-pathogen interactions. *Nature Reviews Genetics*, 11, 539–548.

Dong, S., Qutob, D., Tedman-Jones, J., Kuflu, K., Wang, Y., Tyler, B. M. and Gijzen, M. (2009) The *Phytophthora sojae* avirulence locus *Avr3c* encodes a multi-copy RXLR effector with sequence polymorphisms among pathogen strains. *PLoS One*, 4(5): e5556. doi: 10.1371/journal.pone.0005556.

Dou, D., Kale, S. D., Wang, X., Chen, Y., Wang, Q., Wang, X., Jiang, R. H. Y., Arredondo, F. D., Anderson, R. G., Thakur, P. B., McDowell, J. M., Wang, Y. and Tyler, B. M. (2008a) Conserved C-Terminal Motifs Required for Avirulence and Suppression of Cell Death by *Phytophthora sojae* effector Avr1b. *The Plant Cell*, 20, 1118–1133.

Drenth, A., Tas, I. C. Q., and Govers, F. (1994) DNA fingerprinting uncovers a new sexually reproducing population of *Phytophthora infestans* in The Netherlands. *European Journal of Plant Pathology*, 100, 97–107.

Durrant, W. E., Rowland, O., Piedras, P., Hammond-Kosack, K. E. and Jones, J. D. G. (2000) cDNA-AFLP reveals a striking overlap in race-specific resistance and wound response gene expression profiles. *The Plant Cell*, 12, 963–977.

Eitas, T. K. and Dangl, J. L. (2010) NB-LRR proteins: pairs, pieces, perception, partners and pathways. *Current Opinion in Plant Biology*, 13, 1–6.

Ellis, J. G. and Dodds, P. N. (2011) Showdown at the RXLR motif: Serious differences of opinion in how effector proteins from filamentous eukaryotic pathogens enter plant cells. *Proceedings of the National Academy of Sciences, USA*, 108, 14381–14382.

- Ellis, J. G., Dodds, P. N. and Lawrence, G. J.** (2007a) Flax rust resistance gene specificity is based on direct resistance-avirulence protein interactions. *Annual Review of Phytopathology*, 45, 289–306.
- Elmore, J.M., Lin, Z.J., and Coaker, G.** (2011) Plant NB-LRR signalling: Upstreams and downstreams. *Current Opinion in Plant Biology*, 14, 365–371.
- Fabro, G., Steinbrenner, J., Coates, M., Ishaque, N., Baxter, L., Studholme, D. J., Körner, E., Allen, R. L., Piquerez, S. J., Rougon-Cardoso, A., Greenshields, D., Lei, R., Badel, J. L., Caillaud, M. C., Sohn, K. H., Van den Ackerveken, G., Parker, J. E., Beynon, J. and Jones, J. D.** (2011) Multiple candidate effectors from the oomycete pathogen *Hyaloperonospora arabidopsidis* suppress host plant immunity. *PLoS Pathogens*, 7(11):e1002348.
- Finley, D., Ciechanover, A., and Varshavsky, A.** (2004) Ubiquitin as a central cellular regulator. *Cell*, 116, S29–S32.
- Flier, W. G., Grunwald, N. J., Fry W. E. and Turkensteen L. J.** (2001b) Formation, production and viability of oospores of *Phytophthora infestans* from potato and *Solanum demissum* in the Toluca Valley, central Mexico. *Mycological Research*, 105, 998–1006.
- Flier, W. G., Grünwald, N. J., Kroon, L. P., Sturbaum, A. K., van den Bosch, T. B., Garay-Serrano, E., Lozoya-Saldaña, H., Fry, W. E. and Turkensteen, L. J.** (2003) The Population Structure of *Phytophthora infestans* from the Toluca Valley of Central Mexico Suggests Genetic Differentiation Between Populations from Cultivated Potato and Wild *Solanum* spp. *Phytopathology*, 93, 382–390.
- Flor, H. H.** (1971) Current status of the gene-for-gene concept. *Annual Review of Phytopathology*, 9, 275–296.
- Forch, M., van den Bosch, T., van Bekkum, P., Evenhuis, B., Vossen, J. H. and Kessel, G.** (2010) Monitoring the Dutch *Phytophthora infestans* population for virulence against new *R* genes. PPO-Special Report no. 14, 45–50.
- Forster, H., Coffey, M. D., Elwood, H. and Sogin, M. I.,** (1990) Sequence analysis of the small subunit ribosomal RNA of three zoosporic fungi and implications for fungal evolution. *Mycologia*, 82, 306–312.
- Foster, S. J., Park, T. H., Pel, M., Brigneti, G., Sliwka, J., Jagger, L., van der Vossen, E., and Jones, J. D. G.** (2009) *Rpi-vnt1.1*, a *Tm-22* homolog from *Solanum venturii*, confers resistance to potato late blight. *Molecular Plant–Microbe Interactions*, 22, 589–600.
- Frank, S. A.** (1993) Co-evolutionary genetics of plants and pathogens. *Evolutionary Ecology*, 7, 45–75.
- Fry, W. E.** (2008) *Phytophthora infestans*: the plant (and *R* gene) destroyer. *Molecular Plant Pathology*, 9, 385–402.
- Fry, W. E. and Goodwin, S. B.** (1997) Re-emergence of potato and tomato late blight in the United States. *Plant Disease*, 81, 1349–1357.

Galan, J.E. and Wolf-Watz, H. (2006) Protein delivery into eukaryotic cells by type III secretion machines. *Nature*, 444, 567–573.

Garthwaite, D. G., Barker, I., Parrish, G. and Smith, L. (2008) Pesticide usage survey report 227, *Potato stores in Great Britain*, National Statistics, York UK.

Gassmann, W. and Bhattacharjee, S. (2012) Effector-triggered immunity signalling: from gene-for-gene pathways to protein-protein interaction networks. *Molecular Plant–Microbe Interactions*, 25, 862–868.

Gaulin, E., Madoui, M-A., Bottin, A., Jacquet, C., Mathé, C., Couloux, A., Wincker, P. and Dumas, B. (2008) Transcriptome of *Aphanomyces euteiches*: New oomycete putative pathogenicity factors and metabolic pathways. *PLoS ONE* 3 e1723. doi:10.1371/journal.pone.0001723

Gijzen, M. and Nurnberger, T. (2006) Nep1-like proteins from plant pathogens: Recruitment and diversification of the NPP1 domain across taxa. *Phytochemistry*, 67, 1800–1807.

Gilroy, E. M., Breen, S., Whisson, S. C., Squires, J., Hein, I., Kaczmarek, M., Turnbull, D., Boevink, P. C., Lokossou, A., Cano, L. M., Morales, J., Avrova, A. O., Pritchard, L., Randall, E., Lees, A., Govers, F., van West, P., Kamoun, S., Vleeshouwers, V. G. A. A., Cooke, D. E. L. and Birch, P. R. J. (2011a) Presence/absence, differential expression and sequence polymorphisms between PiAVR2 and PiAVR2-like in *Phytophthora infestans* determine virulence on R2 plants. *New Phytologist*, 191, 763–776.

Gilroy, E. M., Taylor, R. M., Hein, I., Boevink, P., Sadanandom, A. and Birch, P. R. J. (2011b) CMPG1-dependent cell death follows perception of diverse pathogen elicitors at the host plasma membrane and is suppressed by *Phytophthora infestans* RXLR effector Avr3a. *New Phytologist*, 190, 653–666.

Glickman, M. H. and Ciechanover, A. (2002) The ubiquitin-proteasome proteolytic pathway: destruction for the sake of construction. *Physiological Reviews*, 82, 373–428.

Gohre, V. and Robatzek, S. (2008) Breaking the barriers: microbial effector molecules subvert plant immunity. *Annual Review of Phytopathology*, 46, 189–215.

González-Lamothe, R., Tsitsigiannis, D. I., Ludwig, A. A., Panicot, M., Shirasu, K. and Jones, J. D. (2006) The U-box protein CMPG1 is required for efficient activation of defence mechanisms triggered by multiple resistance genes in tobacco and tomato. *The Plant Cell*, 18, 1067–1083.

Goritschnig, S., Krasileva, K. V., Dahlbeck, D. and Staskawicz, B. J. (2012) Computational prediction and molecular characterization of an oomycete effector and the cognate *Arabidopsis* resistance gene. *PLoS Genetics*, 8:e1002502.

Grünwald, N. J. (2012) Genome sequences of *Phytophthora* enable translational plant disease management and accelerate research. *Canadian Journal of Plant Pathology*, 34, 13–19.

Grünwald, N. J. and Flier, W. G. (2005) Biology of *Phytophthora infestans* at its centre of origin. *Annual Review of Phytopathology*, 43, 171–190.

Haas, B. J., Kamoun, S., Zody, M. C., Jiang, R. H., Handsaker, R. E., Cano, L. M., Grabherr, M., Kodira, C. D., Raffaele, S., Torto-Alalibo, T., Bozkurt, T. O., Ah-Fong, A. M., Alvarado, L., Anderson, V. L., Armstrong, M. R., Avrova, A., Baxter, L., Beynon, J., Boevink, P. C., Bollmann, S. R., Bos, J. I., Bulone, V., Cai, G., Cakir, C., Carrington, J. C., Chawner, M., Conti, L., Costanzo, S., Ewan, R., Fahlgren, N., Fischbach, M. A., Fugelstad, J., Gilroy, E. M., Gnerre, S., Green, P. J., Grenville-Briggs, L. J., Griffith, J., Grünwald, N. J., Horn, K., Horner, N. R., Hu, C. H., Huitema, E., Jeong, D. H., Jones, A. M., Jones, J. D., Jones, R. W., Karlsson, E. K., Kunjeti, S. G., Lamour, K., Liu, Z., Ma, L., MacLean, D., Chibucos, M. C., McDonald, H., McWalters, J., Meijer, H. J., Morgan, W., Morris, P. F., Munro, C. A., O'Neill, K., Ospina-Giraldo, M., Pinzón, A., Pritchard, L., Ramsahoye, B., Ren, Q., Restrepo, S., Roy, S., Sadanandom, A., Savidor, A., Schornack, S., Schwartz, D. C., Schumann, U. D., Schwessinger, B., Seyer, L., Sharpe, T., Silvar, C., Song, J., Studholme, D. J., Sykes, S., Thines, M., van de Vondervoort, P. J. I., Phuntumart, V., Wawra, S., Weide, R., Win, J., Young, C., Zhou, S., Fry, W., Meyers, B. C., van West, P., Ristaino, J., Govers, F., Birch, P. R. J., Whisson, S. C., Judelson, H. S. and Nusbaum, C. (2009) Genome sequence and analysis of the Irish potato famine pathogen *Phytophthora infestans*. *Nature*, 461, 393–398.

Hahn, M. and Mendgen, K. (2001) Signal and nutrient exchange at biotrophic plant–fungus interfaces. *Current Opinion in Plant Biology*, 4, 322–327.

Haldar, K., Kamoun, S., Hiller, N.L., Bhattacharje, S. and van Ooij, C. (2006) Common infection strategies of pathogenic eukaryotes. *Nature Reviews Microbiology*, 4, 922–931.

Halterman, D. A., Chen, Y., Sopee, J., Berduo-Sandoval, J. and Sánchez-Pérez, A. (2010) Competition between *Phytophthora infestans* effectors leads to increased aggressiveness on plants containing broad-spectrum late blight resistance. *PLoS ONE*, 5(5): e10536. doi:10.1371/journal.pone.0010536.

Hansen, J.G., Andersson, B., Bain, R., Besnhofer, G., Bradshaw, N., Becena, L., Bugiani, R., Cakir, E., Cooke, L., Dubois, L., Filippov, A., Hannukkala, A., Hausladen, H., Hausvater, E., Heldak, J., Hermansen, A., Kapsa, J., Koppel, M., Lebecka, R., Lees, A., Musa, T., Nugteren, W., Ronis, A., Schepers, H., Spits, H. and Vanhaverbeke, P. (2007) The development and control of *Phytophthora infestans* in Europe in 2006. Tenth Workshop of an European Network for development of an Integrated Control Strategy of potato late blight Bologna (Italy); PPO report No. 12, 13–25.

Hauck, P., Thilmony, R., and He, S. Y. (2003) A *Pseudomonas syringae* type III effector suppresses cell wall-based extracellular defence in susceptible Arabidopsis plants. *Proceedings of the National Academy of Sciences, USA*, 100, 8577–8582.

Haverkort, A., Struik, P., Visser, R. and Jacobson, E. (2009) Applied biotechnology to combat late blight in potato caused by *Phytophthora infestans*. *Potato Research*, 52, 249–264.

Hawkes, J.G. (1990) *The potato: evolution, biodiversity and genetic resources*. Belhaven Press, Oxford, England/Smithsonian Institution Press, Washington, D. C. 259 pp.

- Heath, M. C.** (2000) Non-host resistance and non-specific plant defences. *Current Opinion in Plant Biology*, 3, 315–319.
- Hein, I., Gilroy, E. M., Armstrong, M. R. and Birch, P. R. J.** (2009) The zig-zag-zig in oomycete-plant interactions. *Molecular Plant Pathology*, 10, 547–562.
- Hellens, R. P., Edwards, E. A., Leyland, N. R., Bean, S., Mullineaux, P. M.** (2000) pGreen: a versatile and flexible binary Ti vector for *Agrobacterium*-mediated plant transformation. *Plant Molecular Biology*, 42, 819–832.
- Hershko, A., Heller, H., Elias, S. and Ciechanover, A.** (1983) Components of ubiquitin protein ligase system. Resolution, affinity purification, and role in protein breakdown. *Journal of Biological Chemistry*, 258, 8206–8214.
- Hijmans, R. J. and Spooner, D. M.** (2001) Geographic distribution of wild potato species. *American Journal of Botany*, 88, 2101–2112.
- Hijmans, R. J., Spooner, D. M., Salas, A. R., Guarino, L. and de la Cruz, J.** (2002) *Atlas of wild potatoes*. Systematic and Ecogeographic Studies in Crop Gene pools, 10, IPGRI, Rome.
- Hogenhout, S. A., Van der Hoorn, R. A. L., Terauchi, R. and Kamoun, S.** (2009). Emerging concepts in effector biology of plant-associated organisms. *Molecular Plant–Microbe Interactions*, 22, 115–122.
- Houterman, P. M., Cornelissen, B. J. C. and Rep, M.** (2008) Suppression of plant resistance gene-based immunity by a fungal effector. *PLoS Pathogens* 4: e1000061.
- Huang, S., van der Vossen, E. A. G., Kuang, H., Vleeshouwers, V. G. A. A., Zhang, N., Borm, T. J. A., van Eck, H. J., Baker, B., Jacobsen, E. and Visser, R. G. F.** (2005) Comparative genomics enabled the isolation of the R3a late blight resistance gene in potato. *The Plant Journal*, 42, 251–261.
- Huckelhoven, R.** (2007) Cell wall-associated mechanisms of disease resistance and susceptibility. *Annual Review of Phytopathology*, 45, 101–127.
- Hughes, A. L. and Nei, M.** (1989) Evolution of the major histocompatibility complex: independent origin of nonclassical class I genes in different groups of mammals. *Molecular Biology and Evolution*, 6, 559–579.
- Hunziker, A. T.** (2001) *Genera Solanacearum: the genera of Solanaceae illustrated*, arranged according to a new system. Ruggell, Liechtenstein: A.R.G. Gantner; Königstein, Germany: Koeltz Scientific Books.
- Jamir, Y., Guo, M., Oh, H. S., Petnicki-Ocwieja, T., Chen, S., Tang, X., Dickman, M. B., Collmer, A., Alfano, J. R.** (2004) Identification of *Pseudomonas syringae* type III effectors that can suppress programmed cell death in plants and yeast. *The Plant Journal*, 37, 554–565.
- Jia, Y., McAdams, S. A., Bryan, G. T., Hershey, H. P., and Valent, B.** (2000) Direct interaction of resistance gene and avirulence gene products confers rice blast resistance. *EMBO Journal*, 19, 4004–4014.

- Jiang, R. H. Y. and Tyler, B. M.** (2012) Mechanisms and evolution of virulence in oomycetes. *Annual Review of Phytopathology*, 50, 295–318.
- Jiang, R. H. Y., Tripathy, S., Govers, F. and Tyler, B. M.** (2008) RXLR effector reservoir in two *Phytophthora* species is dominated by a single rapidly evolving super-family with more than 700 members. *Proceedings of the National Academy of Sciences, USA*, 105, 4874–4879.
- Jin, Q., Thilmony, R., Zwiesler-Vollick, J. and He, S. Y.** (2003) Type III protein secretion in *Pseudomonas syringae*. *Microbes and Infection*, 5, 301–310.
- Jones, J. D. G. and Dangl, J. L.** (2006) The plant immune system. *Nature*, 444, 323–329.
- Joosten, M. H. A. J., Vogelsang, R., Cozijnsen, T. J., Verberne, M. C. and de Wit, P. J. G. M.** (1997) The biotrophic fungus *Cladosporium fulvum* circumvents CF-4 mediated resistance by producing unstable AVR4 elicitors. *The Plant Cell*, 9, 367–379.
- Judelson, H. S.** (1997) The Genetics and Biology of *Phytophthora infestans*: Modern Approaches to a Historical Challenge. *Fungal Genetics and Biology*, 22, 65–76.
- Jupe, F., Pritchard, L., Etherington, G. J., MacKenzie, K., Cock, P. J. A., Wright, F., Sharma, S. K., Bolser, D., Bryan, G. J., Jones, J. D. G. and Hein, I.** (2012) Identification and localisation of the NB-LRR gene family within the potato genome. *BMC Genomics*, 13, 75. doi:10.1186/1471-2164-13-75
- Kale, S. D. and Tyler, B. M.** (2011) Entry of oomycete and fungal effectors into plant and animal host cells. *Cellular Microbiology*, 13, 1839–1848.
- Kale, S. D., Gu, B., Capelluto, D. G. S., Dou, D. L., Feldman, E., Rumore, A., Arredondo, F. D., Hanlon, R., Fudal, I., Rouxel, T., Lawrence, C. B., Shan, W. and Tyler, B. M.** (2010) External lipid PI-3-P mediates entry of eukaryotic pathogen effectors into plant and animal host cells. *Cell*, 142, 284–295.
- Kamoun, S.** (2006) A catalogue of the effector secretome of plant pathogenic oomycetes. *Annual Review of Phytopathology*, 44, 41–60.
- Kamoun, S., Huitema, E. and Vleeshouwers, V. G. A. A.** (1999) Resistance to Oomycetes: a general role for the hypersensitive response. *Trends in Plant Science*, 4, 196–200.
- Karimi, M., Inzé, D. and Depicker, A.** (2002) GATEWAY vectors for *Agrobacterium*-mediated plant transformation. *Trends in Plant Science*, 7, 193–195.
- Katagiri, F.** (2004) A global view of defence gene expression regulation: a highly interconnected signalling network. *Current Opinion in Plant Biology*, 7, 506–511.
- Kawasaki, T., Nam, J., Boyes, D. C., Holt III, B. F., Hubert, D. A., Wiig, A. and Dangl, J. L.** (2005) A duplicated pair of *Arabidopsis* RING-finger E3 ligases contribute to the RPM1- and RPS2-mediated hypersensitive response. *The Plant Journal*, 44, 258–270.
- Keeling, P. J., Burger, G., Durnford, D. G., Lang, B. F., Lee, R. W., Pearlman, R. E., Roger, A. J. and Gray, M. W.** (2005) The tree of eukaryotes. *Trends in Ecology and Evolution*, 20, 670–676.

Kemen, E., Gardiner, A., Schultz-Larsen, T., Kemen, A. C., Balmuth, A. L., Robert-Seilaniantz, A., Bailey, K., Holub, E., Studholme, D. J., MacLean, D. and Jones, J. D. G. (2011) Gene gain and loss during evolution of obligate parasitism in the white rust pathogen of *Arabidopsis thaliana*. *PLoS Biology*, 9:e1001094

Kim H. J., Lee H. R., Jo, K. R., Mahdi Mortazavian, S. M., Huigen, D. J., Evenhuis, B., Kessel, G., Visser, R. G. F., Jacobsen, E. and Vossen, J. H. (2012) Broad spectrum late blight resistance in potato differential set plants MaR8 and MaR9 is conferred by multiple stacked *R* genes. *Theoretical and Applied Genetics*, 124, 923–935.

Kirk, J. L., Beaudette, L. A., Hart, M., Moutoglis, P., Klironomos, J. N., Lee, H. and Trevors, J. T. (2004) Methods of studying soil microbial diversity. *Journal of Microbiological Methods*, 58, 169–188.

Kirsch, C., Logemann, E., Lippok, B., Schmelzer, E. and Hahlbrock, K. (2001) A highly specific pathogen-responsive promoter element from the immediate-early activated CMPG1 gene in *Petroselinum crispum*. *The Plant Journal*, 26, 217–227.

Koga, H., Zeyen, R. J., Bushnell, W. R. and Ahlstrand, G. G. (1988). Hypersensitive cell death, autofluorescence, and insoluble silicon accumulation in barley leaf epidermal cells under attack by *Erysiphe graminis* f. sp. *hordei*. *Physiological and Molecular Plant Pathology*, 32, 395–409.

Krasileva, K.V., Dahlbeck, D., and Staskawicz, B.J. (2010) Activation of an *Arabidopsis* resistance protein is specified by the *in planta* association of its leucine-rich repeat domain with the cognate oomycete effector. *The Plant Cell*, 22, 2444–2458.

Kunze, G., Zipfel, C., Robatzek, S., Niehaus, K., Boller, T. and Felix, G. (2004) The N terminus of bacterial elongation factor Tu elicits innate immunity in *Arabidopsis* plants. *The Plant Cell*, 16, 3496–3507.

Lacombe, S., Rougon-Cardoso, A., Sherwood, E., Peeters, N., Dahlbeck, D., van Esse, H. P., Smoker, M., Rallapalli, G., Thomma, B. P. H. J., Staskawicz, B., Jones, J. D. and Zipfel, C. (2010) Interfamily transfer of a plant pattern-recognition receptor confers broad-spectrum bacterial resistance. *Nature Biotechnology*, 28, 365–369.

Gaulin, E., Bottin, A. and Dumas, B. (2010) Sterol biosynthesis in oomycete pathogens. *Plant Signal Behav.*, 5, 258–260.

González-Lamothe, R., Mitchell, G., Gattuso, M., Diarra, M. S., Malouin, F. and Bouarab, K. (2009) Plant Antimicrobial Agents and Their Effects on Plant and Human Pathogens. *International Journal of Molecular Sciences*, 10, 3400-3419.

Lamour, K. H., Stam, R., Jupe, J. and Huitema, E. (2011) The oomycetes broad-host-range pathogen *Phytophthora capsici*. *Molecular Plant Pathology*, DOI: 10.1111/J.1364-3703.2011.00754.X

Lawrence, G. J., Finnegan, E. J., Ayliffe, M. A. and Ellis, J. G. (1995) The L6 gene for flax rust resistance is related to the *Arabidopsis* bacterial resistance gene RPS2 and the tobacco viral resistance gene N. *The Plant Cell*, 7, 1195–1206.

Lehmann, P. (2002) Structure and evolution of plant disease resistance genes. *Journal of Applied Genetics*, 43, 403–414.

Leonelli, L., Pelton, J., Schoeffler, A., Dahlbeck, D., Berger, J., Wemmer, D. E. and Staskawicz, B. (2011). Structural elucidation and functional characterization of the *Hyaloperonospora arabidopsidis* effector protein ATR13. *PLoS Pathogens*, 7(12):e1002428.

Lévesque, C. A., Brouwer, H., Cano, L., Hamilton, J. P., Holt, C., Huitema, E., Raffaele, S., Robideau, G. P., Thines, M., Win, J., Zerillo, M. M., Beakes, G. W., Boore, J. L., Busam, D., Dumas, B., Ferreira, S., Fuerstenberg, S. I., Gachon, C. M. M., Gaulin, E., Govers, F., Grenville-Briggs, L., Horner, N., Hostetler, J., Jiang, R. H. Y., Johnson, J., Krajaeun, T., Lin, H., Meijer, H. J. G., Moore, B., Morris, P., Phuntmart, V., Puiu, D., Shetty, J., Stajich, J. E., Tripathy, S., Wawra, S., van West, P., Whitty, B. R., Coutinho, P. M., Henrissat, B., Martin, F., Thomas, P. D., Tyler, B. M., De Vries, R. P., Kamoun, S., Yandell, M., Tisserat, N. and Buell, C. R. (2010) Genome sequence of the necrotrophic plant pathogen *Pythium ultimum* reveals original pathogenicity mechanisms and effector repertoire. *Genome Biology*, 11: R73

Li, G., Huang, S., Guo, X., Li, Y., Yang, Y., Guo, Z., Kuang, H., Rietman, H., Bergervoet, M., Vleeshouwers, V. G. A. A., van der Vossen, E. A. G., Qu, D., Visser, R. G. F., Jacobsen, E. and Vossen, J. H. (2011b) Cloning and characterization of R3b; Members of the R3 superfamily of late blight resistance genes show sequence and functional divergence. *Molecular Plant–Microbe Interactions*, 24, 1132–1142.

Li, W., Ahn, I. P., Ning, Y., Park, C. H., Zeng, L., Whitehill, J., Lu, H., Zhao, Q., Ding, B., Xie, Q., Zhou, J. M., Dai, L. and Wang, G. L. (2012a) The U-box/ARM E3 ligase PUB13 regulates cell death, defence and flowering time in Arabidopsis. *Plant Physiology*, 159, 239–250.

Li, W., Zhong, S., Li, G., Li, Q., Mao, B., Deng, Y., Zhang, H., Zeng, L., Song, F. and He, Z. (2011) Rice RING protein OsBBI1 with E3 ligase activity confers broad-spectrum resistance against *Magnaporthe oryzae* by modifying the cell wall defence. *Cell Research*, 21, 835–848.

Liu, J., Elmore, J. M., Lin, Z.-J. D., and Coaker, G. (2011). A receptor-like cytoplasmic kinase phosphorylates the host target RIN4, leading to the activation of a plant innate immune receptor. *Cell Host & Microbe*, 9, 137–146.

Liu, J., Li, W., Ning, Y., Shirsekar, G., Wang, X., Dai, L., Wang, Z., Liu, W., and Wang, G. L. (2012) The U-box E3 Ligase SPL11/PUB13 Is a Convergence Point of Defense and Flowering Signaling in Plants. *Plant Physiology Preview*, DOI:10.1104/pp.112.199430.

Lokossou, A. A., Park, T. H., van Arkel, G., Arens, M., Ruyter-Spira, C., Morales, J., Whisson, S. C., Birch, P. R. J., Visser, R. G. F., Jacobsen, E. and Van der Vossen, E. A. G. (2009) Exploiting knowledge of *R/Avr* genes to rapidly clone a new LZ-NBS-LRR family of late blight resistance genes from potato linkage group IV. *Molecular Plant–Microbe Interactions*, 22, 630–641.

Long, M., Betran, E., Thornton, K. and Wang, W. (2003) The origin of new genes: Glimpses from the young and old. *Nature Reviews Genetics*, 4, 865–875.

- Lynch, M. and Conery, J. S.** (2000) The evolutionary fate and consequences of duplicate genes. *Science*, 290, 1151–1155.
- Ma, W. and Guttman, D. S.** (2008) Evolution of prokaryotic and eukaryotic virulence effectors. *Current Opinion in Plant Biology*, 11, 412–419.
- Malcolmson, J. F. and Black, W.** (1966). New *R* genes in *Solanum demissum* Lindl. and their complementary races of *Phytophthora infestans* (Mont.) De Bary. *Euphytica*, 15, 199–203.
- Martin, G. B., Brommonschenkel, S. H., Chunwongse, J., Frary, A., Ganai, M. W., Spivey, R., Wu, T., Earle, E. D and Tanksley, S. D.** (1993). Map-based cloning of a protein kinase gene conferring disease resistance in tomato. *Science*, 262, 1432–1436.
- McCann, H. C. and Guttman, D. S.** (2008) Evolution of the type III secretion system and its effectors in plant–microbe interactions. *New Phytologist*, 177, 33–47.
- McDonald, B. A. and Linde, C.** (2002) Pathogen population genetics, evolutionary potential, and durable resistance. *Annual Review of Phytopathology*, 40, 349–379.
- McHale, L., Tan, X., Koehl, P. and Michelmore, R. W.** (2006) Plant NBS-LRR proteins: adaptable guards. *Genome Biology*, 7, 212. doi:10.1186/gb-2006-7-4-212).
- Medzhitov, R. and Janeway, C. A.** (1997) Innate immunity: the virtues of a nonclonal system of recognition. *Cell*, 91, 295–298.
- Meng, S., Torto-Alalibo, T., Chibucos, M. C., Tyler, B. M. and Dean, R. A.** (2009) Common processes in pathogenesis by fungal and oomycete plant pathogens, described with gene ontology terms. *BMC Microbiology*, 9 (Suppl. 1): S7 doi:10.1186/1471-2180-9-S1-S7.
- Meyers, B. C., Dickerman, A. W., Michelmore, R. W., Sivaramakrishnan, S., Sobral, B. W. and Young, N. D.** (1999) Plant disease resistance genes encode members of an ancient and diverse protein family within the nucleotide-binding superfamily. *The Plant Journal*, 20, 317–332.
- Meyers, B. C., Kozik, A., Griego, A., Kuang, H. and Michelmore, R. W.** (2003) Genome-wide analysis of NBS-LRR-encoding genes in *Arabidopsis*. *The Plant Cell*, 15, 809–834.
- Moon, J., Parry, G., and Estelle, M.** (2004). The ubiquitin-proteasome pathway and plant development. *The Plant Cell*, 16, 3181–3195.
- Mukhtar, M. S., Carvunis, A.-R., Dreze, M., Epple, P., Steinbrenner, J., Moore, J., Tasan, M., Galli, M. Hao, T., Nishimura, M. T., Pevzner, S. J., Donovan, S. E., Ghamsari, L., Santhanam, B., Romero, V., Poulin, M. M., Gebreab, F., Gutierrez, B. J., Tam, S., Monachello, D., Boxem, M., Harbort, C. J., McDonald, N., Gai, L., Chen, H., He, Y., European Union Effectoromics Consortium, Vandehaute, J., Roth, F. P., Hill, D. E., Ecker, J. R., Vidal, M., Beynon, J., Braun, P. and Dangl, J. L.** (2011). Independently evolved virulence effectors converge onto hubs in a plant immune system network. *Science*, 333, 596–601.

Nakagawa, T., Kurose, T., Hino, T., Tanaka, K., Kawamukai, M., Niwa, Y., Toyooka, K., Matsuoka, K., Jinbo, T. and Kimura, T. (2007) Development of series of gateway binary vectors, pGWBs, for realizing efficient construction of fusion genes for plant transformation. *Journal of Bioscience and Bioengineering*, 104, 34–41.

Nicaise, V., Roux, M. and Zipfel, C. (2009) Recent Advances in PAMP-Triggered Immunity against Bacteria: Pattern Recognition Receptors Watch over and Raise the Alarm. *Plant Physiology*, 150, 1638–1647.

Niklaus, J. G. and Wilbert G. F. (2005) The biology of *Phytophthora infestans* at its centre of origin. *Annual Review of Phytopathology*, 43, 171–190.

Oh, S.-K., Young, C., Lee, M., Oliva, R., Bozkurt, T. O., Cano, L. M., Win, J., Bos, J. I. B., Liu, H.-Y., van Damme, M., Morgan, W., Choi, D., Van der Vossen, E. A. G., Vleeshouwers, V. G. A. A. and Kamoun, S. (2009). *In planta* expression screens of *Phytophthora infestans* RXLR effectors reveal diverse phenotypes, including activation of the *Solanum bulbocastanum* disease resistance protein Rpi-blb2. *The Plant Cell*, 21, 2928–2947.

Ori, N., Eshed, Y., Paran, I., Presting, G., Aviv, D., Tanksley, S., Zamir, D. and Fluhr, R. (1997) The *I2C* family from the wilt disease resistance locus *I2* belongs to the nucleotide binding, leucine-rich repeat superfamily of plant resistance genes. *The Plant Cell*, 9, 521–532.

Panstruga, R. (2003) Establishing compatibility between plants and obligate biotrophic pathogens. *Current Opinion in Plant Biology*, 6, 320–326.

Peer, V. D. Y and De Wachter, R. (1997) Evolutionary relationships among crown taxa taken into account site-to-site rate variation in 18s rRNA. *Journal of Molecular Evolution*, 45, 619–630.

Pel, M. A., Foster, S. J., Park, T.-H., Rietman, H., van Arkel, G., Jones, J. D. G., Van Eck, H. J., Jacobsen, E., Visser, R. G. F., and Van der Vossen, E. A. G. (2009) Mapping and cloning of late blight resistance genes from *Solanum venturii* using an interspecific candidate gene approach. *Molecular Plant–Microbe Interactions*, 22, 601–615.

Plett, J. M., Kemppainen, M., Kale, S. D., Kohler, A., Legué, V., Brun, A., Tyler, B. M., Pardo, A. G. and Martin, F. (2011) A secreted effector protein of *Laccaria bicolor* is required for symbiosis development. *Current Biology*, 21, 1197–1203.

Potato Genome Sequencing Consortium (2011) Genome sequence and analysis of the tuber crop potato. *Nature*, 475, 189–195.

Poueymiro, M. and Genin, S. (2009) Secreted proteins from *Ralstonia solanacearum*: a hundred tricks to kill a plant. *Current Opinion in Microbiology*, 12, 44–52.

Raffaele, S., Farrer, R. A., Cano, L. M., Studholme, D. J., MacLean, D., Marco, T., Jiang, R. H. Y., Zody, M. C., Kunjeti, S. G., Donofrio, N. M., Meyers, B. C., Nusbaum, C. and Kamoun, S. (2010) Genome evolution following host jumps in the Irish potato famine pathogen lineage. *Science*, 330, 1540–1543.

- Rehmany, A. P., Gordon, A., Rose, L. E., Allen, R. L., Armstrong, M. R., Whisson, S. C., Kamoun, S., Tyler, B. M., Birch, P. R. J. and Beynon, J. L.** (2005) Differential recognition of highly divergent downy mildew avirulence gene alleles by *RPP1* resistance genes from two *Arabidopsis* lines. *The Plant Cell*, 17, 1839–1850.
- Rietman, H., Bijsterbosch, G., Cano, L. M., Lee, H. R., Vossen, J. H., Jacobsen, E., Visser, R. G. F., Kamoun, S. and Vleeshouwers, V. G. A. A.** (2012) Qualitative and Quantitative Late Blight Resistance in the Potato Cultivar Sarpo Mira Is Determined by the Perception of Five Distinct RXLR Effectors. *Molecular Plant–Microbe Interactions*, 25, 910–919.
- Rivas, S. and Thomas, C. M.** (2005) Molecular interactions between tomato and the leaf mold pathogen *Cladosporium fulvum*. *Annual Review of Phytopathology*, 43, 395–436.
- Robatzek, S. and Saijo, Y.** (2008) Plant immunity from A to Z. *Genome Biology*, 9, 304.1-304.4.
- Romer, P., Hahn, S., Jordan, T., Strauss, T., Bonas, U., and Lahaye, T.** (2007) Plant pathogen recognition mediated by promoter activation of the pepper *Bs3* resistance gene. *Science*, 318, 645–648.
- Rooney, H. C. E., Van't Klooster, J. W., van der Hoorn, R. A. L., Joosten, M. H. A. J., Jones J. D. G. and de Wit, P. J. G. M.** (2005) *Cladosporium* Avr2 inhibits tomato Rcr3 protease required for Cf-2- dependent disease resistance. *Science*, 308, 1783–1786.
- Rose, J. K., Ham, K. S., Darvill, A. G., and Albersheim, P.** (2002) Molecular cloning and characterization of glucanase inhibitor proteins: Co-evolution of a counter defence mechanism by plant pathogens. *The Plant Cell* 14, 1329–1345.
- Roth, C., Rastogi, S., Arvestad, L., Dittmar, K., Light, S., Ekman, D. and Liberles, D. A.** (2007) Evolution after gene duplication: models, mechanisms, sequences, systems, and organisms. *Journal of Experimental Zoology Part B: Molecular and Developmental Evolution*, 308B, 58–73.
- Rowland, O., Ludwig, A. A., Merrick, C. J., Baillieul, F., Tracy, F. E., Durrant, W. E., Fritz-Laylin, L., Nekrasov, V., Sjölander, K., Yoshioka, H. and Jones, J. D. G.** (2005) Functional analysis of Avr9 / Cf-9 Rapidly Elicited genes identifies a protein kinase, ACIK1, that is essential for full Cf-9-dependent disease resistance in tomato. *The Plant Cell*, 17, 295–310.
- Saunders, D.G.O., Breen, S., Win, J., Schornack, S., Hein, I., Bozkurt, T. O., Champouret, N., Vleeshouwers, V. G. A. A., Birch, P. R. J., Gilroy, E. M. and Kamoun, S.** (2012) Host Protein BSL1 Associates with *Phytophthora infestans* RXLR effector AVR2 and the *Solanum demissum* immune receptor R2 to mediate disease resistance. *The Plant Cell*, 24, 3420–3434.
- Schnell, J.D. and Hicke, L.** (2003). Non-traditional functions of ubiquitin and ubiquitin-binding proteins. *Journal of Biological Chemistry*, 278, 35857–35860.

- Schornack, S., van Damme, M., Bozkurt, T. O., Cano, L. M., Smoker, M., Thines, M., Gaulin, E., Kamoun, S. and Huitema, E.** (2010) Ancient class of translocated oomycete effectors targets the host nucleus. *Proceedings of the National Academy of Sciences, USA*, 107, 17421–17426.
- Schulze-Lefert, P. and Panstruga, R.** (2011) A molecular evolutionary concept connecting nonhost resistance, pathogen host range, and pathogen speciation. *Trends in Plant Science*, 16, 117–125.
- Schwessinger, B. and Zipfel, C.** (2008) News from the frontline: recent insights into PAMP triggered immunity in plants. *Current Opinion in Plant Biology*, 11, 389–395.
- Shan, W., Cao, M., Leung, D. and Tyler, B. M.** (2004) The *Avr1b* locus of *Phytophthora sojae* encodes an elicitor and a regulator required for avirulence on soybean plants carrying resistance gene *Rps1b*. *Molecular Plant–Microbe Interactions*, 17, 394–403.
- Sharp, J. K., Valent, B. and Albersheim, P.** (1984) Purification and partial characterisation of a beta-glucan fragment that elicits phytoalexin accumulation in soybean. *Journal of Biological Chemistry*, 259, 11312–11320.
- Singh, V.** (2010) *A Text Book of Botany*. New Delhi: Capital Offset Press. 113 pp. 4th ed.
- Sohn, K. H., Lei, R., Nemri, A. and Jones J. D. G.** (2007) The Downy Mildew Effector Proteins ATR1 and ATR13 Promote Disease Susceptibility in *Arabidopsis thaliana*. *The Plant Cell*, 19, 4077–4090.
- Song, J., Bradeen, J. M., Naess, S. K., Raasch, J. A., Wielgus, S. M., Haberlach, G. T., Liu, J., Kuang, H., Austin-Phillips, S., Buell, C. R., Helgeson, J. P. and Jiang, J.** (2003) Gene *RB* cloned from *Solanum bulbocastanum* confers broad spectrum resistance to potato late blight. *Proceedings of the National Academy of Sciences, USA*, 100, 9128–9133.
- Song, J., Win, J., Tian, M., Schornack, S., Kaschani, F., Ilyas, M., van der Hoorn, R. A. L. and Kamoun S.** (2009) Apoplastic effectors secreted by two unrelated eukaryotic plant pathogens target the tomato defence protease Rcr3. *Proceedings of the National Academy of Sciences, USA*, 106, 1654–1659.
- Spooner, D. M. and Hijmans, R. J.** (2001) Potato systematics and germplasm collecting, 1989–2000. *American Journal of Potato Research*, 78, 237–268.
- Spooner, D. M. and Salas, A.** (2006) Structure, biosystematics, and genetic resources. In: J. Gopal and S. M. P. Khurana (eds) *Handbook of potato production, improvement, and post-harvest management*. Binghamton, NY: The Haworth Press, Inc., doi:10.1300/5776_01.
- Spooner, D. M., McLean, K., Ramsay, G., Waugh, R. and Bryan, G. J.** (2005) A single domestication for potato based on multilocus amplified fragment length polymorphism genotyping. *Proceedings of the National Academy of Sciences, USA*, 120, 14694–14699.
- Staskawicz, B. J., Ausubel, F. M., Baker, B. J., Ellis, J. G. and Jones, J. D. G.** (1995) Molecular genetics of plant disease resistance. *Science*, 268, 661–667.

- Stassen, J. H. M. and Van den Ackerveken, G.** (2011) How do oomycete effectors interfere with plant life? *Current Opinion in Plant Biology*, 14, 1–8.
- Tan, M. Y. A., Hutten, R. C. B., Visser, R. G. F. and Eck, H. J.** (2010) The effect of pyramiding *Phytophthora infestans* resistance genes *RPI-mcd1* and *RPI-ber* in potato. *Theoretical and Applied Genetics*, 121, 117–125.
- Thomma, B. P. H. J., Nürnberger, T. and Joosten, M. H. A. J.** (2011) Of PAMPs and effectors: the blurred PTI-ETI dichotomy. *The Plant Cell*, 23, 4–15.
- Thomma, B. P. H. J., van Esse, H. P., Crous, P. W. and de Wit, P. J. G. M.** (2005) *Cladosporium fulvum* (syn. *Passalora fulva*), a highly specialized plant pathogen as a model for functional studies on plant pathogenic *Mycosphaerellaceae*. *Molecular Plant Pathology*, 6, 379–393.
- Tian, M., Benedetti, B. and Kamoun, S.** (2005) A second Kazal-like protease inhibitor from *Phytophthora infestans* inhibits and interacts with the apoplastic pathogenesis-related protease P69B of tomato. *Plant Physiology*, 138, 1785–1793.
- Tian, M., Huitema, E., Da Cunha, L., Torto-Alalibo, T. and Kamoun, S.** (2004) A Kazal-like extracellular serine protease inhibitor from *Phytophthora infestans* targets the tomato pathogenesis-related protease P69B. *Journal of Biological Chemistry*, 279, 26370–26377.
- Tian, M., Win, J., Song, J., van der Hoorn, R., van der Knaap, E. and Kamoun, S.** (2007) A *Phytophthora infestans* cystatin-like protein targets a novel tomato papain-like apoplastic protease. *Plant Physiology*, 143, 364–377.
- Tian, Z., Liu, J., Wang, B. and Xie, C.** (2006) Screening and expression analysis of *Phytophthora infestans* induced genes in potato leaves with horizontal resistance. *Plant Cell Reporter*, 25, 1094–1103.
- Torto-Alalibo, T., Collmer, C. W., Gwinn-Giglio, M., Lindeberg, M., Meng, S-W., Chibucos, M. C., Tseng T-T., Lomax, J., Biehl B., Ireland, A., Bird, D., Dean, R. A., Glasner, J. D., Perna, N., Setubal, J. C., Collmer, A. and Tyler, B. M.** (2010) Unifying themes in microbial associations with animal and plant hosts described using the gene ontology. *Microbiology and Molecular Biology Reviews*, 74, 479–503.
- Trujillo, M., Ichimura, K., Casais, C. and Shirasu, K.** (2008) Negative regulation of PAMP triggered immunity by an E3 ubiquitin ligase triplet in *Arabidopsis*. *Current Biology*, 18, 1396–1401.
- Tseng, T. T., Tyler, B. M. and Setubal, J. C.** (2009) Protein secretion systems in bacterial–host associations, and their description in the gene ontology. *BMC Microbiology*, 9 (Suppl 1):S2 doi:10.1186/1471-2180-9-S1-S2.
- Tyler, B. M.** (2006) Genomics of Fungal Plant Pathogens. *Encyclopaedia of Plant and Crop Science*. doi: 10.1081/E-EPCS-120019942: 1–5.
- Tyler, B. M.** (2009) Entering and breaking: virulence effector proteins of oomycete plant pathogens. *Cellular Microbiology*, 11, 13–20.

van Damme, M., Bozkurt, T. O., Cakir, C., Schornack, S., Sklenar, J., Jones, A. M. E. and Kamoun, S. (2012) The Irish Potato Famine Pathogen *Phytophthora infestans* Translocates the CRN8 Kinase into Host Plant Cells. *PLoS Pathogens* 8(8): e1002875.

Van der Biezen, E. A. and Jones, J. D. G. (1998) Plant disease-resistance proteins and the gene-for-gene concept. *Trends in Biochemical Sciences*, 23, 454–456.

Van der Hoorn, R. A. L. and Kamoun, S. (2008) From guard to decoy: a new model for perception of plant pathogen effectors. *The Plant Cell*, 20, 2009–2017.

van der Vossen, E. A., Gros, J., Sikkema, A., Muskens, M., Wolters, D., Pereira, A. and Allefs, S. (2005) The *Rpi-blb2* gene from *Solanum bulbocastanum* is an *Mi-1* gene homolog conferring broad-spectrum late blight resistance in potato. *The Plant Journal*, 44, 208–222.

van der Vossen, E., Sikkema, A., Hekkert, B. L., Gros, J., Stevens, P., Muskens, M., Wouters, D., Pereira, A., Stiekema, W. and Allefs, S. (2003) An ancient R gene from the wild potato species *Solanum bulbocastanum* confers broad-spectrum resistance to *Phytophthora infestans* in cultivated potato and tomato. *The Plant Journal*, 36, 867–882.

Van Poppel, P., Guo, J., de Vondervoort, P., Jung, M. W. M., Birch, P. R. J., Whisson, S. C. and Govers, F. (2008) The *Phytophthora infestans* avirulence gene *Avr4* encodes an RXLR-dEER effector. *Molecular Plant–Microbe Interactions*, 21, 1460–1470.

Vanderplank, J. E. (1984) *Disease Resistance in Plants*, 2nd edn. New York, NY, USA: Academic Press.

Vetukuri, R. R., Tian, Z., Avrova, A. O., Savenkov, E. I., Dixelius, C. and Whisson, S. C. (2011) Silencing of the *PiAvr3a* effector-encoding gene from *Phytophthora infestans* by transcriptional fusion to a short interspersed element. *Fungal Biology*, 115, 1225–1233.

Vierstra, R. D. (2009) The ubiquitin-26S proteasome system at the nexus of plant biology. *Nature Reviews Molecular and Cell Biology*, 10, 385–397.

Vleeshouwers, V. G. A. A., Rietman, H., Krenek, P., Champouret, N., Young, C., Oh, S.-K., Wang, M., Bouwmeester, K., Vosman, B., Visser, R. G. F., Jacobsen, E., Govers, F., Kamoun, S., Van der Vossen, E. A. G. (2008) Effector Genomics Accelerates Discovery and Functional Profiling of Potato Disease Resistance and *Phytophthora infestans* Avirulence Genes. *PLoS ONE* 3(8): e2875. doi:10.1371/journal.pone.0002875.

Vleeshouwers, V. G. A. A., Raffaele, S., Vossen, J. H., Champouret, N., Oliva, R., Segretin, M. E., Rietman, H., Cano, L. M., Lokossou, A., Kessel, G., Pel, M. A. and Kamoun, S. (2011) Understanding and exploiting late blight resistance in the age of effectors. *The Annual Review of Plant Biology*, 49, 507–531.

Walter, M., Chaban, C., Schütze, K., Batistic, O., Weckermann, K., Näke, C., Blazevic, D., Grefen, C., Schumacher, K., Oecking, C., Harter, K. and Kudla, J. (2004) Visualization of protein interactions in living plant cells using bimolecular fluorescence complementation. *The Plant Journal*, 40, 428–438.

Wang, Q., Han, C., Ferreira, A. O., Yu, X., Ye, W., Tripathy, S., Kale, S. D., Gu, B., Sheng, Y., Sui, Y., Wang, X., Zhang, Z., Cheng, B., Dong, S., Shan, W., Zheng, X., Dou, D., Tyler, B. M. and Wang, Y. (2011) Transcriptional Programming and Functional Interactions within the *Phytophthora sojae* RXLR Effector Repertoire. *The Plant Cell*, 23, 2064–2086.

Wang, Y. S., Pi, L. Y., Chen, X., Chakrabarty, P. K., Jiang, J., De Leon, A. L., Liu, G. Z., Li, L., Benny, U., Oard, J., Ronald, P. C. and Song, W. Y. (2006) Rice XA21 binding protein 3 is a ubiquitin ligase required for full Xa21-mediated disease resistance. *The Plant Cell*, 18, 3635–3646.

Wawra, S., Agacan, M., Boddey, J. A., Davidson, I., Gachon, C. M., Zanda, M., Grouffaud, S., Whisson, S. C., Birch, P. R. J., Porter, A. J. and van West, P. (2012a) Avirulence Protein 3a (Avr3a) from the Potato Pathogen *Phytophthora infestans* Forms Homodimers through Its Predicted Translocation Region and Does Not Specifically Bind Phospholipids. *Journal of Biological Chemistry*, 287, 38101–38109.

Wawra, S., Bain, J., Durward, E., de Bruijn, I., Minor, K. L., Matena, A., Löbach, L., Whisson, S. C., Bayer, P., Porter, A. J., Birch, P. R. J., Secombes, C. J. and van West, P. (2012b) Host-targeting protein 1 (SpHtp1) from the oomycete *Saprolegnia parasitica* translocates specifically into fish cells in a tyrosine-O-sulphate-dependent manner. *Proceedings of the National Academy of Sciences, USA*, 109, 2096–2101.

Westerink, N., Brandwagt, B. F., de Wit, P. J. G. M. and Joosten, M. H. A. J. (2004) *Cladosporium fulvum* circumvents the second functional resistance gene homologue at the *Cf-4* locus (*Hcr9-4E*) by secretion of a stable Avr4E isoform. *Molecular Microbiology*, 54, 533–545.

Whisson, S. C., Avrova, A. O., Boevink, P. C., Armstrong, M. R., Seman, Z. A., Hein, I. and Birch, P. R. J. (2011) Exploiting knowledge of pathogen effectors to enhance late blight resistance in potato. *Potato Research*, 54, 325–340.

Whisson, S. C., Boevink, P. C., Moleleki, L., Avrova, A. O. and Morales, J. G. (2007) A translocation signal for delivery of oomycete effector proteins into host plant cells. *Nature*, 450, 115–118.

Wilton, M. and Desveaux, D. (2010). Lessons learned from type III effector transgenic plants. *Plant Signaling and Behavior*, 5, 746–748.

Win, J., Krasileva, K. V., Kamoun, S., Shirasu, K., Staskawicz, B. J. and Banfield, M. J. (2012) Sequence Divergent RXLR Effectors Share a Structural Fold Conserved across Plant Pathogenic Oomycete Species. *PLoS Pathogens*, 8(1): e1002400. doi:10.1371/journal.ppat.1002400.

Win, J., Morgan, W., Bos, J., Krasileva, K. V., Cano, L. M., Chaparro-Garcia, A., Ammar, R., Staskawicz, B. J. and Kamoun, S. (2007) Adaptive evolution has targeted the C-terminal domain of the RXLR effectors of plant pathogenic oomycetes. *The Plant Cell*, 19, 2349–2369.

Xiang, T., Zong, N., Zou, Y., Wu, Y., Zhang, J., Xing, W., Li, Y., Tang, X., Zhu, L., Chai, J. and Zhou, J. M. (2008) *Pseudomonas syringae* effector AvrPto blocks innate immunity by targeting receptor kinases. *Current Biology*, 18, 74–80.

- Yaeno, T., Li, H., Chaparro-Garcia, A., Schornack, S., Koshiba, S., Watanabe, S., Kigawa, T., Kamoun, S. and Shirasu, K.** (2011) Phosphatidylinositol monophosphate-binding interface in the oomycete RXLR effector Avr3a is required for its stability in host cells to modulate plant immunity. *Proceedings of the National Academy of Sciences, USA*, 108, 14682–14687.
- Yang, C. W., González-Lamothe, R., Ewan, R. A., Rowland, O., Yoshioka, H., Shenton, M., Ye, H., O'Donnell, E., Jones, J. D. G. and Sadanandom, A.** (2006) The E3 ubiquitin ligase activity of *Arabidopsis* PLANT U-BOX17 and its functional tobacco homolog ACRE276 are required for cell death and defence. *The Plant Cell*, 18, 1084–1098.
- Zeng, L. R., Qu, S., Bordeos, A., Yang, C., Baraoidan, M., Yan, H., Xie, Q., Nahm, B. H., Leung, H. and Wang, G. L.** (2004) Spotted leaf11, a negative regulator of plant cell death and defence, encodes a U-box/armadillo repeat protein endowed with E3 ubiquitin ligase activity. *The Plant Cell*, 16, 2795–2808.
- Zhou, J. M. and Chai, J.** (2008) Plant pathogenic bacterial type III effectors subdue host responses. *Current Opinion in Microbiology*, 11, 179–185.
- Zhu, S., Li, Y., Vossen, J. H., Visser, R. G. F. and Jacobsen, E.** (2011) One step stacking of three potato late blight resistance genes; the use of avirulence genes to select for functionality. *Transgenic Research*, 21, 89–99.
- Zipfel, C. and Rathjen, J.P.** (2008) Plant Immunity: AvrPto Targets the Frontline. *Current Biology*, 18, R218–R220.